Characterisation of the geochemical properties of a clay liner at a landfill site

Gabriela Muñoz-Meléndez

A thesis submitted for the degree of Doctor of Philosophy of the University of London and the Diploma of Imperial College.

November, 1999

T. H. Huxley School of Environment, Earth Sciences and Engineering - Environmental Analysis Section, Imperial College of Science, Technology and Medicine (University of London) Silwood Park, Ascot, Berkshire SL5 7TE

To three wonderful women: my mother, Angélica and Ana

Abstract

This thesis describes the chemical, mineralogical and spatial characterisation of a new cell of engineered Oxford Clay in an existing landfill site. The clay content, organic carbon content, soil pH, cation exchange capacity and exchangeable cations were determined for 35 samples taken from the bottom of the cell. Three elements Cr, Cu and Zn were also determined in fractions bound to carbonates, Fe-Mn oxides, organic matter and exchangeable sites as well as total concentrations in the compacted clay used as liner. These elements were characterised in the soil solution as well.

Stability diagrams were used to identify which inorganic species would be in the soil solution. Inorganic species were quantified using the geochemical equilibrium model, Geochem-PC.

Geostatistics were used to describe the spatial variability of the soil pH, organic matter and metals bound to soil solid phases. Variograms were calculated using Variowin 2.1; the ordinary kriging and crossvalidation process were carried out using Gslib.

It was possible, through the chemical, mineralogical and spatial characterisation, to identify the presence of a layer rich in pyrite underneath the liner system. The spatial characteristics of the landfill cell are complex and to a large extent are associated with the mineralogical composition of the site, particularly with the oxidation of pyrite in the surface, that causes the pH to be low. pH spatial variation correlates with the distribution of Cu, Cr and Zn in the soil.

This work shows that it is possible to predict the behaviour of trace elements through the characterisation of geochemical parameters; even more, the mineral, chemical and spatial characterisation of geochemical parameters in a clay liner can reveal trends and natural hazards in a landfill site, and could be used to reduce risks and optimise the monitoring designs.

BRITISH LIBRARY

ETHOS

Boston Spa, Wetherby
West Yorkshire, LS23 7BQ
www.bl.uk

PAGE MISSING IN ORIGINAL

Contents

ABSTRACT 3

ACKNOWLEDGEMENTS 4

TABLE OF CONTENTS 5

LIST OF TABLES 8

LIST OF FIGURES 11

HYPOTHESES 16

CHAPTER 1. RESEARCH AIMS AND OBJECTIVES 17

CHAPTER 2. GENERAL REVIEW 24

2.1. INTRODUCTION 24
2.2. OVERVIEW OF WASTE DISPOSAL 24
2.3. THE LANDFILL SYSTEM 25
2.4. FOCUS ON CLAY LINERS 33
2.5. SOIL SAMPLING 41
2.6. SOIL SAMPLE PREPARATION 45
2.7. CHEMICAL ANALYSIS TO DETERMINE REACTIVY OF HEAVY METALS ON SOIL SAMPLES 46
2.8. THE SOIL SOLUTION 47
2.9. SPATIAL VARIABILITY 53
2.10. CONCLUSIONS 59

CHAPTER 3. L-FIELD SITE 60

3.1. INTRODUCTION 60
3.2. L-FIELD SITE 60
3.3. HISTORICAL DEVELOPMENT 61
3.4. GEOLOGY 63
3.4.1. OXFORD CLAY 64
3.4.2. KELLAWAY BEDS 66
3.4.3. CORNBRASH LIMESTONE 66
3.4.4. BLISWORTH CLAY 67
3.4.5. GREAT OOLITE LIMESTONE OR BLISWORTH LIMESTONE 67
3.5. RAINFALL AND EVAPORATION 68
3.6. DRAINAGE 70
3.7. WATER SUPPLY 70
3.8. CONCLUSIONS 71

CHAPTER 4. THE EXPLORATORY CAMPAIGN 72

4.1. INTRODUCTION 72
4.1.1. OBJECTIVE 72
4.2 SAMPLING 73

4.3. Analytical methods and techniques used on the exploratory samples 74
4.4. Results from the exploratory samples characterisation 75
4.4.1. Preparation of trace-element solutions for ICP-MS analysis HF-$HClO_4$ method 79
4.4.2. Common single extraction scheme for soil analysis 80
4.4.2.1. Comparison of the analytical determination of the common single extraction scheme for soil analysis by ICP-AES 82
4.4.3. Sequential Extraction Procedure for the Speciation of Particulate Trace Metals 83
4.4.3.1. Comparison of the analytical determination of the sequential extraction scheme by ICP-AES 86
4.4.3.2. Degradation of the extractable fraction versus time 87
4.4.3.3. Confirmation of the sequential extraction scheme 90
4.4.4. Determination of the mineralogy composition 97
4.4.5. Measuring of soil pH 100
4.5. Assessment of the Sampling Proposal 101
4.6. Conclusions 102

CHAPTER 5. THE ASSESSMENT CAMPAIGN 104

5.1. Introduction 104
5.2. the assessment sampling 104
5.3. Sample pre-treatment 105
5.4. Analytical determinations on the assessment samples 105
5. 5. Result from the assessment sample characterisation 107
5.5.1. Total digestion using the HF-$HClO_4$ method and ICP-AES 107
5.5.2. Determination of soil pH 107
5.5.3. The mineralogical composition 109
5.5.4. Determination of organic carbon content by the Loss-On-Ignition method 112
5.5.5. The cation exchange capacity and the exchangeable cations. 112
5.5.6. The fractionation of Ni, Cu, Zn, Cd and Pb in solid phases using a sequential extraction method and ICP-AES 114
5.5.7. Characterisation of the soil solution 124
5.5.7.1. The saturation extract 124
5.5.7.2. The soil-water Extract 124
5.5.7.3. Determination of the cation content using ICP-AES 126
5.5.7.4. Determination of the anion content 127
5.5.6. Conclusions 131

CHAPTER 6. INORGANIC METAL SPECIES IN SOLUTION 133

6.1. Introduction 133
6.2. Stability diagrams 134
6.2.1. Stability diagram of the major mineral components of the liner 136
6.2.1.1. Clay fraction 136
6.2.1.2. Carbonates 137
6.2.1.3. Pyrite 139
6.2.2. Stability diagrams for the inorganic species in solution 139
6.2.2.1. Sodium 140
6.2.2.2. Magnesium 140
6.2.2.3. Aluminium 141
6.2.2.4. Potassium 141
6.2.2.5. Calcium 143
6.2.2.6. Iron 144
6.2.2.7. Zn 146
6.2.3. Final remarks on the use of stability diagrams for chemical speciation 148
6.3. Inorganic metal speciation using the geochemical equilibrium model: GEOCHEM-PC 148
6.3.1. Analytical scheme for the geochemical equilibrium model confirmation 148
6.3.2. Modelled inorganic species in soil solution 148
6.4. Conclusions 151

CHAPTER 7. STATISTICAL ANALYSIS OF THE MEASURED PARAMETERS IN THE LINER 152

7.1. INTRODUCTION 152
7.2. DESCRIPTIVE STATISTICS 152
7.3. GEOSTATISTICS 153
7.4. RESULTS 155
7.4.1. SOIL pH 155
7.4.2. ORGANIC MATTER CONTENT 158
7.4.3. CEC AND EXCHANGEABLE CATIONS 161
7.4.4. Cr, Cu AND Zn 163
7.4.4.1. EXCHANGEABLE FRACTION 163
7.4.4.2. FRACTION BOUND TO CARBONATES 167
7.4.4.3. FRACTION BOUND TO Fe-Mn OXIDES 169
7.4.4.4. FRACTION BOUND TO ORGANIC MATTER 173
7.4.4.5. TOTAL CONCENTRATION 183
7.5. CONCLUSIONS 192

CHAPTER 8. CONCLUSIONS 194

REFERENCES 199

APPENDIX 1.THE CERTIFIED VALUES OF THE REFERENCE MATERIAL AND THE RECOVERY PERCENTAGE OF EXPLORATORY SAMPLES 213

APPENDIX 2. THE ASSESSMENT SAMPLING REPORT 216

APPENDIX 3. THE HEXAQUO ION $[M(H_2O)_6]^{N+}$ 217

List of Tables

Table 2.1. Leachate analysis (parameters with differences between acetic and methanogenic phase) (Ehrig, 1988) 26

Table 2.2. Leachate analysis (no difference between phases could be observed) (Ehrig, 1988) 27

Table 2.3. Tessier *et at* (1979) sequential extraction steps. 47

Table 2.4. Common laboratory method to obtain soil solution. 51

Table 2.5. Ions of major interest in soil solution. 52

Table 2.6. Variogram models 58

Table 3.1. Input and outputs from the pit area of the L-field site 69

Table 3.2. Results for the analysis of groundwater taken from the borehole 1/73 71

Table 4.1. Total concentration of selected metals on exploratory samples from the L-field site, (values are given in mg kg^{-1}). 79

Table 4.2. Limits of detection for the HF-$HClO_4$ method. 79

Table 4.3. Concentration of bioavailable metals on exploratory samples from the L-field site (values are given in mg kg^{-1}). 80

Table 4.4. Concentration of exchangeable cation fraction of selected metals on exploratory samples from the L-field site (values are given in mg kg^{-1}). 81

Table 4.5. Limits of detection for the 0.05 mol/l EDTA and mol/l acetic acid single extraction methods using ICP-MS. 81

Table 4.6. Wavelengths used for ICP-AES determination. 82

Table 4.7. Concentration of bioavailable metals on exploratory samples from the L-field site (values are given in mg kg^{-1}) determined by ICP-AES. 82

Table 4.8. Concentration of exchangeable cation fraction of selected metals on exploratory samples from the L-field site (values are given in mg kg^{-1}) determined by ICP-AES. 83

Table 4.9. LoD for the EDTA and acetic acid methods using ICP-AES technique. 83

Table 4.10. Soil pools, importance of the determination of heavy metals bound to an specific fraction and proposed reagent to operationally defined them 84

Table 4.11. Concentrations of heavy metals bound to soil fractions for the exploratory sample S1 85

Table 4.12. Concentrations of heavy metals bound to soil fractions for the exploratory sample S2 85

Table 4.13. Concentrations of heavy metals bound to soil fractions for the exploratory sample S3 85

Table 4.14. Concentrations of heavy metals bound to soil fractions for the exploratory sample liner 86

Table 4.15. Limits of detection for the Tessier *et al* (1979) method, using ICP-MS 86

Table 4.16. Concentrations of heavy metals bound to soil fractions for the exploratory sample S1 determined by ICP-AES. 87

Table 4.17. Limits of detection for the Tessier *et al* (1979) method, using ICP-AES. 87

Table 4.18. Exchangeable fraction determined by ICP-AES, at selected intervals after extraction, values are given in mg/kg 88

Table 4.19. Fraction bound to carbonates determined by ICP-AES, at selected intervals after extraction, values are given in mg/kg. 89

Table 4.20. Fraction bound to Fe-Mn oxides determined by ICP-AES, several days after extraction, values are given in mg/kg 89

Table 4.21. Fraction bound to organic matter determined by ICP-AES, several days after extraction, values are given in mg/kg 90

Table 4.22. Mineralogical composition for bulk rock and clay fraction for exploratory samples of Oxford Clay samples from the L field site. Values given in % wt. 97

Table 4.23. The properties of the clay minerals in the exploratory samples 98

Table 4.24. Soil pH measurement in water for exploratory samples. 101

Table 4.25. Number of samples to take during the assessment sampling. 102

Table 5.1. Total concentration of heavy metals on assessment samples. 108

Table 5.2. Results for the soil pH measurement 109

Table 5.3. Mineralogical composition of the two pH zones. 110

Table 5.4. Organic matter content determined by LOI method. 113

Table 5.5. CEC and exchangeable cation in the assessment samples, values are given in centimoles of cation charge per kilogram ($cmol_c kg^{-1}$) 115

Table 5.6. Results for the fraction of heavy metals as exchangeable forms, values are given in mg kg^{-1} 116

Table 5.7. Results for the heavy metal fraction bound to carbonates, values are given in mg kg^{-1}. 117

Table 5.8. Results for the heavy metal fraction bound to Fe-Mn oxides, values are given in mg kg^{-1} 118

Table 5.9. Results for the heavy metal fraction bound to organic matter, values are given in mg kg^{-1} 119

Table 5.10. Results for the heavy metal in the residuals, values are given in mg kg^{-1}. 120

Table 5.11. Comparison between the total concentration of Zn versus the sum of concentration of Zn in solid fractions, values are given in mg kg^{-1}. 121

Table 5.12. Comparison between the total concentration of Cu versus the sum of concentration of Cu in solid fractions, values are given in mg kg^{-1} 122

Table 5.13. Comparison between the total concentration of Cr versus the sum of concentration of Cr in solid fractions, values are given in mg kg^{-1} 123

Table 5.14. Analytical details for the determination of cations in the ICP-AES system and the cation content in soil solution 127

Table 5.15. Analytical details for the determination of anions in soil solution using the UV/visible spectrophotometer Ultrospec III Pharmacia LKB 128

Table 5.16. Concentrations of bicarbonate and carbonate calculated from the alkalinity expressed in terms of $CaCO_3$. 129

Table 5.17. Retention time, resolution and limit of detection for 5 anions and the anion concentration in the sample. 130

Table 6.1. Measured concentrations of chemical species in soil solution extracted from compacted virgin Lower Oxford Clay. 135

Table 6.2. Predicted versus observed values for a 0.01 M HCl solution. 148

Table 6.3. Primary distribution of metals and ligands in the soil solution extracted from the Lower Oxford Clay samples 150

Table 7.1. Rank correlation coefficients. 153

Table 7.2. Rank correlation coefficients for geochemical parameters in 24 liner samples 162

List of Figures

Figure 2.1. Typical envelope of acceptability for placed and compacted clay in terms of moisture content and dry density at which appropriate permeability requirements are met (Parker and Rae, 1998). 36

Figure 2.2. The adsorption of an hydrated divalent metal cation [$M(H_2O)_6^{2+}$] by the interlayer surfaces of montmorillonite (McBride *et al*, 1991) 40

Figure 2.3. The specific sorption of divalent heavy metals by Fe oxide (McBride *et al*, 1991). 40

Figure 2.4. Variogram showing the exponential model 57

Figure 3.1. L-field landfill site. 62

Figure 3.2. Location of Stewartby. 63

Figure 3.3. Geological cross-section of the Marston Vale, Bedfordshire 64

Figure 4.1. Exploratory sampling locations. 74

Figure 4.2.a. Spectral profiles of the standard, blank and sample of the leachate corresponding to the exchangeable fraction extraction for Al 92

Figure 4.2.b. Spectral profiles of the standard, blank and sample of the leachate corresponding to the exchangeable fraction extraction for Ca 92

Figure 4.2.c. Spectral profiles of the standard, blank and sample of the leachate corresponding to the exchangeable fraction extraction for Si 92

Figure 4.3.a. Spectral profiles of the standard, blank and sample of the leachate corresponding to the fraction bound to carbonates extraction for Al 93

Figure 4.3.b. Spectral profiles of the standard, blank and sample of the leachate corresponding to the fraction bound to carbonates extraction for Ca 93

Figure 4.3.c. Spectral profiles of the standard, blank and sample of the leachate corresponding to the fraction bound to carbonates extraction for Si 93

Figure 4.4.a. Spectral profiles of the standard, blank and sample of the leachate corresponding to the fraction bound to Fe-Mn oxides extraction for Al 96

Figure 4.4.b. Spectral profiles of the standard, blank and sample of the leachate corresponding to the fraction bound to Fe-Mn oxides extraction for Ca 96

Figure 4.4.c. Spectral profiles of the standard, blank and sample of the leachate corresponding to the fraction bound to Fe-Mn oxides extraction for Si 96

Figure 4.5.a. Spectral profiles of the standard, blank and sample of the leachate corresponding to the fraction bound to organic matter extraction for Al 97

Figure 4.5.c. Spectral profiles of the standard, blank and sample of the leachate corresponding to the fraction bound to organic matter extraction for Si 97
Figure 5.1. The assessment sampling location at L-field site landfill. 105
Figure 5.2. The assessment sampling points. 106
Figure 6.1. Stability diagram of the liner clay fraction. 137
Figure 6.2. Stability diagram for the system calcite-gypsum 137
Figure 6.3. Stability diagram for jarosite. 139
Figure 6.4. Complexes of Na^{+} in solution 140
Figure 6.5. Chloride and carbonates of Mg^{2+} in solution 141
Figure 6.6. Hydrolysis, sulphate and phosphates of Mg^{2+} in solution 141
Figure 6.7. Hydrolysis species of Al^{3+} in equilibrium with Illite. 142
Figure 6.8. Sulphate species of Al^{3+} in equilibrium with Illite 142
Figure 6.9. Species of K^{+} 142
Figure 6.10. Chloride, carbonates and hydrolysis species of Ca^{2+} in equilibrium with calcite and $CO_{2(g)}$. 143
Figure 6.11. Phosphates and sulphate species of Ca^{2+} in equilibrium with calcite and $CO_{2(g)}$ 143
Figure 6.12. Hydrolysis species of Fe^{3+} in equilibrium with $Fe(OH)_3$-soil 144
Figure 6.13. Sulphate and phosphates species of Fe^{3+} in equilibrium with $Fe(OH)_3$-soil 144
Figure 6.14. Hydrolysis species of Fe^{2+} 145
Figure 6.15. Complexes of Fe^{2+} in solution 145
Figure 6.16. The hydrolysis species of Zn^{2+} in equilibrium with Zn-soil 146
Figure 6.17. Chloride complexes of Zn^{2+} in solution 147
Figure 6.18. Sulphate and phosphates of Zn in solution 147
Figure 7.1.a. Histogram and descriptive statistics for the original pH population. 156
Figure 7.1.b. Histogram and descriptive statistics for the transformed pH population. 156
Figure 7.2. Directional variograms characterising the spatial distribution of transformed pH population 157
Figure 7.3. Histogram and descriptive statistics of the ordinary kriging estimates for the transformed pH population 157
Figure 7.4. Scatterplot of observed versus estimated values for the soil transformed pH population 157
Figure 7.5. Histogram of errors for the transformed pH kriging estimates. 158
Figure 7.6. Directional variograms of errors for the pH transformed kriging estimates. 158
Figure 7.7. Map of pH transformed kriging estimates 159
Figure 7.8. Histogram and descriptive statistics for the organic matter content 160

Figure 7.9. Histogram and descriptive statistics of the organic matter ordinary kriging estimates.....160

Figure 7.10. Directional variograms characterising the spatial distribution of the organic matter content population. 160

Figure 7.11. Scatterplot of observed versus estimated values for the organic matter content population. 160

Figure 7.12. Histogram of errors for the organic matter content kriging estimates. 161

Figure 7.13. Directional variograms of errors for the organic matter content kriging estimates 161

Figure 7.14. Gray scale map of organic matter kriging estimates. 162

Figure 7.15. The Bayes theorem applied on the exchangeable Zn results.....165

Figure 7.16. The Bayes theorem applied on the exchangeable Cu results. 166

Figure 7.17. The Bayes theorem applied on the exchangeable Cr results. 167

Figure 7.18. The Bayes theorem applied to the Zn bound to carbonates results. 168

Figure 7.19. The Bayes theorem applied on the Cu bound to carbonates results. 169

Figure 7.20. Histogram and descriptive statistics of Zn bound to Fe-Mn oxides. 170

Figure 7.21. Histogram and descriptive statistics of the Zn bound to Fe-Mn oxides ordinary kriging estimates.....170

Figure 7.22. Directional variograms characterising the spatial distribution of Zn bound to Fe-Mn oxides. 170

Figure 7.23. Scatterplot of observed versus estimated values for Zn bound to Fe-Mn oxides 171

Figure 7.24. Histogram of errors for the Zn bound to Fe-Mn oxides estimates. 171

Figure 7.25. Directional variograms of the errors for the kriging estimates of Zn bound to Fe-Mn oxides. 172

Figure 7.26. Gray scale map of the Zn bound to Fe-Mn oxides kriging estimates. 172

Figure 7.27. Histogram and descriptive statistics for Cu bound to organic matter. 174

Figure 7.28. Histogram and descriptive statistics of the ordinary kriging estimates for Cu bound to organic matter.....174

Figure 7.29. Directional variograms characterising the spatial distribution of Cu bound to organic matter. 174

Figure 7.30. Scatterplot of observed versus estimated values for Cu bound to organic matter 175

Figure 7.31. Histogram of errors for the Cu bound to organic matter estimates.....175

Figure 7.32. Directional variograms of the ordinary kriging errors for Cu bound to organic matter. 175

Figure 7.33. Gray scale map of Cu bound to organic matter kriging estimates. 176
Figure 7.34. Histogram and descriptive statistics of Cr bound to organic matter. 177
Figure 7.35. Histogram and descriptive statistics of the ordinary kriging estimates for Cr bound to organic matter. 177
Figure 7.36. Directional variograms characterising the spatial distribution of the Cr bound to organic matter. 177
Figures 7.37. Scatterplot of observed versus estimated values for Cr bound to organic matter 178
Figure 7.38. Histogram of errors for Cr bound to organic matter ordinary kriging estimates. ..178
Figure 7.39. Directional variograms of errors for the Cr bound to organic matter estimates. ..178
Figure 7.40. Gray scale map of the Cr bound to organic matter kriging estimates. 179
Figure 7.41. Histogram and descriptive statistics of the Zn bound to organic matter. 180
Figure 7.42. Histogram and descriptive statistics of Zn bound to organic matter ordinary kriging estimates. 180
Figure 7.43. Directional variograms characterising the spatial variability of the Zn bound to organic matter. 180
Figure 7.44. Scatterplot of observed versus observed values for Zn bound to organic matter..181
Figure 7.45. Histogram of errors for Zn bound to organic matter estimates....181
Figure 7.46. The directional variograms of errors for Zn bound to organic matter estimates...181
Figure 7.47. Gray scale map of Zn bound to organic matter kriging estimates....182
Figure 7.48. Histogram and descriptive statistics of the total concentration of Cr....184
Figure 7.49. Histogram and descriptive statistics of the ordinary kriging estimates for Cr total 184
Figure 7.50. Directional variograms characterising the spatial variability of the total concentration of Cr. 184
Figure 7.51. Scatterplot of observed versus estimated values for Cr total....185
Figure 7.52. Histogram of errors for the Cr total estimates....185
Figure 7.53. Directional variograms of errors for Cr total estimates. 185
Figure 7.54. Gray scale map of total concentration of Cr kriging estimates....186
Figure 7.55. Histogram and descriptive statistics of the total concentration of Cu. 186
Figure 7.56. Histogram and descriptive statistics of Cu total ordinary kriging estimates....187
Figure 7.57. Directional variograms characterising the spatial distribution of the total concentration of Cu....187
Figure 7.58. Scatterplot of the observed versus the estimated values for Cu total. 188
Figure 7.59. Histogram of errors for Cu total estimates....188
Figure 7.60. Directional variograms of errors for the Cu total estimates. 188

Figure 7.61. Gray scale map of total concentration of Cu kriging estimates. 189

Figure 7.62. Histogram and descriptive statistics of the total concentration of Zn. 190

Figure 7.63. Histogram and descriptive statistics of the ordinary kriging estimates for Zn total 190

Figure 7.64. Directional variograms characterising the spatial distribution of the total concentration of Zn, without the highest value. 190

Figure 7.65. Scatterplot of observed versus estimated values for Zn total. 191

Figure 7.66. Histogram of errors for Zn total estimates. 191

Figure 7.67. Directional variogram of errors for Zn total estimates 191

Figure 7.68. Gray scale map of the total concentration of Zn kriging estimates. 192

Figure 7.69. Summary figure showing grey scale maps of: **a)** pH, **b)** organic matter, **c)** Zn bound to Fe-Mn oxides, **d)** Cr bound to organic matter, **e)** Cu bound to organic matter, **f)** Zn bound to organic matter, **g)** Total concentration of Cr, **h)** Total concentration of Cu, and **i)** Total concentration of Zn 193

Figure A2.1 Fe^{3+} hexahydronium ion. 214

Hypotheses

The hypotheses for this research were that:

- The chemical, mineral and spatial characteristics of the compacted clay liner influence all components of the clay, including heavy metals, and so, these characteristics should be taken into account when estimating the mass transfer of components from the soil to other environments.
- The spatial variability description of geochemical parameters can reveal trends and areas of reactivity, that can impact on the liner performance to attenuate landfill leachate.

Chapter 1. Research aims and objectives

The excessive generation of waste constitutes one of the most serious problems of our time. Several options for dealing with the waste management problem have been developed, however, none of these options have fully solved the problem and they all have an impact on the environment. Currently, containment landfill is the most used and cost-effective waste management option. The main end-products of waste degradation in a landfill are leachate and gas (methane) and both of them impact on the environment. In contrast to gas, which represents an economically attractive source of regenerable energy, leachate remains a critical issue. Several factors influence the generation of leachate; most of them are carefully controlled through legal and engineering requirements. Most of the responsibility to attenuate leachate falls on the adequate performance of the liner system or, to put it in more specific terms, the attenuation depends on the type of material the liner is made of. There is no such thing as the perfect impermeable material, and it is known that each material has a different effectiveness to attenuate leachate, and not all elements or compounds are equally removed or reduced in concentration.

There are several types of liner systems, however compacted clay liners are still the most common liner system chosen. Strict engineering criteria are applied to the selection, preparation, compaction, placement, and protection of the clay to be used as the liner. A special emphasis is put on the physical parameters that influence attenuation on compacted clay liners. However, similar focus has not been directed on geochemical parameters. Surprisingly enough, even though the objective is to construct an effective, continuous clay liner, none of these parameters have been spatially or temporally described.

The liner system is not the only factor to consider during the design, construction, management, closure and aftercare of a landfill. Among other factors, the collection, removal, monitoring and cover systems can be listed. A critical factor is the selection of a site to be used as a landfill, which should take into account a number of parameters including proximity to the waste generator, availability of transportation systems to move waste, climate, geology, hydrogeology, surface hydrology, proximity of airports, demographics, land use, impact on the local community and economy. The ideal site to host a waste disposal facility is one that fulfils all these factors to the degree desired.

Despite the enormous complexity and intricate number of influencing factors in a landfill, the efficiency of compacted clay liner systems is still a critical issue. A study on the geochemical parameters that influence attenuation is necessary to fully describe the performance of the compacted clay liner systems. This study should consider the spatial variation of the geochemical parameters on the clay liner to effectively assess its performance and to identify possible sources of natural. This study will not be complete without considering that the distribution, mobility and biological availability of chemical elements depend not simply on their concentration but, critically, on the chemical form, or species, that occur in natural systems. As a result, the attenuation effectiveness will vary with different elements and compounds.

Based on the above considerations the objectives of this research were identified as follows:

- Characterise a number of geochemical parameters on the clay liner
- Describe spatially the geochemical parameters of the clay liner
- Characterise the species of a number of specific elements
- Describe spatially the species of the elements chosen
- Assess the performance of the clay liner

This study focussed on a real containment landfill site, the L-field site at Stewartby, Bedfordshire; managed by Shanks & McEwan (Southern Waste Services) Limited. The L-field site is an old (nineteen years) above-ground composite containment landfill, partially filled and has a compacted clay liner system made of weathered Oxford Clay.

The geochemical parameters characterised were soil pH, cation exchange capacity (C.E.C.) and exchangeable cations, clay content, iron/manganese hydrous-oxide, organic matter content and acid/base neutralisation potential.

The heavy metals considered initially were: chromium, copper, cadmium, lead, nickel and zinc. The selection of these was based on the regulated metal concentrations in soils, previous environmental studies and potential toxicity. The heavy metals finally selected were copper, chromium and zinc; the others were omitted mainly due to analytical complications.

The research approach was as follows:

I. ***Collection of information*** on the L-field site included historical information about the site, water supply, rainfall and drainage rates and geology

II. ***Exploratory sampling*** was carried out using a random collection pattern on a slope of an uncompacted Lower Oxford Clay and liner. The samples collected were mainly used to try the first proposed analytical methods and techniques, which were:

* Preparation of trace-element solutions for inductively coupled plasma mass spectrometry (ICP-MS) analysis using an HF-$HClO_4$ method of digestion
* Common single extraction scheme for soil analysis using 0.05 mol/l EDTA and 0.43 mol/l acetic acid; using ICP-MS
* Tessier *et al* (1979) sequential extraction method, using ICP-MS

* Mineralogical composition for bulk rock and clay fraction by X-ray Diffraction (XRD)
* Soil pH by measurement in water

The analytical methods and techniques were chosen based on the results from the exploratory sample determinations. A sampling protocol to carry out the detailed sampling was also proposed

III. ***Detailed sampling*** was carried out following a regular grid pattern with thirteen metre interval to the south-west and ten metre interval to the north-east. 27 samples and eight sampling duplicates were collected from the area covering a total of 4800 square metres. The chemical analyses used to characterise geochemical parameters were as follows:

* Clay content and iron/ manganese hydrous-oxide content were calculated from the mineralogical composition using XRD
* Organic carbon content was determined by weight loss-on-ignition method
* Soil pH was determined by the 0.01 M calcium chloride ($CaCl_2$) method
* The cation exchange capacity was determined by the method developed by Amrhein and Suarez (1990) for soil containing carbonates

The geochemical parameters were selected to the bound form of the selected heavy metals as determined by sequential extraction (Tessier *et al*, 1979) and ICP-AES. The sequential extraction performance was confirmed. The total concentration of these metals was determined using the HF-$HClO_4$ method and ICP-AES.

When enough values of the geochemical parameters and the populations of the operationally defined metal species were determined, a statistical/geostatistical methodology consisting of three stages was applied, as follow:

- Descriptive statistics, summary statistics and histograms were prepared for each population.
- Test of normality, each population was tested for normality using the Kolmogorv-Smirnoff test. If the population departed from normality, a Box-Cox transformation was applied.
- Geostatistical treatment, directional experimental variograms were prepared for each population data set; followed by model fitting that describe the spatial variability shown in the directional experimental variograms. The next step in the geostatistical treatment was the crossvalidation process, in which estimated and observed values were compared and the differences (better known as errors) among these populations,were calculated. The last step in the geostatistical treatment was the analysis of errors. When a population was transformed, both populations (the original and the transformed) were geostatistically treated and both were compared during the error estimate analysis. The population with the better performance of error estimates was chosen for interpretation

When insufficient data were obtained, Bayesian probability was applied to the results to calculate a posterior probability given an observed ocurrence of an event.

For the exchangeable cations and CEC, rank correlation coefficients were calculated.

Finally, a brief study on the best way to determine cation and anion concentrations in the the soil solution was carried out. Cation content was determined using ICP-AES and UV-visible spectrophotometry. Anion content was determined using ion chromatography.

IV. ***Interpretation of results***. Natural hazards that could represent a risk to the effective containment of waste were identified, mainly the oxidation of the pyrite layer at the bottom of the landfill cell and the effects of solubilisation on metals. The continuity of geochemical parameters that control attenuation was spatially described and the performance of the compacted clay liner was assessed

Through this study it was possible to:

- Identify the risk due to a natural hazard such as the oxidation of a pyrite layer underneath a compacted clay liner system in a containment landfill
- Describe spatially the geochemical parameters that influence attenuation in a compacted clay liner system
- Use the spatial description of geochemical parameters as a tool to assess the attenuating role of clay liners
- Identify the impact of the geochemical parameters on operationally defined species of copper, chromium and zinc in a compacted clay liner
- Describe spatially the operationally defined species of copper, chromium and zinc bound to compacted clay liner pools

This thesis describes the above study. The structure as presented in the document is as follows:

Chapter 2 presents a general review of waste generation, management and regulation; containment landfill; the compacted clay liner system; the sampling methods commonly used on soil surveys; the chemical analytical methods usually applied on soil studies, particularly sequential extraction and the soil solution determination; and the spatial variability and geostatistics as a tool to model it. This last topic includes a more detailed review on basic geostatistical concepts. Chapter 3 gives the most

relevant information on the L-field site. Chapter 4 presents the sampling techniques and chemical methods used on samples collected during the exploratory campaign. Chapter 5 provides a detailed explanation of the chemical analysis, procedures, results and modifications (when needed) of methods to determine geochemical parameters and heavy metals on samples taken during the assessment campaign. Chapter 6 shows stability diagrams for the major minerals components of the compacted clay liner and inorganic species in solution; this chapter includes a quantification of the main inorganic species in the soil solution extracted from the compacted clay liner. Chapter 7 shows the statistical and geostatistical treatment of data and results. Conclusions are given in chapter 8.

Chapter 2. General Review

2.1. Introduction

All the topics considered important for the research described in this thesis are presented in this chapter. Thus, an overview of waste disposal is briefly introduced, before giving a more detailed description on landfill as an option for waste disposal. After these two topics are reviewed, a section dedicated to the use of clay as a liner system is presented. A description of the main soil sampling concepts to take into account when characterising the clay properties is presented afterwards. A summary of the sample preparation follows the sampling section which is followed by a review of chemical analyses used to characterise the reactivity of heavy metals in soil samples. Soil solution characterisation is given as an independent section from the chemical analysis, to emphasise the importance of the soil solution on the chemical speciation of heavy metals. Finally a review of spatial variability, and geostatistics as a tool to describe its pattern is presented.

2.2. Overview of waste disposal

The production of waste is a natural consequence of life in an industrialised society. While living in a such a society, all of us are involved in generating waste. In general terms, anything which is discharged is presumed to be a waste, unless the contrary is proven. In scientific, engineering terms; "waste is any substance which constitutes a scrap material or an effluent or other unwanted surplus substance arising from the application of any process; and any substance or article which requires to be disposed of as being broken, worn out, contaminated or otherwise spoiled" (Ball and Bell, 1994). There are several types of classification of wastes, depending on: the generating source,

the legal regulations, the characteristics of the waste and the attitude of the person or authority responsible for disposing of the waste.

Waste generation, however, is not a recent phenomenon and it has been around with us since the evolution of mankind. Until the nineteenth century, the different types and more importantly the volume of waste was not posing a problem and dumping places were the recurrent solution. Ideas such as the possibility of land contamination was not considered. Since the late nineteenth century, the volume and hazardous nature of waste generated has increased considerably, and has led to the development of several waste management options, each of them related to specific pollution problems. The actual trend in waste management tends to waste minimisation, followed by recycling and then by safe disposal in the following order of preference: combustion as fuel, incineration and landfill (Hester and Harrison, 1995). At present, waste management is still struggling between the recycling and re-use stage, and the safe disposal stage. Among the available alternatives already in use are: incineration, chemical transformation, biological treatment and landfilling. With the exception of landfilling, the other options are still costly to implement and maintain. The most cost-effective way, so far, has been landfilling, which is the prime means of waste disposal. As a result, the regulations relating to landfill design, management, and closure and aftercare have also been increasing. In the United Kingdom there are approximately 4000 licensed landfill sites where approximately 85% of controlled waste and 70% of hazardous waste are disposed (Hester and Harrison, 1995).

2.3. The landfill system

A landfill is "the engineered deposit of waste onto and into land in such a way that pollution or harm to the environment is prevented and through restoration, land provided

which may be used for another purpose" (Skitt, 1992). The so called engineered deposit, which can be a cavity naturally occurring or excavated specifically for the purpose of landfilling, is covered with layers of liner followed by waste and then driven over with compacting equipment, to be followed with a cover material. A completely covered compacted solid waste unit is called a cell.

Waste, does not stop being a source of concern after being deposited in a landfill site. Waste will be modified by physical, chemical and biological processes once in the landfill. The transformation effect of these processes, plus the water -either contained within the solid waste; or that entering in the landfill and migrating through the wastes- produce a liquid called leachate. Tables 2.1. gives results for leachate analysis where parameters show differences between acetic and methanogenic phase. Table 2.2. shows results for the leachate analysis where parameters did not show any difference between phases.

Table 2.1. Leachate analysis (parameters with differences between acetic and methanogenic phase) (Ehrig, 1988).

	acetic	**phase**	**methanogenic**	**phase**
	average	*range*	*average*	*range*
pH (-)	6.1	4.5 - 7.5	8	7.5 - 9
BOD_5 (mg/l)	13000	4000 - 40000	180	20 - 550
COD (mg/l)	22000	6000 - 60000	3000	500 - 4500
BOD_5/ COD (-)	0.58	-	0.06	-
SO_4 (mg/l)	500	70 - 1750	80	10 - 420
Ca (mg/l)	1200	10 - 2500	60	20 - 600
Mg (mg/l)	470	50 - 1150	180	40 - 350
Fe (mg/l)	780	20 - 2100	15	3 - 280
Mn (mg/l)	25	0.3 - 65	0.7	0.03 - 45
Zn (mg/l)	5	0.1 - 120	0.6	0.03 - 4

COD, chemical oxygen demand; BOD_5, biochemical oxygen demand (determination of oxygen levels over a period of five days)

Table 2.2. Leachate analysis (no difference between phases could be observed) (Ehrig, 1988).

	average	*range*
Cl (mg/l)	2100	100 - 5000
Na (mg/l)	1350	50 - 4000
K (mg/l)	1100	10 - 2500
alkalinity (mg $CaCO_3$/l)	6700	300 - 11500
NH_4 (mg/l)	750	30 - 3000
orgN (mg/l)	600	10 - 4250
total N (mg/l)	1250	50 - 5000
NO_3 (mg N/l)	3	0.1 - 50
NO_2 (mg/l)	0.5	0 - 25
total P (mg/l)	6	0.1 - 30
AOX (µg Cl/l)	2000	320 - 3500
As (µg/l)	160	5 - 1600
Cd (µg/l)	6	0.5 - 140
Co (µg/l)	55	4 - 950
Ni (µg/l)	200	20 - 2050
Pb (µg/l)	90	8 - 1020
Cr (µg/l)	300	30 - 1600
Cu (µg/l)	80	4 - 1400
Hg (µg/l)	10	0.2 - 50

AOX, adsorbable organic halogen

The chemicals contained in the leachate may eventually escape from the landfill base and become potential groundwater contaminants.

Leachate is not the only end-product of degradation within a landfill, gas (methane) will be generated as well. Three trophic groups of anaerobic bacteria are required for the production of methane from biological polymers (cellulose, hemicellulose and protein) (Wolfe, 1979). The first group are hydrolytic and fermentative microorganisms, which are responsible for the hydrolysis of biological polymers and for the fermentation of the initial products of the hydrolysis process (soluble sugars, amino acids, long chain

carboxylic acids and glycerol). The fermentation products generated by the action of hydrolytic and fermentative organisms are short-chain carboxylic acids, alcohols, carbon dioxide, hydrogen and acetate (a direct precursor of methane). The second group of bacteria involved in the production of methane from biological polymers is the obligate proton reducing acetogens, these oxidise the fermentation products produced by the first group of bacteria to acetate, carbon dioxide and hydrogen; the conversion of fermentation intermediates like butyrate, propionate and ethanol is only favourable at very low hydrogen concentration, this is when the obligate proton-reducing acetogenic bacteria can function in syntrophic association with a hydrogen scavenger such as sulphate reducing organism. The third group of bacteria are the methanogens, they can use only a limited number of substrates including formate, methanol, methylamines, hydrogen plus carbon dioxide and acetate (Wolin and Miller, 1985). Methanogens are important in anaerobic digestion, because they (Zeikus, 1980):

- control the pH of their ecosystem by the consumption of acetate
- regulate the flow of electrons by the consumption of hydrogen, creating thermodynamically favourable conditions for the catabolism of alcohols and acids
- excrete organic growth factors including vitamins and amino acids which are used by other heterotrophic bacteria in the ecosystem

The production of methane from acetate yields only 31 kJ/mole CH_4 produced. The conversion of hydrogen and carbon dioxide to methane yields 135.6 kJ/ mole CH_4 produced. Thus, the production of methane is more favourable when it is produced from hydrogen and carbon dioxide. The methanogens are most active in the pH range 6.8 to 7.4 (Zehnder, 1978).

It can be seen that both gas and leachate depend on the contents of the landfill, the local climate, and the design, construction, operation and management of the facility

itself. Regulations in relation to landfill contents change in different countries. For example, in most European countries with the exception of Britain, regulations have become strict on hazardous waste and disposal without previous treatment is prohibited (Daniel, 1993). However, there are still numerous landfills with mixed contents inherited from times before more strict regulations were introduced. In Britain, the co-disposal policy has typically been followed (Ball and Bell, 1994). Co-disposal is the calculated and monitored treatment of industrial and commercial, liquid and solid wastes by interaction with biodegradable wastes in a controlled landfill site (Skitt, 1992).

In terms of landfill design and management, three major principles have been recognised (Hester and Harrison, 1995):

- Dilute and attenuate was the most used principle of landfilling until 1980. It had little or no engineering on site, and leachate was allowed to migrate to the surroundings. There, all responsibility fell on the attenuating properties of soil and dilution by groundwater
- Containment is the most accepted principle of landfilling nowadays. It has a higher degree of engineering with the objective of containing wastes long enough to allow biodegradation and attenuation processes to take place. However, because there is no known material perfectly impermeable to all constituents in a leachate, this will migrate from the landfill base. Even in the most sophisticated engineering sites; releases to the environment will occur
- Entombment, is based on the containment principle but differs in that waste, rather than being disposed of, is stored indefinitely in a relatively dry form, thus preventing the release of degradation products to the environment. The ultimate objective is to gain time until effective new technologies are developed

A more detailed review on containment, the most acceptable principle of landfilling design and management, will be carried out in the remaining paragraphs. Bearing in mind that not all containment systems are the same, local and national regulations are expected to introduce changes depending on the landfill location. Thus, the selection of the landfill location should be the very first concern. Once the location has being chosen, the next concerns would be:

- *Design of the landfill itself.* A general idea is that landfills are all below-ground, making use of old quarries. This is very common, but not the only possibility for containment of wastes. Landfills could be above-ground or above-and below ground. The above ground design is better for sites with shallow water-tables; the construction of liners and drainage is easy because it will be made almost at ground level and leachate can be drained by gravity. Above-and below design have the advantage of allowing more waste to be disposed, make use of construction material from the excavation to bury waste, and permit the use of a place with a relatively flat surface after closure
- *Liners* are natural or synthetic materials, the purpose of which is to act as environmental protection. They serve as a hydraulic barrier to the flow of fluids. To do so, they must have low hydraulic conductivity for long periods of time. They act mainly on retaining the leachate. Among the natural material used, three types could be identified: naturally occurring clay liners, compacted clay liners and geosynthetic clay liners. In addition there are several types of synthetic material to make up geomembrane liners such as: high density polyethylene, very low density polyethylene, chlorinated polyethylene, chlorosulphonated polyethylene, ethylene interpolymer alloy, polyvinyl chloride. Both natural and synthetic liners differ in their chemical, mechanical and physical properties and the way they enhance

protection to the environment. For example, clay liners have inherent attenuation capacities, are relatively stable to organic and inorganic compounds, are not as impermeable as synthetic liners are, however, these last ones are sensitive to organic compounds. In most developed countries both types of liners are used to optimise complementary properties. The system based on the mixed use of liners is called "composite" landfill liner system. There is one more system, the multiple layer system which, besides multiple liners, includes monitoring layers. It is increasing in popularity in U.S.A. and some parts of Europe, despite the known problem of layers slipping due to sheer forces or the associated risk of using a permeable layer as monitoring system

- *Collection and removal systems* could be separated into four types each with regulated technical characteristics: primary leachate collection system (PLCS), secondary leachate collection system (SLCS), surface water collection system (SWCS) and methane gas collection (MTG)

  PLCS consists of a drain (made of gravel), filter (usually made of geotextile), sump and removal manhole/pipe. SLCS is used in systems having double liners, where between them, the SLCS or "leak detection liner" is installed. It has the same components as the primary liner and is highly influenced by it. For example, when the primary one is a geomembrane the leak detection liner could be made of gravel or a geonet. The SWCS is built in the landfill cap after closure. It consists of a drain sheet (made of gravel or composite liner) protected by a filter (sand or geotextil, depending of the drain material) and a removal system at the perimeter of the facility (perforated pipe or geocomposite edge drain). MTG consists of drainage layer (sand or geotextile), vent, flare or gas collection and piping system

- *Monitoring systems*. The design, frequency, extent and type of monitoring systems will depend on waste composition and volume, rate of gas produced, surrounding geology and legal requirements
- *Cover system*. The purpose of the cover system is particularly to restrict infiltration of water into the waste. Other secondary objectives are to separate buried waste from surface environment and the control release of gas from the waste. The most common components of the cover system are: surface layer, protection layer, drainage layer, barrier layer and gas collection layer, made of natural or synthetic material. Their life time will depend highly on the nature of waste, the site hydrology and maintenance. The most critical component of the cover system is the barrier layer, because it is the one that would minimise percolation

The above paragraphs outlined the most common principles of landfill design, the main end-products of degradation within the landfill and the three major principles of landfill management. Now, the future of the facility once the operational phase is completed should be considered.

The post-operation phase should last until the landfill has stabilised. The point of landfill completion varies in different countries. In Britain, the statutory guidance is the "Waste Management Paper 26A" (Landfill Completion) (Department of the Environment, 1993), in which criteria for leachate are given to decide if the landfill has reached the completion stage. This is defined as "that point at which a landfill has stabilised physically, chemically, and biologically to such a degree that the undisturbed contents of the waste are unlikely to cause pollution to the environment or harm to human health. At completion, post-closure pollution controls, leachate management, and gas-removal systems are no longer required" (Department of the Environment, 1993). The criteria for leachate are based on the Drinking Water Directive (80/778/EEC)

(Commission of the European Communities), assuming at least ten-fold dilution of the leachate within an aquifer. There are more factors to be satisfied prior to completion such as present and future quality and volume of leachate, flow and concentration of gas, future impact and generation of degradation products, instability of and presence of waste that could represent a hazard in future.

The regulatory legislation which helped to minimise the polluting effects caused by waste disposal are as follows in chronological order (Walker, 1991): Town and Country Planning Act 1971; Deposit of Poisonous Waste Act, 1972; Control of Pollution Act, 1974; EEC Directive (80/68/EEC) on the protection of Ground Water against Pollution caused by Certain Dangerous Substances; The Collection and Disposal of Waste Regulations, 1988; The Water Act, 1989; The Environmental Protection Act, 1990.

The future for landfill as a waste disposal option is uncertain as current regulations tend in other directions such as waste minimisation. Landfilling still remains an essential waste management option, for which new concepts such as "sustainable" and "fail-safe" are being developed. Policies on degradation acceleration or waste pre-treatment prior to landfill are already available and even waste separation is proposed as a way to control degradation products.

2.4. Focus on clay liners

Each issue related to containment landfill could be a research topic by itself, and many have been. Improvements on landfill design and management have come from a better understanding of the mechanisms controlling phenomena such as waste degradation or attenuation capacity of soil. Leachate remains a critical matter in landfill containment and one relies on the performance of liners as effective tools. It is true that new materials have been developed and used, but economical and political factors are perhaps the most

important aspects for the liner system choice. A real scenario related to landfills in Britain is a co-disposal containment with a system of compacted clay liners, known as lift. A clay liner is so called, not because it is entirely made of clay, but to emphasise that it is the clay that is the material largely responsible for the low hydraulic conductivity (Daniel, 1993). Compacted clay liners are made commonly of natural soil material, however processed material such as bentonite or even synthetic material can be incorporated. These materials should comply with the following minimum requirements:

- Hydraulic conductivity $\leq 1 \times 10^{-9}$ cm/s
- Percentage fines $\geq$ 20-30 %
- Plasticity index $\geq$ 7-10 %
- Percentage gravel $\leq$ 30 %
- Maximum particle size: 25 -50 mm

Percentage fines is the percent by dry weight passing the US No 200 sieve, with openings of 75 μm. Plasticity index criteria is determined according to ASTM D4318. Percentage of gravel is the percent by dry weight retained on a No 4 sieve with openings of 4.76 mm.

The construction process of clay liners consists of following parts (Daniel, 1993):

- *Material processing*, where lumps of material are broken down, stones are sieved out, soil is moistened and additives such bentonite are incorporated. An important part in this step is to moisten the soil to a certain point; when soil is dried water can be added and should be mixed uniformly,. Soil should be dried uniformly if it is wet. The process of hydration/dehydration usually takes from 2 to 3 days. Frozen soil should not be used to construct clay liners (Figure 2.1)

- *Surface preparation*, this should be rough, rather than smooth, between overlying and underlying lifts to assure an effective bonding
- *Soil placement*, in here soil is placed on lifts, special importance is put to control the soil thickness layer to less than 230 mm. Small quantities of water are usually added to the composition to recover water losses in the process (Figure 2.1)
- *Compaction* is used to homogenise the soil into a mass free of voids. The water content of soil and the compaction method are critical factors for the future performance of compacted liners (Figure 2.1)
- *Protection*, once compacted the lift should be protected from desiccation and freezing that can cause cracking of clay and increase hydraulic conductivity. This can be avoided if the lift is temporally covered with a plastic sheet until used, if the surface is left in an impermeable state or if the lift is regularly moisten

The clay liner has the ability to interact geochemically with the leachate. The result of this interaction, known as attenuation, should lead to partial or total immobilisation of potential groundwater contaminants (Daniel, 1993). Attenuation by sorption is often the most important process controlling the behaviour of contaminants in the subsurface (Piwoni and Keeley, 1990). However, the degree of attenuation accomplished by sorption depends to a large extent, but not only, on the clay characteristics. The contaminant characteristics and the transporting fluid media characteristics also influence the attenuation processes.

The **clay properties** that affect attenuation can be divided in two categories : physical and geochemical properties. The physical properties in question, permeability/porosity, texture and homogeneity, are achieved during the construction of liners. Actually there is extensive testing of the quality and extent of these parameters before and after

construction of clay liners. The geochemical parameters that can affect the attenuation are: clay content, cation exchange capacity and exchangeable cations, iron and manganese hydrous-oxide content, organic carbon content, soil pH and acid/base neutralisation potential (Daniel, 1993). The overall effect of these parameters determine the material attenuation capacity. The possible chemical interactions that may occur in the compacted clay liner are usually evaluated through laboratory tests (sequential batch-contact, column percolation and biochemical test), and field tests (for example lysimeters).

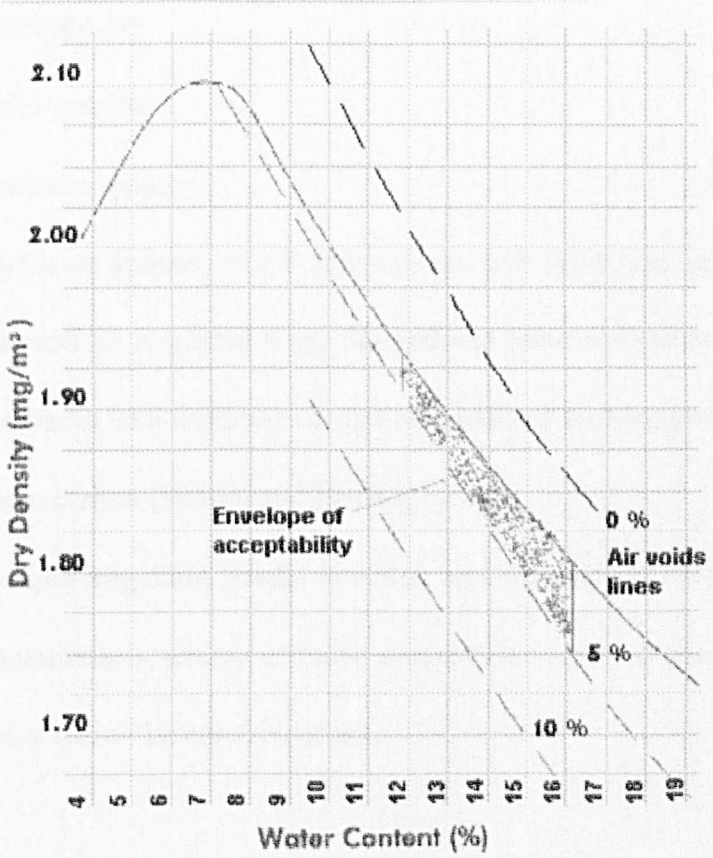


Figure 2.1. Typical envelope of acceptability for placed and compacted clay in terms of moisture content and dry density at which appropriate permeability requirements are met (Parker and Rae, 1998)

The **contaminant properties** that affect sorption depend upon the contaminant types. Numerous tests have been carried out to predict the chemical attack of liquid on clay

liners. For example, acid and alkaline liquids can dissolve the components in the clay, create channels and increase hydraulic conductivity. Inorganic liquids may influence the hydraulic conductivy of the clay liner due to their high conductivities. Organic liquids, sufficiently concentrated, can cause "syneresis" (flocculation of clay particles and crack of soil) due to its low dielectric constant.

If contaminants are classified in groups that consider the mobility properties of the contaminant, rather than in general categories as organic or inorganic ones, then three general groups can be identified:

- Ionic or charged species
- Uncharged polar species
- Uncharged nonpolar species

The chemical forms or species of the contaminant will determine the sorption and hence mobility in the soil. In a general way, charged and polar compounds interact with charged and polar surfaces, and nonpolar compounds interact with nonpolar components of soil, usually organic carbon (Piwoni and Keeley, 1990).

The primary **transporting fluid media** is water, and its characteristics can influence the behaviour of contaminants, mainly of those susceptible to gain or loss a proton. The characteristics of the water to be considered are:

- pH
- Salt content
- Dissolved Organic Matter
- Redox potential

Several parameters should be considered when describing the sorption of contaminants by the clay liner. To focus on the research described in this thesis, the

sorption of metal ions by soils and their constituents will be reviewed in the following paragraphs.

Among the mechanisms involved with the sorption of heavy metals by soil, the following four mechanisms should be mentioned:

- ***Cation exchange*** or non specific adsorption. Exchangeable sites for cations are permanent negative charge on 001 faces of clay minerals. Cations are sorbed to 001 faces mainly by coulombic forces, keeping their hydration spheres more or less intact (Figure 2.2). Water molecules take part in the bonding of H-bonds with surface O atoms (McBride *et al*, 1991). The strength of the binding increases when the hydratation sphere decreases. The exchange of cations bound to 001 faces sites will depend on the cation nature, the clay surface, concentration of cations to be exchange and environmental conditions.
- ***Specific adsorption*** or surface complexation. Sites for cations are transitory negative charges produce by the reversible, pH-dependent dissociation of H^+ from amphoteric surface OH groups of oxides and edge faces of clay minerals. Cations are bound directly to surface OH groups and O atoms, which work as ligands and displace water molecules from the dissolved metal cations by ligand exchange and forming bridges linking the cations to structural cations in the mineral (Figure 2.3). Bonds are intermediate between ionic and covalent. Specific adsorption is not easily reversible, however cations specifically sorbed can be substituted by other cations (Pickering, 1979). Selective sorption correlates with metal hydrolysis, stability and degree of covalence of the metal, pH and structure and composition of the mineral (Parker and Rae, 1998; Harmsen, 1977).
- ***Co-precipitation***. This mechanism is similar to sorption, the main difference is that sorbed metals are assimilated into a growing mass of oxide as it precipitates. Oxide

stability depends on Eh, pH and complexing agents. Metals that are co-precipitated are not easily released back into solution unless environmental conditions change causing solubilisation of the oxide (Parker and Rae, 1998)

- ***Organic complexation***. Metal adsorption on soil organic matter shows similarities with the chemisorption or specific adsorption mechanism (McBride, 1994). Some metals coordinate directly to soil organic matter functional groups, forming strong ionic and covalent bondings, a further contribution to the stability in metal-organic matter complexes is the "chelate effect", that is the entropy created by the complexing reaction. The metal selectivity for organic matter depends on:

1. The chemical nature of the organic ligand (functional group). Soil organic matter has many different functional groups, such as carboxylic, phenolic, amine, carboxyl, and possibly sulphydryl.
2. The degree of adsorption on the organic matter. A degree of adsorption preference can be established if soil organic matter ligands are classified as Lewis bases (O>N>S), and metal cations as Lewis acids.
3. pH. Metals compete with H^+ for bonding on functional groups
4. The ionic strength of the solution. This will determine intensity of competition by other cations for the complexing sites

Because metals are strongly bound to soil organic matter, they are most slowly desorbed. A large activation energy may be needed to break the ligand-metals bond.

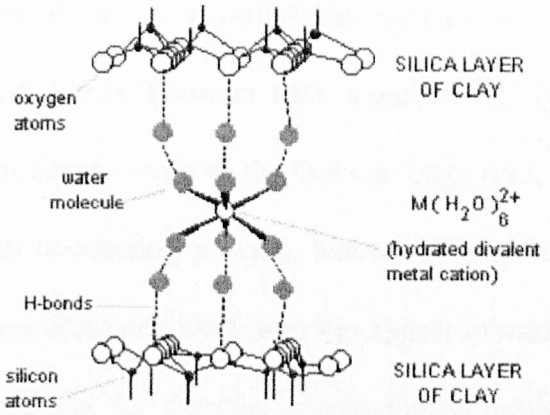


Figure 2.2. The adsorption of an hydrated divalent metal cation $[M(H_2O)_6^{2+}]$ by the interlayer surfaces of montmorillonite (McBride *et al*, 1991).

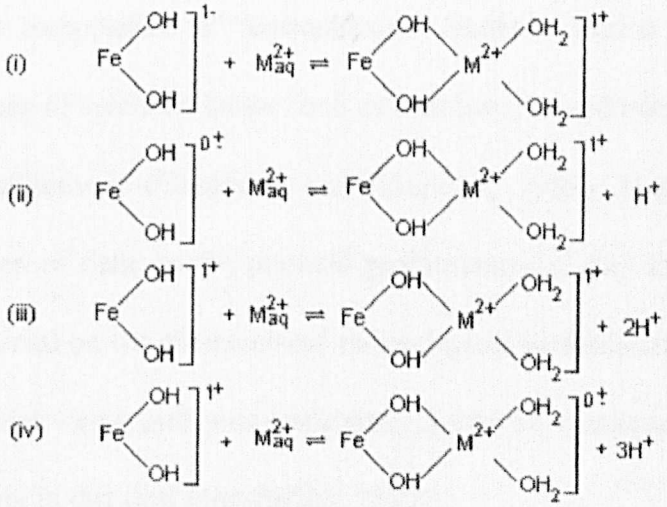


Figure 2.3. The specific sorption of divalent heavy metals by Fe oxide (McBride *et al*, 1991).

In the above paragraphs, the construction, technical details and metal binding mechanism in compacted clay liners have been reviewed. A logical thought could be to question the reliability of these liner systems.

Hydraulic conductivity of clay as a barrier has been extensively described for real scenarios (Quingley *et al*, 1986), however little attention had been paid to chemical properties of the clay, this could be due to the fact that clays used as landfill liners are at the end of the geological weathering process; hence, the clays chosen as barriers are believed to be largely inert. Research work into the impact of various chemicals on clay minerals have been carried out for decades. Contradicting results are reported; some authors showed that acids dissolved aluminium, iron, alkali metals and alkali earths from clay minerals whereas bases dissolved silica (Daniel and Liljestrand, 1984). The impact of organic compounds on the increase of effective permeability has also been reported (Brown and Thomas; Johnson *et al*, 1989). On the other hand, some authors have reported no major alterations in the liner occur on exposure to leachate (Peters, 1993; Quigley *et al*, 1986). Nowadays, it is widely accepted that clay liners are generally compatible with the composition of "conventional" leachate (Parker and Rae, 1998). More than this, the use of synthetic liners, such as bentonite, in addition to clay liners are reported to work effectively (Grantham and Robinson, 1988). Despite the steadily growing accumulation of data on the physical performance of clay liners, only limited studies have been carried on the chemical and mineralogical performance of clay liners in short, long and spatial terms and more research should be developed to clarify and increase understanding in this field (Batchelder, 1995).

2.5. Soil sampling

Before performing a chemical analysis to characterise clay properties, sampling must be carried out to collect representative samples of the soil under investigation. However, it is not an easy task to assess the representativeness of samples because soil is a dynamic system, subject to short-term fluctuations that could affect the form and biovailability of

elements (Alloway, 1990). Soil can show marked spatial variability in physical and chemical properties at the macro and micro-scales, thus emphasising the need for thorough sampling to include the range of variance in parameters. Soil properties vary not only from one location to another but also among the horizons of a given profile (Sparks, 1996). Thus when sampling soil populations it is necessary to divide them, both horizontally and vertically.

The sampling plan has the objective to design which units of the population are to be included in the sample (commonly a soil volume). There are always a number of different plans or designs available, some more precise or cost-effective than others. In general the best sampling design is one that provides the maximum precision to the lowest cost (Sparks, 1996).

Some types of soil sampling are given below:

Simple random. This is the most commonly used and simplest method. It is based on equal and independent probability of sampling units to be drawn. The location of the point at which each sampling unit will be taken is often reached in two steps (Sparks, 1996). The first one serves to chose approximately one point in the field. To do so a map of the area should be prepared and two base lines at right angles which intersect at an arbitrary origin should be established. A scale should be defined. Two random numbers should be drawn, and locate the intersection of the two distances in the field as the approximately sampling point. The second step in getting a simple random sample is to take the first point as the origin of a new coordinate system and a second random coordinate is measured off to select an exact sampling point. If more than one sampling unit is included in the sample, the random sample gives a mean and variance estimate of the sampling error, as follows:

$$\bar{y} = \frac{\sum_{i=1}^{n} y_i}{n}$$

$$V_y = \frac{\sum_{i=1}^{n} \left(y_i - \bar{y} \right)}{n(n-1)} = \frac{s^2}{n}$$

where:
y_i is the value observed for the ith sampling unit
n is the number of unit samplings

$\bar{y}$ is the mean

$V_{(\bar{y})}$ is the mean variance

Confidence limits can be calculated once the variance is known, as usual:

$$L = \bar{y} \pm t_\alpha \sqrt{\frac{s^2}{n}}$$

where:
L is the confidence limit
t_α is the Student's t with (n-1) degrees of freedom at the α probability level

Knowing the mean variance allows an estimate of the number of samples to collect in future sampling to obtain a given precision with a specified probability, using:

$$n = t_\alpha^2 \frac{s^2}{D^2}$$

where:
D is the specified limit

The simple random model is often a satisfactory method when sampling highly homogeneous fields. However if the variance is known, a more suitable method can be applied (Tan, 1996).

Stratified random, in this type of sampling, a whole population is broken into subpopulations, and a simple random sample is taken from each one. It is mainly applied to heterogeneous fields; the objective being to improve the precision level. At least a

couple of samples should be taken from each strata. The mean and variance estimate are given by:

$$\bar{y} = \frac{\sum_{h=1}^{L} N_h \bar{y}_h}{N}$$

$$V_y = \frac{1}{N^2} \sum_{h=1}^{L} N_h^2 \left(\frac{s_h^2}{n_h} \right)$$

where:
N_h is the total number of units in the hth stratum
L is the total number of strata

Systematic sampling. The selected units are at regular distances from each other, either in one or two dimensions (Sparks, 1996). If the population is one dimensional, the first unit is assumed to be selected at random from the first k units and subsequent units at each kth interval. If the population is in two dimensions the field is considered to be composed of strata of common size and shape. Systematic sampling frequently offers more accurate results than simple random sampling, because the samples are more evenly distributed over the population (Tan, 1996). The sample mean is calculated from each sample, and these means are treated as the data from the simple random sample size equal to the number of separately systematic data (Sparks, 1996). There are three popular designs:

- Regular grid
- Herringbone
- "W" design

In all sampling types, the error sources could be divided in three categories; sampling, selection and measurement.

Characterisation of the whole sample taken is not always cost-effective and subsampling should be made to estimate some characteristics of the larger sampling unit

without measuring the whole sample collected. However, it will decrease the precision because additional components of variation are introduced. One cost saving approach is to work on composite rather than simple samples. The procedure is based on collecting single samples that represent the population under study and mix them to form a bulk sample on which chemical analysis will be carried out.

The tools to sample include soil sampling tubes, augers and till spades or shovels, depending on the depth (shallow and deep) and types of sampling mechanisms.

2.6. Soil sample preparation

Once the sample has been collected, care must be taken to avoid contamination and prevent the occurrence of further chemical reaction taking place. Air drying is the most acceptable procedure for sampling preparation. This drying could be accelerated using air flow, but the temperature should not exceed 35 °C, because changes in physical and geochemical characteristics of soil had been reported (Hesse, 1972). This drying method however will impact on some properties of soil under study; for example redox sensitive elements, such as sulphur; will oxidise producing SO_4^{-2}; causing the pH to decrease. When this occurs and low pH values are obtained, it is recommended to carry out the characterisation on fresh samples.

Once the sample is dried it should be stored in a air-tight non-reactive material container; with the purpose of avoiding gases to be adsorbed onto the sample.

After drying, the next concern is to homogenise the sample, using grinding and sieving. The objective is that during subsampling every particle has an equal chance of being chosen by thorough mixing. The soil fraction passing through a 2 mm sieve is the internationally accepted for chemical analysis (Tan, 1996). The main errors found during the sample preparation stage are due to contamination by grinding or sieving, oxidation

of the sample and loss or gain of moisture. The last concern before analysis is to reduce the sample, either automatically (riffle sampler) or manually (quartering).

If volatile organic compounds (VOC) content is to be determined, the sample must be taken in a wide mouth glass container with a Teflon-lined septum cap, preserved at 4°C for up to 2 weeks prior to extraction and placed in separate plastic bags containing activated carbon, to check for diffusion of VOCs through the screw cap septum.

A final consideration is that despite the theories and established methods, which are all very idealised, problems are bound to be encountered when dealing with environmental sampling. This idealistic approach should be considered as useful guide to be adapted to a particular situation and its effectiveness should be monitored.

2.7. Chemical analysis to determine reactivy of heavy metals on soil samples

The most important chemical processes, affecting the behaviour and bioavailability of metals in soil are those concerned with the adsorption of metals from the liquid phase onto the solid phase (Alloway, 1990). These processes can involve the following mechanisms: cation exchange capacity, specific adsorption, co-precipitation, organic complexation, selectivity of adsorbents.

Immobilisation of metals by mechanisms of adsorption and precipitation, will prevent movement of the metals to groundwater (McLean and Bledsoe, 1992). Metal-soil interaction is such that when metals are introduced at the soil surface downward transportation does not occur to any great extent, unless the metal retention capacity of the soil is overloaded, or metal interactions with the associated waste matrix enhances mobility.

Multiphase equilibria must be considered when defining metal behaviour in soil (Alloway, 1990). Metals in soil solution are subject to mass transfer out of the system by

leaching to groundwater, plant uptake, or volatilisation (potentially important mechanism for volatile metals such as mercury). At the same time metals participate in chemical reaction with the soil solid phase.

The reactivity of heavy metals in soil can be described in terms of speciation and "localisation" of heavy metals in the different solid phases of soils. Speciation of heavy metals in soils can be defined in many ways. First, it can be defined as the extraction and quantification of a soil phase which is functionally designated in its element contents (i.e. the species extracted is defined by its role or function, for example, available to plants). Second, speciation can be defined operationally, i.e. by the extraction technique itself. The extractions are usually designed to extract elements associated or bound to a particular soil phase. However, in practice the soil phase may be ill-defined and the extracts not specific to the phase. The use of selective extractants to quantify the element content in a particular phase is based on the concept of "pools" in soils. Elements of different solubility and mobilities are bound to different pools, that can be selectively sampled by extractants of different strengths.

The extraction scheme should combine both features, to obtain adequate recovery and to prevent losses, especially destruction of the analyte. If standard addition is applied to test recovery, it should be considered that the recovery of the spike does not always correspond with the analyte of the sample.

In order to assess the reactivity in solid soil, both single and sequential extraction procedures are being applied, and are being proposed as methods of measurements in the European Community (Ure *et al*, 1993; Quevauviller and Maier, 1994). An extensive review on metal speciation in solid matrices is given by Das *et al* (1995), where performance of sequential and selective extractions is discussed and a list of major techniques for the characterisation of chemical species in various matrices is given.

Among these techniques are atomic absorption spectrometry (AAS), inductively coupled plasma-atomic emission spectrometry (ICP-AES), X-ray fluorescence (XRF), neutron activation analysis (NAA), anodic stripping voltametry (ASV), X-ray diffraction (XRD), infrared and raman spectrometry, nuclear magnetic resonance (NMR), mass spectrometry (MS), mössbauer spectrometry, circular dichroism, molecular ultraviolet absorption and luminescence. Separation techniques in speciation analysis for organometallic species have been extensively described in literature (Szpunar-Lobinska *et al*, 1995). Despite the reported disadvantages of the sequential extraction procedures, such as non-selectivity of the chemical reagents used in the methods (Bermoind, 1992; Xiao-Quan and Chen, 1993; Bermoind *et al*, 1998), operational simplicity and rapidity renders it most suitable for routine species identification. However, the distribution of a given metal between various fractions can be only considered as operationally defined by the method of extraction (Lake *et al*, 1984). In order to assess the performance of chemical extractants used for the partitioning of trace metals species in oxidised estuarine sediments, a statistical approach had been proposed (Luoma and Bryan, 1981). Continuing with the assessment of the partitioning of trace metals in sediments using a sequential extraction procedures, factors that affect this partitioning have been described (Rapin *et al*, 1986). A final work on assessing sequential extractions, that should be mentioned, is one that proposes a dynamic analysis on the partitioning of heavy metals using a sequential extraction method. It considers an approach in which kinetics versus equilibrium rates should be established for the speciation of metal complexes with ligands from soil and water (Langford and Cook, 1995).

When trying to speciate heavy metals in soil the problems are not only due to non-selectivity of reactants used during the sequential extraction procedure. Changes in chemical speciation can take place during the sampling, or even during the transportation

of the samples to be speciated. Changes in the chemical speciation of heavy metals during reactive transport of samples have been studied and partial equilibrium models have been suggested to deal accurately with the variations (Liddell, 1994). Approaches to sampling and sample treatment for metal speciation in soil and sediment have been published previously (Rubio and Ure, 1993), and steps in quality control in speciation investigations have also been recommended (Michalke, 1994).

Among all the sequential extraction methods the best well known is the developed by Tessier, Campbell and Bisson (1979), many current methods were modified from this one. A summary of this method is given in Table 2.3.

Table 2.3. Tessier *et at* (1979) sequential extraction steps.

Fraction	Extraction period (hr)	Temperature (°C)	Extraction process
exchangeable	1	room	with 8 mL of magnesium chloride solution (1M $MgCl_2$, pH = 7.0) and continuous agitation
bound to carbonates	16	room	with 8 mL of 1M sodium acetate solution adjusted to pH 5.0 with acetic acid
bound to Fe-Mn oxides	6	96	with 20 mL of hydroxylamine hydrochloride in 25% (v/v) acetic acid with occasional agitation
bound to organic matter	2	85	with 3 mL of 0.02 M nitric acid solution and 5 mL of hydrogen peroxide 30 % solution adjusted to pH 2 with nitric acid
	3	85	After a second aliquot of hydrogen peroxide must be added
	0.5	room	After cooling 5 mL of 3.2 M ammonium acetate must be added and the sample must be taken to 20 mL and agitated continuously

2.8. The soil solution

Analysis of soil solution is a way of detailing analysis of whole soils or soil extracts. Soil solution chemistry focuses on the available fraction of chemicals occurring in the soil

environment, at any point in time and it is a useful predictor of mass transfer from the soil to other environmental compartments. The goal of the soil solution analysis is to give information of both a static and dynamic nature, for describing nature, direction, extent, and rate of chemical reactions. Soil solution is the aqueous liquid phase of soil at field moisture contents. It differs from soil water, the "moisture that fills the pores between soil particles", in that it represents the aqueous phase of the soil at or below field capacity (Wolt, 1994).

Measurement of soil solution chemical components *in situ* is not possible, due to its dynamic nature and variation with soil moisture content, especially in weakly buffered soils. Consequently, soil solution is often operationally defined by the particular method whereby it is obtained. Uncertainties regarding the physical origin of lysimeter water result in uncertain interpretations regarding chemical processes governing the chemical composition of lysimeter soil solution. In contrast, uncertainties concerning the contribution of soil solution in diffuse soil water - as measured by laboratory displacement of soil solution - result in uncertain conclusions regarding flux of solutes through the soil profile (Table 2.4). Plant nutrient availability, phytotoxicity, and soil metabolism are best related to chemical composition of diffuse water as reflected in composition of displaced soil solution. Considerations of chemical transport, however, are more clearly reflected in soil solutions obtained by lysimetry, provided the solutions obtained represent mobile water in the soil environment.

The parameters that have an overt controlling influence over chemical concentration, speciation, and activity in the soil solution (or master variables) (Wolt, 1994) are:

- Soil pH
- Ionic strength
- Redox potential

- Suspended colloidal matter

Table 2.4. Common laboratory method to obtain soil solution.

Technique	Method
Centrifugation displacement	Low-Pressure
	High-Pressure
Column displacement	Traditional
	Vacuum
	Syringe-Pressure
Pressure Membrane Extraction	
Saturation Extraction	Saturation Paste
Water Extraction	
Complexation and Exchange	Variable Mole Fraction
	Mass Balance/Iteration

Comprehensive soil solution analysis typically requires measurement of soil solution pH and the total concentration of major exchangeable cations and the anions that balance charge in the aqueous phase (Table 2.5.). Comprehensive soil solution analysis is necessary for applications where computational approaches are used to model ion speciation and free ion concentration, or activity, in soil solution. There are many chemical equilibria and reaction models available, such as: GEOCHEM-PC (Parker, 1997) and MINTEQA2/PRODEFA2 (Allison *et al*, 1991). These tools have an extensive set of thermodynamic data and are able to model important classes of reactions such as hydrolysis, complexation, dissolution/precipitation, oxidation/reduction, ion exchange and adsorption. There is a need to examine the validity of prediction of elemental speciation provided by various chemical models, and analytical schemes have been suggested (Loeppert *et al*, 1995).

Among the analytical techniques used to determine ions in soil solution, ion chromatography has proved to be efficient (Fernandez-Boy *et al*, 1998). Specific-ion electrodes have also been used to determine cadmium activities in natural waters and synthetic soil solutions (Gardiner, 1974). Comparison exercises have been carried out

previously among techniques, to determine which analytical techniques would be the more suitable to determine a specific cation activity in soil solution. For example, ion selective electrode and the Donan dialysis have been compared to determine copper activities in soil solution (Minnich and McBride., 1987). For cadmium activities in sludge-amended soil, four methods were compared and similarities were found for ion-selective electrode measurements and predicted values calculated by Geochem-PC (Candelaria *et al*, 1995).

Table 2.5. Ions of major interest in soil solution (Wolt, 1994).

Ion	Comments
	Major Exchangeable Cations
Ca^{2+}	Major Exchangeable Cations
Mg^{2+}	occur predominantly as exchangeable cations in soils; these ions are
Na^{+}	relatively easily manipulated by liming, irrigation, or acidification;
K^{+}	exchangeable Al^{3+} is characteristic of, though rarely the predominant
NH_4^{+}	exchangeable cation in, acid soils; productive agricultural soils are
$Al^{3+}(H^{+})$	rich in exchangeable Ca^{2+}
	Major Anions
NO_3^{-}	Present in considerably lower concentrations than the major cations in all but
SO_4^{2-}	the most coarse-textured and strongly saline soils, where they are essentially
Cl^{-}, F^{-}	equal; sulphate and nitrate are important nutrient sources for plants; sulphate
HCO_3^{-}, CO_3^{2-}	chloride and bicarbonate salts accumulate in saline soils.

The concentration of ions determined by analytical techniques are given in most of the cases as total concentrations, which should be corrected to actual ionic concentrations and ion activities in soil solution (Adams, 1971). Among the corrections, the ion-pair correction could be the most important when estimating activity coefficients in aquatic systems and soil extract from their electric conductivity (Griffin and Jurinak, 1973).

Correction of the concentration of ions because formation of species are not the only factor to consider when determining ionic activities in soil solution, the principal limitations on the determination of ionic activities in soil solution and suspensions had been described by Amacher (1984).

2.9. Spatial Variability

Physical and geochemical parameters that influence natural attenuation in clay liners and in soils in general have some location in space and are subject to changes in time. A set of data with a spatial correlation structure cannot be treated by classical statistics, because the assumptions of independence are not longer valid. These kind of data sets cannot be studied using a deterministic approach, because they are the result of complex systems with unknown leading physical and chemical properties. Geostatistics is concerned with data that fluctuate in space and/or time (Olea, 1991) and offers statistical tools to model spatial variability.

Introductory readings of geostatistical theory can be found in Issaks and Srivastava (1989) and Goovaerts (1997). More advanced theoretical geostatistical treatments are illustrated in Cressie (1993) and Journel and Huijbregts (1978). There are many computer-based tools to capture, manipulate, process and display spatially related data; the choice of a specific software will depend on the nature of the work carried out. GSLIB (Deutsch and Journel, 1998) is a powerful tool and maybe the most popular public domain geostatistical software and GEO-EAS (Englund and Sparks, 1991) is a introductory computer-based tool of geostatistical analysis.

Geostatistics has its origins in mining and has been used extensively in geology (Burgess and Webster, 1980a, 1980b and 1980c) and natural resources characterisation. However, there are other multiple applications in ecology (Robertson, 1987; Rossi *et al*,

1992), entomology (Liebhold *et al*, 1993)., agriculture (Viera *et al*, 1983; Lake *et al*, 1997; Husson, 1998), human and medical geography (Cliff and Ord, 1975; Gesler, 1986), and environmental sciences (Myers, 1997).

Prior to applying any spatial statistical treatment, descriptive statistics of the data set should be carried out. The objectives of doing so are to organise, present and summarise this set of data. One of the most common and useful presentations of data is the histogram, which can capture important data features by few summary statistics. These include the well known: measures of location (mean, median, mode, minimum, maximum, quartiles, quantiles), measures of spread (variance, standard deviation, interquartile range) and measures of shape (coefficient of skewness, coefficient of variation) (Issaks and Srivastava, 1989). From the histogram and the statistics it is possible to identify outliers and determine whether a distribution is normal or departs from normality. A test of normality such as Kolmogorov-Smirnoff test (Sokal and Rohlf, 1995), can be applied on the data set during the descriptive statistics stage. In the case of non-normality, a transformation can be applied on the data to normalise them. From all the known transformations, the Box-Cox is particularly recommended, because it is a tailor-made transformation to the data in question (Krebbs, 1999). The relationship between two variables can also be described by the correlation coefficient or rank correlation coefficients (Pannatier, 1995) and represented graphically in plots such as p-p plots (a graph plotting the quantiles of one distribution versus the quantiles of another, which is used to compare two distributions) and scatterplots. A map of the data locations should be prepared during the descriptive statistics stage; which allows the identification of data set features such as clusters, trends, discontinuities and bad recordings. When the descriptive statistics stage is completed, the appropriate number of data (30-50) at each

location should be checked. A final check for outliers and data already transformed should be carried out, before the spatial statistical treatment.

Estimation in geostatistics is based on probabilistic models, accounting for the uncertainties at unsampled locations where complex processes occur. Any unsampled value, z, is viewed as a result of a random process, so it can be considered as a random variable (RV) Z. The probability distribution of these RVs depends on the location, therefore any random variable can be expressed in terms of a location coordinate vector **u** and can be written as {Z(**u**), **u** $\in$ study area} and is known as Random Function (Issaks and Srivastava, 1989).

The distribution function of a continuous RV or outcome set, can be conditioned to neighbouring data values on the same attribute z or another related attribute y.

If estimation is carried out, the restriction of stationary must be introduced; that is, the expected values of the sample values are equal to the expected value of the true value at the unsampled location. Optimal estimates for the unsampled values can be derived using different methods (Deutsch and Journel, 1998). The estimation methods for a global estimation are polygonal and cell declustering; whereas for a point estimation polygonal, local sample mean, inverse distance and triangulation can be listed. Most techniques give more weight to samples closer to the point being estimated.

The parameters that describe the probability distribution of the Random Function can then be calculated. They do not represent a sample statistics, but parameters of a conceptual model. Usually two univariate parameters: mean and variance, are enough to characterise the probability distribution; then the stationary model is said to be of second order. Other parameters that are commonly used to summarise the bivariate behaviour of a stationary random function are: the covariance $C_{(h)}$, correlogram $\rho_{(h)}$ and variogram $\gamma_{(h)}$

The geostatistics approach consists of two parts. One is the calculation of an experimental variogram from the data and model fitting, and the second is the estimation or prediction of values at unsampled locations.

A ***variogram*** is used to describe the spatial relationship between points separated by vector h. It gives a measurement of similarity ($\gamma_{(h)}$) or how a close pair of data vary together (co-variance). It can be expressed as:

$$\gamma_{(h)} = \frac{1}{2N_{(h)}} \sum \left(Z_{(x+h)} - Z_{(x)} \right)^2$$

If the variogram (Figure 2.4) rises and stabilises around some value; then reaches a sill (C), that is theoretically the sample variance. It could be the case that the variogram does not reach a sill, indicating that it corresponds to phenomena with an unlimited capacity for dispersion. The distance at which the variogram reaches the sill is called range (a) and beyond it data are independent. Discontinuities at the variogram origin could also be present. Such an unstructured component of variation at h=0 is known as the nugget effect (Co) and among causes for it are sampling errors and short scale variability. The calculation of the experimental variogram is carried out in several directions to assess if the spatial variability is the same. If it is the same, it is characterised isotropic, otherwise is anisotropic.

Once the variogram is calculated, a model (Table 2.6) must be fitted to it. Models that reach a sill, that is have a finite variance and covariance, are called transition models. Such are the spherical, exponential, gaussian and hole effect models. The most important model that does not reach a sill, is the power model. It is possible to have a combination of two or more models (nested structure), with a total variance of the sum of variances of each model.

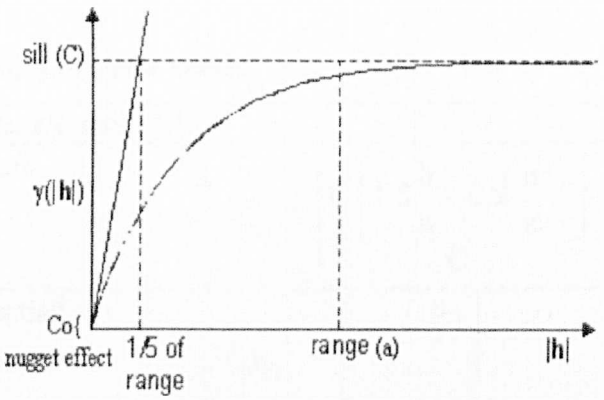


Figure 2.4. Variogram showing the exponential model.

From the several estimation methods, ***kriging*** is the most popular because it "is a collection of generalised linear regression techniques for minimising an estimation variance defined from a prior model for a covariance" (Olea, 1991). Kriging is not just used to estimate unsampled areas, it is also used to build probabilistic models of uncertainty about these unknown values (Deutsch and Journel, 1998). The traditional kriging methods are simple and ordinary, providing the "best" linear unbiased estimate (BLUE) for unsampled areas, with the kriging variance being used to define Gaussian-type confidence intervals. There are other types of kriging such as non-linear, universal and factorial, which are applied under specific restrictions to particular cases. Kriging is generally carried out using data on the same attribute as that being estimated. However, it is possible to apply kriging on data defined on different attributes, this technique is called co-kriging. The spatial continuity of a single variable is described using (semi) variograms, however it is possible to describe the cross-continuity between two variable by using the cross-variogram (Isaaks and Srivastava, 1989).

Table 2.6. Variogram models.

Models with a sill	
Spherical	$\gamma_{(h)} = \begin{cases} C\left[1.5\frac{h}{a} - 0.5\left(\frac{h}{a}\right)^3\right] & \text{, if } h \le a \\ C & \text{, if } h \ge a \end{cases}$
Exponential[1]	$\gamma_{(h)} = C\left[1 - e^{\left(-\frac{3h}{a}\right)}\right]$
Gaussian[1]	$\gamma_{(h)} = C\left[1 - e^{\left(-\frac{(3h)^2}{a^2}\right)}\right]$
Hole effect[2]	$\gamma_{(h)} = C\left[1.0 - \cos\left(\frac{h}{a} * \pi\right)\right]$
Models without a sill	
Power	$\gamma_{(h)} = C\,h^{\omega},\ 0 < \omega < 2$
de Wij[3]	$\gamma_{(h)} = A\ln(h) + B$

[1] These variogram models reach their sill asymptotically, the effective range is defined as the distance at which $\gamma(a) = 0.95\ C$

[2] It is defined by a length a to the first peak and positive variance contribution value C

[3] A is the slope (equals to 3 times the absolute coefficient of dispersion) and B is related to the length of the samples

Checking the model performance and refining the chosen parameters is carried out through a ***crossvalidation*** process, during which known values are re-estimated using the best conditions in the kriging model. A comparison can then be made between the true and the estimate values. The next step is the ***analysis of cross-validated residual or errors***, which must fulfil the following requirements:

- The distribution of N errors should be symmetrical, centred on a zero mean, with a minimum spread (to verify this a histogram should be prepared)
- The N errors for a given procedure should be independent one from another (this can be checked preparing a variogram of the errors)

The kriging estimates can be mapped, to reveal the overall trend of data. ***Maps*** provide helpful visual displays of the spatial variability in the field under study and can be

used as a summary and representation of soil properties where natural hazards can be identified (Goodchild, 1993).

2.10. Conclusions

In this chapter the most relevant topics involved in the development of this research have been reviewed and the theoretical basis for the practical work developed in the remaining chapters have been outlined. The review includes legal, technical and scientific references - when appropriate - for each section.

Chapter 3. L-field site

3.1. Introduction

This chapter describes the landfill from which the liner samples were taken for this research. Relevant information for the research such as geology, is detailed, not only for the stratum from which liner is made; but for all the strata present in the area. Information which is non-relevant for this research, but important if considering the possible environmental impact on the surroundings - particularly water- that this landfill can have; such as rainfall, drainage and water supply are also presented. The rainfall input will influence the generation of the landfill leachate; whereas the rainfall outputs and volatilisation should be considered when listing the possible releases of the contaminants contained in the leachate to the environment. The groundwater quality in the area is well known and is monitored periodically, to measure and control any impact that the landfill leachate release can cause.

3.2. L-field site

The containment landfill under study is known as the "L-field site"; at present it is licensed to Shanks & McEwan (Southern Waste Services) Limited. The L-field site, grid reference TL 0155 435, is rectangular in shape with its long axis lying roughly north east/south west. It is some 1300 m in length by about 760 m in width at the northern end and about 450 m in width at the southern end (Figure 3.1.). The original void was $10x10^6$ m^3 with an approximate depth of 20 m.

It is located within the Marston Vale, approximately 9.7 km east of the M1 motorway and 9.7 miles south west of Bedford in Bedfordshire and covers approximately 76 hectares. The site is situated adjacent to Stewartby Brick Works, the village of Stewartby (Figure 3.2) is approximately three quarters of a mile to the east. The site's main transport links are serviced by the A421 trunk road and the Bedford to Betchley rail link. Before excavation the natural ground surface was gently undulating with ground contours varying from 33.5 to 41 m O.D., with a fall to the east and north east where any run off is to the brook, running from south west to north east and which eventually finds its way into the River Ouse at Willington (SME LTD, 1976).

The approximate value of front line plant is of £ 3 million, the fuel used per annum is 750, 000 litres. There are 120 gas wells with an average depth of 18 metres. The total length of gas extraction pipe work is of 53 km. The liner lift consists of 6 layers of compacted Oxford Clay (SME LTD, 1996).

3.3. Historical development

The quarry operation started in 1953 and worked until 1960. The original excavation was for quarrying the Lower Oxford Clay for the brick making industry (London Brick Company). The clay has a particular characteristic of being high in organic content, that gives it the capability of self-combustion once the clay reaches a certain temperature.

This type of clay is economically attractive to make bricks, because only small amounts of additional fuel are required to start the process and this will keep almost self-sustained.

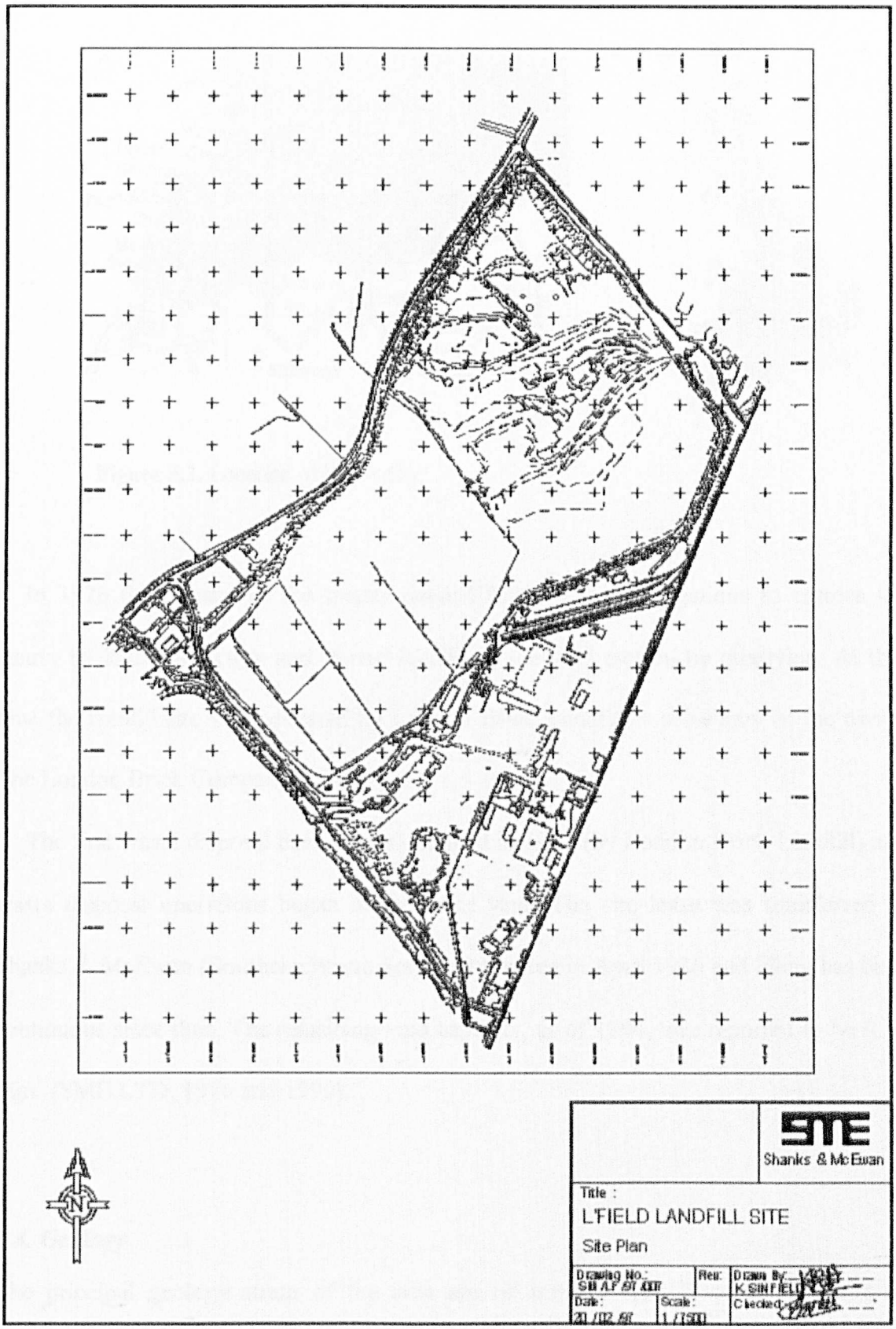


Figure 3.1. L-field landfill site.

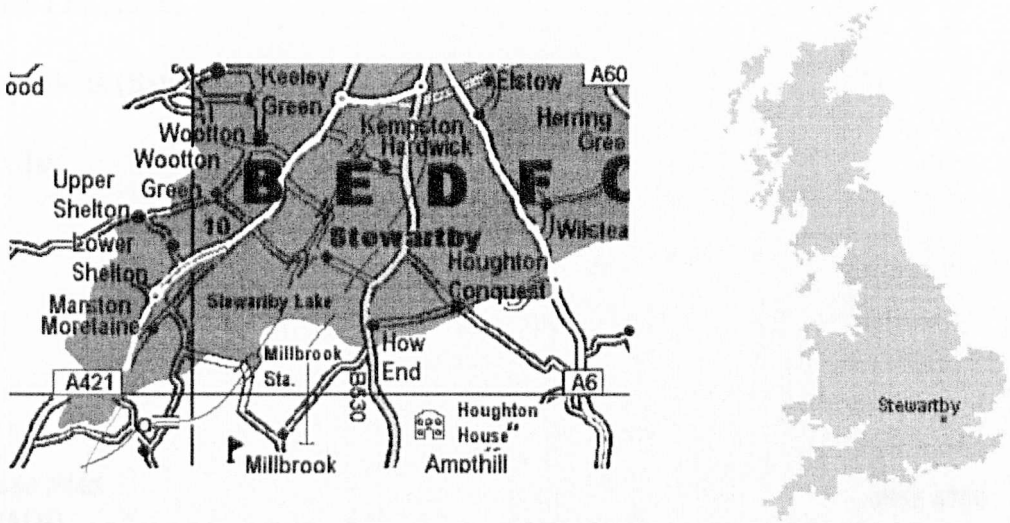


Figure 3.2. Location of Stewartby.

In 1976 the owners of the quarry needed to fulfil their obligations to restore the quarry back to agriculture and started landfilling the void created by quarrying. At that time the landfill site was operated by London Brick Landfill, a subsidiary of the owner The London Brick Company (LBC).

The first waste disposal license was obtained in 1977 (by London Brick Landfill) and waste disposal operations began in the same year. The site lease was transferred to Shanks & McEwan (Southern Waste Services) Limited in April 1986 and filling has been continuous since then. The remaining void capacity, as of 1994, was reported to be 6.16 Mm^3 (SME LTD, 1976 and 1996).

3.4. Geology

The principal geology strata of the area are of Jurassic age. They are in order of increasing age (Figure 3.3) (SME LTD, 1996):

Great Oolite Limestone

Blisworth Clay

Cornbrash Limestone

Kellaways Beds (Sand and Clay)

Oxford Clay

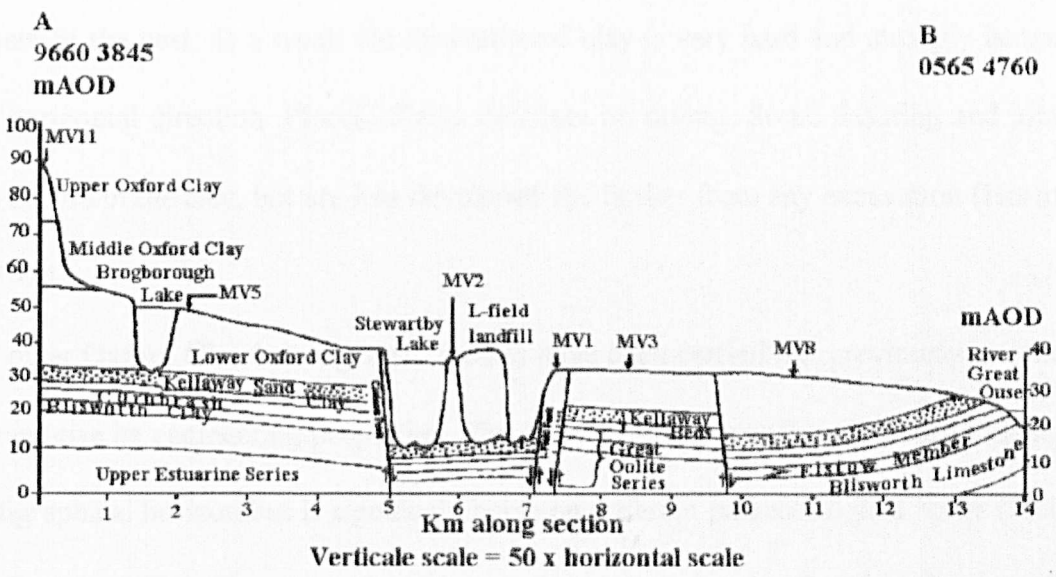


Figure 3.3. Geological cross-section of the Marston Vale, Bedfordshire.

In the following paragraphs each stratum will be detailed.

3.4.1. Oxford Clay.

The Oxford Clay extends from the surface (except for the soil profile) to depths varying in general from about 12 m at the north east end to 27.5 m at the south end. The main mass of the clay is weathered Oxford Clay of medium grey colour. Weathering has occurred at the top of the deposit to depths between 2.7 and 5.8 m. The weathered clay

is mottled brown, orange and grey in colour. Numerous fossil remains are present throughout the clay either in a calcareous or pyritic form. Selenite crystals ($CaSO_4 \cdot 2H_2O$) are common in the overburden, particularly near the base of the weathered zone. (Horton *et al*, 1974)

The Lower Oxford Clay and a small depth of the Middle Oxford Clay present in the area is heavily over-consolidated as a result of great depths of overlying sediment being present in the past; as a result the unweathered clay is very hard and strongly laminated in a horizontal direction. Pieces of clay defoliate on drying. Some fissuring and jointing also occurs in the clay, but are less developed the farther from any excavation (Horton *et al*, 1974)

Lower Oxford Clay heterogeneity studies have been carried out previously in order to characterise its engineering properties. The depth of burial was found to vary little in any stratigraphical horizon but is significant between different palaentological zones (Jackson and Fookes, 1974). However alterations at close intervals were found in the slope faces of brick-pits in the Lower Oxford Clay. These short-term weathering characteristics of clay-shales have been influenced by the their preferred orientation (Jackson, 1973). Weathering of the Lower Oxford Clay results in the reaction of redox-sensitive minerals, especially pyrite, and organic matter. The two main consequences of these reactions are decreased sedimentary permeability resulting from the dissolution of gypsum and calcite, and the enhancement of sorption and cation exchange properties of the Lower Oxford Clay as ferric oxyhydroxide and smectite components increase (Milodowski *et al*, 1986). The chemical and mineralogical stability of the Oxford Clay as a mineral liner for landfill has been studied using a series of batch equilibrium experiments with the mudrock and a synthetic leachate (Batchelder, 1995; Batchelder *et al*, 1998).

Liners are made of Virgin Callow (Batchelder, 1995), after compaction. The compacted clay liner must have reached a permeability < 1 x 10^{-9} m/s before being placed on site.

3.4.2. Kellaway Beds (Horton *et al*, 1974).

Underlying the Oxford Clay are the Kellaway beds. Two subdivisions of the Kellaways Beds are generally recognised, The Kellaway Clays below and the Kellaway Sands above. The Kellaway Beds have a total thickness of 3.0 to 6.1 m. The Kellaway Clay comprises uniform medium to dark grey, somewhat shaly mudstones, with occasional bivalves, gastropods and a few ammonites. It varies in thickness from 0 to 2.1 m. It generally resembles the Oxford clay, but is very much less bituminous and fossiliferous and may be more pyritic. It weathers to a pale gray selenitic clay. The sandy beds are commonly bioturbated and may be locally cemented into dogger-like masses by calcite, showing lustre mottling.

3.4.3. Cornbrash limestone

The Cornbrash rests non-sequentially upon the Blisworth Clay, the top of which is penetrated by shallow burrows infilled with shell-debris-rich clay. The upper contact with the Kellaways Beds, is sometimes abrupt, with some recementation of the Cornbrash and the Kellaway Beds. There was an increase of the basin of sedimentation at the end of the deposition of the Upper Cornbrash because the same lithology is developed where the Kellaways Clay overlaps onto the Lower Cornbrash. A variety of detrital limestones make up the greater part of the Cornbrash. The most typical lithology is a pale to medium grey, blue hearted rock, with much fine to medium, well rounded shell debris

with a micritic (lime mud) matrix making up a small but variable proportion of the whole; the shell debris and occasional ooliths are darker than this matrix, possible due to the presence of pyrite (Horton *et al,* 1974).

3.4.4. Blisworth Clay

This has characteristic bright greenish, violet and mottled colours. The formation generally varies from 4 to 5.9 m in thickness. It is predominantly argillaceous, although calcareous bed may be present. The limestones are of two distinct types: a coarse blue-hearted shell-detrital limestones overlain by grey mudstones, a second calcareous comprises pale green-tinted grey porcellanous micritic limestone interbedded with pale greenish grey marls and mudstones. The argillaceous beds weather at the surface to oyster-rich marls and clays. These beds contrast strongly with the bluish grey shell-detrital limestones of the overlying Cornbrash and the junction is commonly marked by a bored or burrowed surface with pipes of dark grey shell-debris clay extending down into the calcareous facies of the Blisworth Clay. A similar non-sequence occurs at the base of this facies and separates it from the typical Blisworth Clay sediments upon which it rests. The precise age of this calcareous facies has not been proven (Horton *et al,* 1974).

3.4.5. Great Oolite Limestone or Blisworth Limestone (Horton *et al,* 1974).

This limestone is considerably younger than much of the White Limestone, and with the overlaying Blisworth Clay, is of Upper Bathonian age. It comprises three major types of stones. In the unweathered state all the lithologies are coloured in shades of grey. They commonly contain well rounded shell debris. The rock types are arbitrarily classified, there being an apparently continuous variation in the proportion of the constituents;

grains, clay matrix and lime matrix (either micrite or granule calcite). In the limestones the predominant particles are rolled shell fragments, but these may be associated with superficial ooliths, ooliths and pellets. The matrix is commonly micritic, but fine grained sparry calcite is also present. In certain limestones the particles are well stratified, and this sometime shows cross-bedded units, which possess basal clay flake layers (eroded micritic or clay pellets). These granular-bedded units may be separated by parting or beds of micrite devoid of particles. With decreasing particles-grain size these interbedded units pass into thinly laminated beds which sometimes show ripple drif microscoss-stratification. As the proportion of clay and micrite matrix increases the internal structures of the limestones tend to have been entirely obliterated by bioturbation and finally then give way to marls. The mudstones are usually dark grey I colour but may show shades of greyish green. They range from beds packed with shells and shell debris (of lumachelle type) with layers or lenses of shell fragments. A geological fault crosses the north west corner of the site which has displaced the level of the beds on the north side upwards relative to those on the south side by about 3 m.

3.5. Rainfall and Evaporation

The annual average rainfall in the vicinity of Stewartby, for the period 1953 to 1975 was 549 mm (SME LTD, 1996). At Stewartby the highest rainfall recorded in one month during this period was 113.2 mm in November 1963, and the maximum in one day was 45.7 mm on March 5th 1970. The average annual evaporation from a free water surface measured at Cardington is 566 mm and the annual average transpiration from an area of full cover of shallow rooted vegetation is of the order of 517 mm according to the

Ministry of Agriculture and Fisheries, Meteorological Department, Cambridge (SME LTD, 1996).

Since excavation of the L-field has ceased in 1960, the pit was partially filled with water and in recent years water has been pumped out. From the information available, the input to and the output from the pit area is estimated as given in Table 3.1.

Table 3.1. Input and outputs from the pit area of the L-field site.

Input	
a) Rainfall 1960 to 1975 totalled 8935 mm	
Catchment area 1960 to 1971 = 119.6 ha (295 acres)	
Catchment area 1971 to 1975 = 86.4 ha (213 acres)	
Therefore, water input from rainfall amounts to 9797 million l (2,155 million gal)	
b) water pumped into pit area 1964 to 1968 was of the order of 1923 million l (423 million gal)	
Total water entering the pit area is therefore	11720 million l (2578 million gal)
Output	
Evaporation from free water surface - 4632 million l (1019 million gal) (area of flooded pit 58.5 ha (144.4 acres))	
Transpiration 1960 - 1970 = 3487 million l (767 million gal) (area of ground 61.1 ha (151 acres))	
Transpiration 1971 - 1975 = 727 million l (160 million gal) (area of ground 27.9 ha (69 acres))	
Water pumped out to empty pit 1973 - 1975 = 2955 million l (650 million gal)	
Total water leaving the pit area is therefore	11801 million l (2596 million gal)

Water used to spread the L-field appears to have been retained by the callow, as works were not able to rely on sufficient volume of this water to become available for recirculating.

3.6. Drainage

Some 33.2 ha (82 acres) of arable land west of the Woburn Road drain under the road leading to site and, together with the L-field site, drain eastward to the brook which eventually finds its way to the River Ouse at Willington. After the site was excavated, drainage from the area west of Woburn Road was diverted into Stewartby Lake, via the western brook diversion. The only drainage entering the excavated area was from the edges of the excavation, and the accumulating surface area of the sluiced overburden eventually 27.9 ha (69 acres).

3.7. Water Supply

The main groundwater supplied in the area is from the Anglian Water Authority mains. In the period about 1890 - 1900 wells were dug in the area for the local water supplies. Seven of these wells, dug at Wootton, passed through the Oxford Clay into the Kellaways Sand and are reported to have given good supplies of water. This is contrary to LBC's experience with bores and excavations made into the Kellaway sand. Three other wells which were sunk to the Great Oolite Limestones or just below are also of interest, one at Marston Moretaine and two in the Kempston area at Kemston Bury and Meadow Farm, which produce hard saline water. Water taken by LBC in 1973 from borehole 1/73 in the north west corner of L-field sunk to the Great Oolite was saline to taste. The results for the analysis of this water is given Table 3.2 (SME LTD, 1996).

The water present in the Great Oolite Limestone in this area is saline due to the high concentration of dissolved salts and it is not suitable for use as a potable water supply.

Table 3.2. Results for the analysis of groundwater taken from the borehole 1/73.

Parameter	Concentration, mg/litre*
pH	7.5
Calcium, as Ca^{2+}	131
Magnesium, as Mg^{2+}	21
Sodium, as Na^{+}	1080
Potassium, as K^{+}	22
Sulphate (SO_4^{2-})	470
Chloride (Cl^{-})	1510

* pH is given in pH units

3.8. Conclusions

Water can gain access to the L-field site pit by one of three ways by rainfall, through the weathered clay and through the Oxford Clay and Kellaway Beds. The effective average annual rainfall over the area, that is the difference between precipitation and evapotranspiration, is small (about 32 mm), so that after the pit is filled, capped and covered by vegetation, ingress of water from this source would appear to be limited. The horizontal permeability of the Oxford Clay is of the order of 1.7×10^{-7} cm $\cdot$ sec^{-1} and the vertical permeabilities of the underlying Kellaway Beds even less. Therefore, it is unlikely that any significant amount of water will enter the pit through these deposits. This implies that the water entering the landfill will not enhance in a significant way the generation of leachate, and this is expected to be effectively contained by the strata in the area.

Chapter 4. The exploratory campaign

4.1. Introduction

After reviewing the information collected on the L-field site, an exploratory visit was carried out aiming to identify a representative and minimally disturbed area where an exploratory sampling would be carried out. The north side of the L-field site was chosen because there, landfill cells had not been used yet. It is estimated that it would take seven years to fill that pit. The study was focused on the strata within which the landfill is built. The stratigraphic units are known as the Lower Oxford Clay. The compacted clay liner system are made of Virgin Callow.

Once the place and horizon were chosen, an exploratory sampling was carried out.

In this chapter the sampling and analytical determinations applied on the exploratory samples are detailed and the results are discussed.

4.1.1. Objective

The objective of this limited study were to identify characteristics that can influence sampling campaigns, and the key chemical properties of the Oxford Clay that can affect attenuation.

Several analytical methods and techniques were tested on the samples collected, to identify possible interferences arising from the sample matrix and to compare results from this study versus others previously carried out on the characterisation of the Lower Oxford Clay (Jackson, 1973; Jackson and Fookes, 1974; Milodowski *et al*, 1986; Batchelder, 1995; Batchelder *et al*, 1998).

A limited number of samples were taken as representative of the stratum (Lower Oxford Clay) assuming that the area would not show a high degree of variability. That is, no dramatic changes due to spatial variability or compaction were expected. Thus, three samples from the Lower Oxford Clay, before compaction, were taken from the cell walls; and one composite sample of the Lower Oxford Clay already engineered and placed on the cell bottom was collected as well.

4.2. Sampling

The exploratory sampling was carried out on February 7th, 1997 around 13:00 hours at the north site of the L-field site. The sampling site was located on a slope of approximate ten metres length, composed entirely of Lower Oxford Clay. The top was a narrow step followed by six metres of Weathered Oxford Clay. Three samples were taken from the Lower Oxford Clay at random positions, each of them with its respective duplicate. One composite sample was also collected from the liner. The sampling locations are shown in Figure 4.1. Samples were collected as listed below:

i) the first sample (S1) was collected on the slope at approximately 4 m below of the top at a depth of approximately 30 cm.

ii) the second sample (S2) was dug at around 12 m to the north of point one and 10 m from the top at the same depth of 30 cm.

iii) the third sample (S3) was collected from the narrow step at a depth of 30 cm.

The samples were labelled and kept in plastic bags, taken to the laboratory and stored in the refrigerator at temperature of 5 °C.

4.3. Analytical methods and techniques used on the exploratory samples

The following analytical methods and techniques were applied to determine the concentrations of Cr, Cu, Cd, Pb, Ni and Zn in the exploratory samples:

- Preparation of trace element solutions ICP-MS analysis, using the HF-$HClO_4$ method
- Common single extraction scheme for soil analysis using 0.05 mol/l EDTA and 0.43 mol/l acetic acid (Quevauviller and Maier, 1994)
- Sequential extraction method to speciate trace elements (Tessier *et al*; 1979)

The following determinations were also applied to exploratory samples:

- A mineralogical composition determination for bulk rock and clay fraction was carried out using X-ray diffraction
- Soil pH was determined by measurement in water as described by Carter, 1993

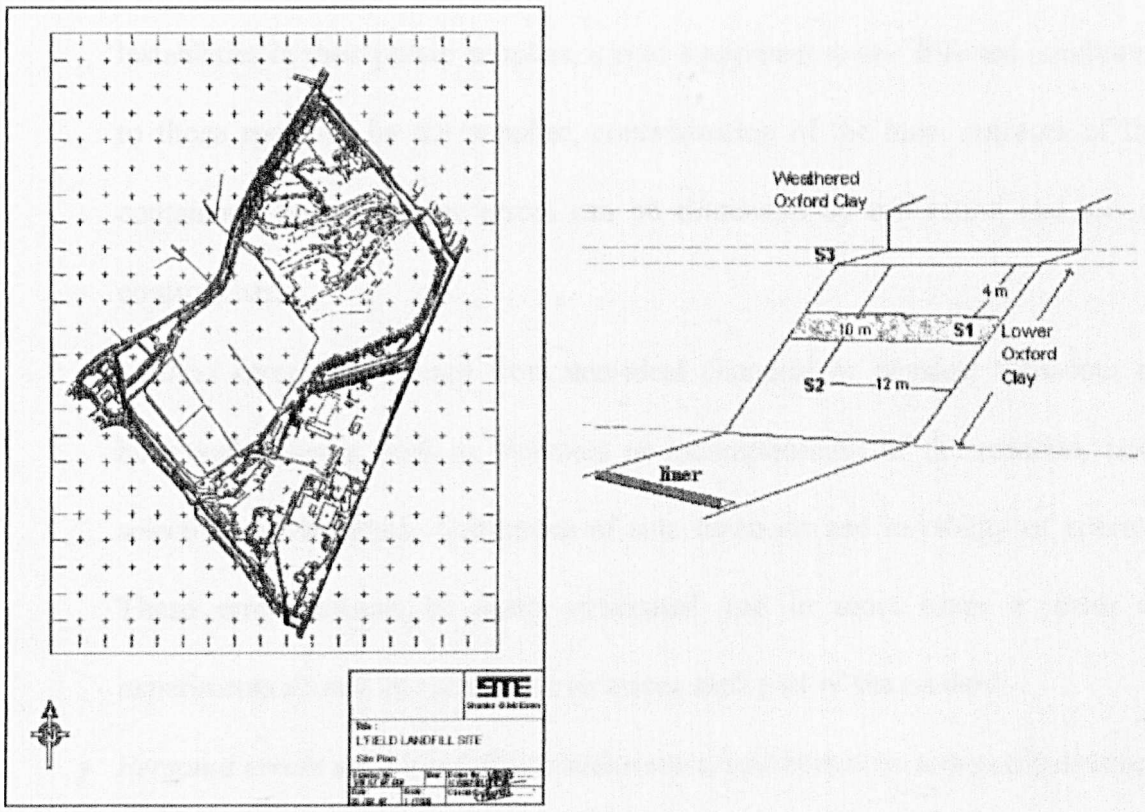


Figure 4.1. Exploratory sampling locations.

4.4. Results from the exploratory samples characterisation

Prior to reporting of results, two topics should be reviewed briefly; 1) errors in chemical analysis and 2) limit of detection (LoD) calculation.

1) Errors in chemical analysis. There are many uncertainties that will influence the measurements when performing a chemical analysis, since no result of chemical analysis is totally free of errors or uncertainties. Measurement errors cannot be completely eliminated, but they can be minimised and their size can be estimated. Chemical analyses are affected by at least two types of errors (Skoog *et al*, 1997):

- ***Systematic (or determinate) errors***, are errors that affect the accuracy (closeness of a result to its true or accepted value) of results, causing the mean of a set of data to differ from the acceptable value. There are three types of systematic errors:
  - *Instrumental errors* are caused by imperfections in measuring devices, instabilities in their power supplies, use of equipment under different conditions to those specified by the supplier, contamination of the inner surfaces of the containers. Most of these errors can be eliminated by calibration and use of control charts
  - *Method errors* are caused from non-ideal chemical or physical behaviour of analytical systems, such as slowness or incompleteness of the reaction, non-selectivity of reagents, occurrence of side reactions and instability of species. These errors cannot be easily eliminated and in most cases a series of experiments should be carried out to assess each part of the method
  - *Personal errors* are caused from carelessness, inattention or personal limitations of the experimenter
- ***Random (or indeterminate) errors***, are errors that affect the precision (closeness of data to other data that have been obtained in exactly the same way) of the

measurement, causing data to be scattered more or less symmetrically to the mean value. These types of error can be evaluated by the methods of classic statistics, assuming that random errors follow (in most of the cases) a gaussian or normal distribution and the standard deviation is a measure of precision.

In this research, errors in chemical analysis were minimised using a quality assurance program, that consisted of the following:

- ***Control charts*** were prepared for the:
  - *Balance*, the standard masses of 20, 10, 5, 3, 2 and 1 g "Stanton Instrument Ltd" serial No. 12344, were measured for 15 consecutive days, three times per day. Estimates of the population mean, standard deviation and upper and lower control limits were computed. A weekly exercise was to weigh a standard of 1 g before using the balance
  - *ICP-AES*, deionised water of 18 megaohm-cm resistivity was introduced to the instrument during 20 consecutive days; the process was repeated five times a day. The objective was to measured the contribution of instrumental background on the wavelengths of interest. Estimates of mean, deviation standard and control limits were computed. These background levels were checked every three months
  - *IC*, deionised water of 18 megaohm-cm, was injected to the instrument and baselines were taken during 15 consecutive days to determined the stability of the equipment. Estimates of mean, standard deviation and control limits were calculated. Background levels were verified monthly
  - *Pipettes* of 100-1000 μL, 1000-5000 μL, 1-10 mL and 2-5 mL were check in their performance by taking 1 mL of deionised water, which was disposed into a vial on the already calibrated balance.

- ***Instrumental Stability*** is checked periodically by the supplier for major instruments such as ICP-AES and ICP-MS. It is carried out annually for some minor equipment such as balances. Calibration for equipment such as pHmeters, is performed prior to use of equipment using standards; as described: pHmeter was calibrated using two buffer solution pH 4 and 7 certified by BDH, when the pHmeter was used after a long period of not being used, the probe was soaked for a period of two hours in a pH 7 solution prior to measurement
- ***Verification of analytical method*** using certified standards and reference material. The analytical methods verified by using standards were:
  - the HF-$HCLO_4$ method that was verified using the GSS-1 Brown soil standard certified by the National Research Centre for CRMs (China). The recovery percentage for the samples and certified concentrations of the reference material are given in Appendix 1
  - Loss-on-ignition method that was verified using the BIR-1 Icelandic Basalt standard certified by the US Geological Survey (USA)

The verification of the performance of the sequential extraction method was not carried out using standards, this is because there are no certified reference materials of metal species bound to solid phases. The performance of this method was verified through a series of experiments described in sections 4.4.3.2., 4.4.3.3. and based on stoichiometric calculations considering the mineralogical composition

- **Calculation and reporting of results**:
  - *The standard deviation of computed results*. The calculation of the standard deviation (s_y) for a set of measurements, eachone of which has a known sample deviation (s_a, s_b and s_c), was calculated as follows:

$$s_y = \sqrt{s_a^2 + s_b^2 + s_c^2}\ ,\ \text{for addition or substraction}$$

  - *Reporting of computed results*. The precision of data was indicated by the standard deviation. The uncertainty associated with the result was considered by rounding results up to two significant figures. To round data the next statement was followed: "the number of unit steps from the smallest to the largest measurement in an array should usually be between 30 and 300 units" (Sokal and Rohlf, 1995)
- **2) Calculation of Limits of Detection** was carried out as described:
  - The matrix matched blank (blank, without addition of standard solution of metals, with the same matrix as the samples, for example $MgCl_2$ at pH 7, and considering dilution in samples) was measured 10 times (in the wavelength or retention time of interest). Estimates of the mean and standard deviation were computed. The standard deviation was multiplied by a factor of 3 (***3s***)
  - The standard solution with the highest concentration used to prepare the calibration curve, was measured 10 times. The mean and standard deviation of the measurement were calculated and corrected by blank subtraction. The resulting mean was divided by the concentration (usually this was 5 mgL^{-1}), to express the mean in terms of concentration (x_{conc})

- The limit of detection was equal to the division of *3s* (the three times standard deviation of the matrix matched blank) by x_{conc}. The result was corrected by dilution factor and expressed relative to a mass of air-dry soil

4.4.1. Preparation of trace-element solutions for ICP-MS analysis using the HF-$HClO_4$ method

The total digestion method was used to determine the *total* concentration of metals of interest in the four exploratory samples. The results are shown in Table 4.1, the number next to the element symbol stands for the isotope analysed, the value next to the mean is the standard deviation. The limits of detection for the method using the ICP-MS technique are given in Table 4.2.

Table 4.1. Total concentration of selected metals on exploratory samples from the L-field site, (values are given in mg kg^{-1}).

Sample	Cr 52	Ni 60	Cu*	Zn 66	Cd 111	Pb 208
S1	155.2±1.2	69.1±4.5	41.9±2.6	142±10	< 1.06	15.6±1.6
S2	145.0±4.4	56.6±0.5	32.7±2.3	104±21	< 0.53	12.8±1.3
S3	157.5±1.8	67.9±1.1	45.8±2.2	145±3	1.38±0.21	15.4±1.0
liner	118.3±0.3	52.0±3.8	24.7±2.2	95±26	< 0.53	17.3±2.0

* This value corresponds to the average value of Cu 53 and 55

Table 4.2. Limits of detection for the HF-$HClO_4$ method.

Element	LoD, µg g^{-1}
Cr	0.36
Ni	0.88
Cu	0.39
Zn	0.77
Cd	0.53
Pb	0.14

Observations:

- The method is time consuming and both acids need to be handled with extremely care

- The sample solutions were too concentrated to be analysed as they were, a dilution factor of 2000 was applied; this indicated that the concentrations of the selected metals can be easily detected by other less sensitive techniques
- The total concentration of the selected metals, with the exception of Pb, is lower in the liner sample. The total concentration distribution, with the exception of Pb and Ni, decreases from the top to the bottom of the north site of L-field
- Cd was detected in only one sample
- The total element concentration determined in the exploratory samples showed similarities with those determined by Milodowski *et al* (1986), in Elstow, Bedforshire, an area close to where the exploratory sampling was carried out

4.4.2. Common single extraction scheme for soil analysis

The single extraction procedure was used to determine extractable contents of Cd, Cr, Cu, Ni, Pb and Zn using 0.05 mol/l EDTA and 0.43 mol/l acetic acid. The EDTA extraction is used to indicate the organically bound fractions present in the soil, that is why this method is one of the most commonly used in soil-transfer studies. The acetic acid extracts are equivalent to exchangeable cation fractions. Results for the EDTA and acetic acid extractions are given in Tables 4.3 and 4.4, respectively. Limits of detection for the 0.05 mol/l EDTA and 0.43 mol/l acetic acid single extraction methods using ICP-MS are given in Table 4.5.

Table 4.3. Concentration of organically bound metals on exploratory samples from the L-field site (values are given in mg kg^{-1}).

Sample	Cr 53	Ni 60	Cu 63	Zn 66	Cd 111	Pb 208
S1	"	4.15±0.41	1.84±0.18	6.0±0.2	0.09±0.02	0.52±0.03
S2	"	3.81±0.14	1.45±0.47	2.8±0.4	0.04±0.01	0.46±0.03
S3	"	5.73±0.40	3.5±0.18	14.2±0.2	0.30±0.04	0.06±0.03
Liner	"	5.30±0.44	2.14±0.20	3.5±0.2	0.02±0.01	1.20±0.05

Table 4.4. Concentration of exchangeable cation fraction of selected metals on exploratory samples from the L-field site (values are given in mg kg^{-1}).

Sample	Cr 52	Ni 60	Cu 63	Zn 66	Cd 111	Pb 208
S1	ii	8.6±0.7	1.0±0.3	26.3±2.3	0.44±0.01	0.90±0.22
S2	ii	7.2±0.4	0.8±0.2	19.7±7.1	0.17±0.03	0.58±0.24
S3	ii	12.8±0.6	3.8±2.8	32.0±3.0	0.75±0.09	1.16±1.22
Liner	ii	11.2±2.0	1.7±0.6	8.1±0.3	0.05±0.04	1.66±0.81

Table 4.5. Limits of detection for the 0.05 mol/l EDTA and mol/l acetic acid single extraction methods using ICP-MS.

Element	LoD µg g^{-1}	
	EDTA	acetic acid
Cr	ii	ii
Ni	0.075	0.24
Cu	0.090	0.54
Zn	0.143	2.55
Cd	0.015	0.09
Pb	0.008	0.15

ii isobaric interference

Observations:

- An isobaric interference was presented on ^{52}Cr when both EDTA and acetic acid extraction schemes were used, this is because the carbon (^{12}C) present in the extractant solution, ($[CH_2N(CH_2COOH)_2]$ for EDTA and CH_3COOH for acetic acid, can react with the argon (^{40}Ar) (auxiliary, cooled and carried gas) of the plasma. ICP-AES, could be used instead of ICP-MS to avoid this interference
- The organically complexed metal distribution decreases from the top of the slope to the bottom, with exception of Zn
- In sample S1 the exchangeable cation fraction concentrations for Cr and Zn are apparently higher than the corresponding organically complexed forms
- In sample S2 the exchangeable cation fraction concentration for Zn is apparently higher than the corresponding organically complexed form

- In samples S3 and liner the exchangeable cation fraction concentrations are lower than the corresponding organically complexed forms
- Only in sample S3, Cd was found as exchangeable and organically complexed forms

4.4.2.1. Comparison of the analytical determination of the common single extraction scheme for soil analysis by ICP-AES

In order to determine in a reliable way the concentration of metals extracted by reagents with carbon in their chemical structure, all the exploratory samples were analysed by ICP-AES and the results compared with those for same samples analysed by ICP-MS.

Although the best wavelengths were chosen to carry out the experiment (Table 4.6.), neither Ni nor Pb gave satisfactory results. The limits of detection were very poor and so none of the results are reported. The results for Cu, Cr and Zn as exchangeable and organically complexed forms are shown in Tables 4.7 and 4.8.

Table 4.6. Wavelengths used for ICP-AES determination.

Element	Wavelength (λ), nm
Cu	324.754
Cr	267.716
Zn	213.856

Table 4.7. Concentration of organically bound metals on exploratory samples from the L-field site (values are given in mg kg^{-1}) determined by ICP-AES.

Sample	Cr	Cu	Zn
S1	0.21±0.02	1.18±0.02	4.81±0.11
S2	0.20±0.04	0.90±0.05	2.22±0.05
S3	< 0.05	1.84±0.04	9.06±0.12
Liner	0.31±0.06	1.20±0.02	2.56±0.03

Observations:

- The use of ICP-AES instead of ICP-MS improved significantly the analytical determination of Zn, Cu and Cr extracted with reagents with carbon in their chemical formula. However Pb and Ni could not be determined

Table 4.8. Concentration of exchangeable cation fraction of selected metals on exploratory samples from the L-field site (values are given in mg kg^{-1}) determined by ICP-AES.

Sample	Cr	Cu	Zn
S1	< 0.46	1.05±0.19	16.39±0.55
S2	< 0.46	0.81±0.24	14.50±0.48
S3	< 0.46	1.39±0.44	22.81±0.22
Liner	< 0.46	1.68±0.28	5.20±0.29

The limits of detection for both methods using ICP-AES are given in Table 4.9.

Table 4.9. LoD for the EDTA and acetic acid methods using ICP-AES technique.

Element	LoD µg g^{-1}	
	EDTA	**Acetic acid**
Cr	0.05	0.46
Cu	0.08	0.44
Zn	0.02	0.46

4.4.3. Sequential Extraction Procedure for the Speciation of Particulate Trace Metals

The relevant importance of determining the soil pool to which metals are bound and the proposed reagents used by Tessier *et al* (1979) to speciate operationally trace metals are given in table 4.10.

The analytical technique used was ICP-MS, despite the possible interferences to be presented by use of organic extractants. Results of the sequential extraction scheme on exploratory samples are given in Table 4.11 to 4.14. Limits of detection using ICP-MS for each metal in each fraction are given in Table 4.15.

Observations:

- The elements were difficult to determine by ICP-MS, because of the interferences presented by the organic extractants used in four of the five steps in the Tessier *et al* (1979) method. In order to improve the analytical performance another technique, such as ICP-AES, that does not present interferences at presence of organic should be used
- The concentration and distribution of metals in specific soil pools between the samples of LOxC and the liner sample are remarkably different
- The concentration of Cd in the soil solid phases of the exploratory samples, with the exception of the residual fractions of samples S1 and S3, is below the limit of detection

Table 4.10. Soil pools and the importance of the of heavy metals fraction and proposed reagents to operationally define them.

FRACTION	REASONS	REAGENTS
Exchangeable	Changes in water ionic composition are likely to affect sorption-desorption processes	1M $MgCl_2$, pH 7.0
Bound to Carbonates	Significant trace metal concentrations can be associated with them. This fraction would be susceptible to changes of pH	1M NaOAc, pH 5
Bound to Iron and Manganese Oxides	Iron and manganese oxides are as nodules, concentrations, cement between particles, or simply as a coating on particles. These oxides are excellent scavengers for trace metals and are thermodynamically unstable under anoxic conditions	0.04 M $NH_2OH.HCl$ in 25 % (v/v) HOAc
Bound to Organic Matter	Trace metals may be bound to various forms of organic matter: living organisms, detritus, coatings on mineral particles, etc. The complexation properties of natural organic matter are well recognised as in the phenomenon of bioacumulation in certain living organisms	H_2O_2, pH 2 (HNO_3) + NH_4OAc
Residual	The residual solid should contain mainly primary and secondary minerals, which may hold trace metals within their crystal structure. These metals are not expected to be released in solution over a reasonable time span under the conditions normally encountered in nature	HF - $HClO_4$

Table 4.11. Concentrations of heavy metals bound to soil fractions for the exploratory sample S1.

Element	Fractions				
	Exchangeable	Bound to Carbonates	Bound to Fe-Mn oxides	Bound to organic matter	Residual
Cr	19.2 ± 7.1	1.5	25 ± 3	5.6 ± 0.5	105 ± 2
Ni	2.3 ± 0.6	10.5 ± 0.8	50 ± 2	1.4 ± 0.1	< 0.9
Cu	< 0.2	< 0.4	< 0.1	6.8 ± 0.8	34.3 ± 2
Zn	< 0.7	19.5 ± 0.5	46 ± 14	9.9 ± 0.9	64 ± 9
Cd	< 0.1	< 0.2	< 0.1	< 0.8	0.3 ± 0.01
Pb	< 0.1	1.1 ± 0.1	13 ± 1	3.2 ± 0.3	< 0.1

Table 4.12. Concentrations of heavy metals bound to soil fractions for the exploratory sample S2.

Element	Fractions				
	Exchangeable	Bound to Carbonates	Bound to Fe-Mn oxides	Bound to organic matter	Residual
Cr	< 18.2	< 1.5	29 ± 3	6.4 ± 0.5	103 ± 3
Ni	2.6 ± 0.7	22 ± 1	32 ± 3	1.6 ± 0.1	< 0.9
Cu	< 0.2	< 0.4	< 0.1	19.0 ± 0.8	15 ± 2
Zn	< 0.7	38 ± 2	47 ± 21	8.9 ± 0.9	12 ± 1
Cd	< 0.1	< 0.2	< 0.1	< 0.8	< 0.5
Pb	< 0.1	3 ± 0	12 ± 1	1 ± 0.3	< 0.1

Table 4.13. Concentrations of heavy metals bound to soil fractions for the exploratory sample S3.

Element	Fractions				
	Exchangeable	Bound to Carbonates	Bound to Fe-Mn oxides	Bound to organic matter	Residual
Cr	< 18.2	< 1.5	< 0.3	5 ± 0.3	151 ± 2
Ni	2.5 ± 1	22 ± 0.8	$8 \pm 0_{.4}$	1.0 ± 0.1	30 ± 2
Cu	< 0.2	< 0.4	< 0.1	5.9 ± 0.6	40 ± 2
Zn	< 0.7	40 ± 1.8	36 ± 2.0	19.8 ± 1	46 ± 4
Cd	< 0.1	< 0.2	< 0.1	< 0.8	$1 \pm 0.0_1$
Pb	< 0.1	3 ± 0.3	$1 \pm 0_{.2}$	3 ± 0.3	$8 \pm 0_{.1}$

- The sequential extraction scheme renders more information than the single extraction schemes, because it will provide information about the distribution of trace metals among soil components. This is important for assessing the potential of soil to supply micronutrients for plant growth and sequestriation of trace metals, and for determining amelioration procedures for soil at risk of causing the trace metal contamination of waterways (Ure and Davidson, 1995)

Table 4.14. Concentrations of heavy metals bound to soil fractions for the exploratory sample liner.

Element	Fractions, μg g^{-1}				
	Exchangeable	Bound to Carbonates	Bound to Fe-Mn oxides	Bound to organic matter	Residual
Cr	< 18.2	< 1.5	< 0.3	4.0 ± 0.3	109 ± 1
Ni	< 0.9	< 0.5	48 ± 3	< 1.0	4 ± 0.$_2$
Cu	< 0.2	< 0.4	< 0.1	11.0 ± 0.9	15 ± 1
Zn	< 0.7	< 0.5	24 ± 1	28.2 ± 1.2	42 ± 4
Cd	< 0.1	< 0.2	< 0.1	< 0.8	< 0.5
Pb	< 0.1	< 2.3	< 0.1	2.0 ± 0.1	11 ± 0.$_3$

Table 4.15. Limits of detection for the Tessier *et al* (1979) method, using ICP-MS.

Element	LoD, μg g^{-1}				
	Exchangeable	bound to carbonates	bound to Fe-Mn oxides	bound to organic matter	bound to residue
Cr	18.2	1.5	0.3	1.2	0.4
Ni	0.9	0.5	0.3	1.0	0.9
Cu	0.2	0.4	0.1	0.5	0.4
Zn	0.7	0.5	2.5	3.0	0.8
Cd	0.1	0.2	0.1	0.8	0.5
Pb	0.1	2.3	0.1	3.0	0.1

4.4.3.1. Comparison of the analytical determination of the sequential extraction scheme by ICP-AES

Three replicates of one sample of Lower Oxford Clay (S1) were determined by ICP-AES to compare performance versus ICP-MS. The wavelengths used were those shown in Table 4.7, with the exception of the determination of the residual, when λ = 327.396 nm, λ = 205.552 nm, and λ = 481.053 nm were used to determine Cu, Cr and Zn. The wavelengths used to determine Ni and Pb were λ = 221.647 nm and λ = 220.353 nm, respectively for all fractions, despite the fact that some problems will arise during their determinations. The results are shown in Table 4.16, and limits of detection for the method are given in Table 4.17.

Table 4.16. Concentrations of heavy metals bound to soil fractions for the exploratory sample S1 determined by ICP-AES.

Element	Fractions, μg g^{-1}				
	Exchangeable	Bound to carbonates	Bound to Fe-Mn oxides	Bound to organic matter	Residual
Cr	17.0 ± 0.7	0.9 ± 0.2	19 ± 1	2.3 ± 0.1	110 ± 3
Ni	3.0 ± 0.2	7.1 ± 0.4	44 ± 1	< 0.02	12 ± 1
Cu	< 0.13	$0.4 \pm 0.0_7$	$2 \pm 0._1$	2.4 ± 0.3	37 ± 2
Zn	< 1.67	21.0 ± 0.4	$33 \pm 0._4$	8.3 ± 0.2	75 ± 4
Pb	---	---	---	---	$15 \pm 0._3$

Observations:

- ICP-AES offers a better determination to Zn, Cu and Cr; however Pb will not be determined effectively by using this technique.

Table 4.17. Limits of detection for the Tessier *et al* (1979) method, using ICP-AES.

Element	LoD, μg g^{-1}				
	Exchangeable	bound to carbonates	bound to Fe-Mn oxides	bound to organic matter	bound to residue
Cr	1.17	0.30	0.29	0.19	0.09
Ni	2.41	0.20	0.21	0.02	0.09
Cu	0.13	0.02	0.08	0.03	0.06
Zn	0.13	0.29	0.13	0.06	0.06
Cd	1.67	0.91	0.48	0.18	0.10
Pb					0.32

4.4.3.2. Degradation of the extractable fraction versus time

Duplicates of one sample of Lower Oxford Clay (S1) were treated according to the sequential extraction scheme of Tessier *et al* (1979). ICP-AES was used to determine the heavy metal fractions bound to five different pools in a landfill cell. Each fraction was

determined in subsequent weeks. The metal concentration decreased with time. This change happened after one week, in all the fractions, with the exception of the fraction bound to organic matter, in which case a change in the metal concentrations took place after two weeks. It was necessary to monitor this fraction for up to 37 days, to be sure that the metal concentration changed with time.

Exchangeable fraction:

This was the most unstable fraction, and so it was determined daily. A reduction of metal concentration occurred after seven days of being extracted, as shown in Table 4.18.

Table 4.18. Exchangeable fraction determined by ICP-AES, at selected intervals after extraction, values are given in mg kg^{-1}.

Element	fresh	after 7 d	after 15 d	after 37 d
Cr	16.2 ± 0.6	14.1 ± 0.9	0.8 ± 0.02	3.0 ± 0.02
Ni	2.6 ± 0.7	1.9 ± 0.3	0.4 ± 0.03	1.0 ± 0.04

d. days

It would appear that the exchangeable cations are susceptible to degradation, such as precipitation but that a small fraction of them will be released again.

Fraction bound to Carbonates:

The results of the comparison for extractions carried out with NaOAc are shown in Table 4.19. This step takes 16 h, because of the time spent in centrifugation and dilution. The determination was carried out one day after the extraction.

Table 4.19. Fraction bound to carbonates determined by ICP-AES, at selected intervals after extraction, values are given in mg kg^{-1}.

Element	fresh	after 7 d	after 15 d	after 37 d
Zn	22.1 ± 1.7	19.3 ± 1.5	15.6 ± 0.2	13.7 ± 0.3
Ni	7.2 ± 3.2	6.5 ± 0.8	4.9 ± 0.04	4.6 ± 0.1
Cr	1.0 ± 0.1	$0.5 \pm 0.0_2$	< 1.5	< 1.5
Cu	$0.5 \pm 0.0_1$	< 0.4	< 0.4	< 0.4

The concentration of metals bound to carbonates remains more stable than those in the exchangeable fraction. However, determinations on the heavy metals bound to carbonates should not be carried out on extractions older than one week.

Fraction bound to Fe-Mn oxides:

This fraction takes one working day for preparation. Thus, with centrifugation and dilution steps, the solution is determined two or three days after the extraction step. The results for this extraction are given in Table 4.20.

Table 4.20. Fraction bound to Fe-Mn oxides determined by ICP-AES, several days after extraction, values are given in mg kg^{-1}.

Element	fresh	after 7 d	after 15 d	after 37 d
Cr	17.9 ± 0.6	17.07 ± 0.5	5.02 ± 0.4	2.0 ± 0.9
Ni	40.9 ± 3.6	38.7 ± 2.6	27.1 ± 0.5	10.7 ± 0.9
Zn	34.1 ± 4.3	32 ± 2.9	28.0 ± 2.8	23 ± 3.8
Cu	1.9 ± 0.1	1.8 ± 0.5	0.8 ± 0.5	< 0.1

Fraction bound to Organic Matter:

This fraction also takes one working day for preparation and so the diluted solution is usually analysed by ICP-AES two or three days after the extractions are carried out. The results for this extraction are given in Table 4.21.

Table 4.21. Fraction bound to organic matter determined by ICP-AES, several days after extraction, values are given in mg kg^{-1}.

Element	fresh	after 7 d	after 15 d	after 37 d
Cr	2.6 ± 0.6	2.5 ± 0.5	2.0 ± 0.4	2.0 ± 0.9
Zn	9.0 ± 0.4	8.9 ± 0.9	8.0 ± 1.1	7.3 ± 3.8
Cu	2.7 ± 0.1	2.8 ± 0.5	0.8 ± 0.3	< 0.5

Conclusions:

It is clear that the effect of time on the extractions is crucial, particularly in the exchangeable fraction. For this reason it is recommended to extract and determine the elements on the same day, or no later than a couple of days. For the rest of the fractions, analysis should not be carried out within five days after the extraction.

4.4.3.3. Confirmation of the sequential extraction scheme

In order to improve reliability of the analysis throughout sequential extraction, a validation was carried out. The selectivity of each extraction step was assessed through measurements of Ca (for carbonates), Al (for hydroxyl fractions) and Si (for clay lattice) in the leachate of samples. ICP-AES was used with standards matched to each extraction step matrix . A "profile" of the best spectral line to the conditions was measured for the standard, sample and a blank.

The hypothesis was that none of these elements - Al, Ca, Si -, should be in the leachate if the extraction step is effective and does not attack the subsequent fractions. Thus neither Ca, Si nor Al should be found in the leachate corresponding to the exchangeable fraction, the fraction bound to Fe-Mn oxides and the fraction bound organic matter. Ca should be found in copious quantities in the leachate corresponding to the fraction bound to carbonates but neither Si nor Al. The mineralogical composition of

the exploratory samples was determined at the same time, the results for this study will be shown in the next section.

Leachate corresponding to the exchangeable metal fraction extraction

This leachate corresponds to the extraction of exchangeable metals. The sample, blank and standard are in a matrix of 1M $MgCl_2$ at pH 7.0.

The spectral profiles for the standard, blank and sample at the optimum wavelengths (for this conditions) for Al (λ = 396 nm), Ca (λ = 393.366 nm) and Si (λ = 251.611 nm) are shown in Figures 4.2a, b and c, respectively.

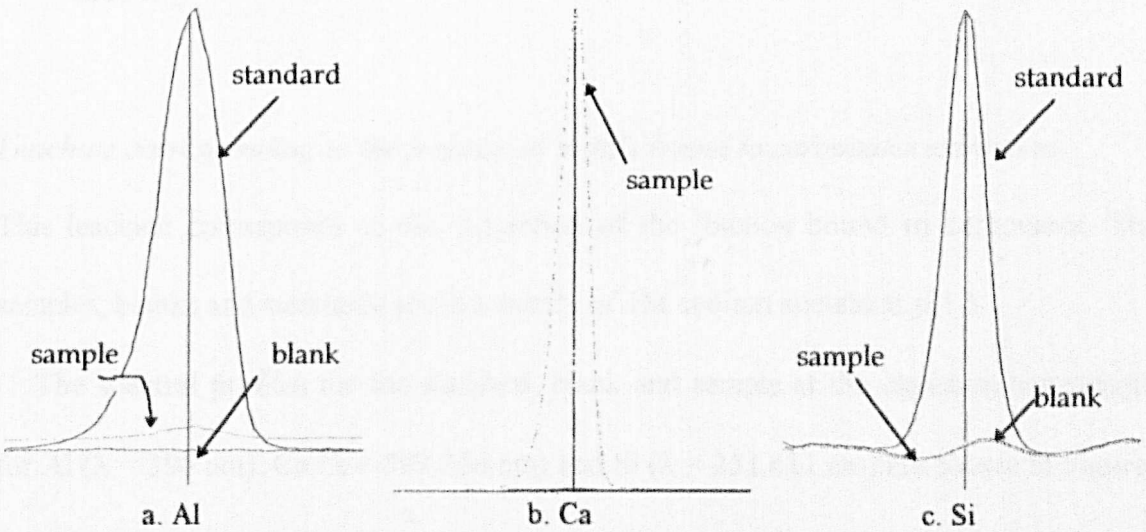


Figure 4.2. Spectral profiles of the standard, blank and sample of the leachate corresponding to the exchangeable fraction extraction.

Observations:

- The reagents are free of detectable amounts of Al, Ca and Si
- The extraction of the exchangeable metals does not attack Al in the clay in a significant way. Only traces of aluminium - around 2 μgmL^{-1}- were found in the leachate. The standard signal shown in Figure 4.2a. corresponds to a concentration of 10 μgmL^{-1}

- There is a small right wing interference on silica, as seen in Figure 4.2b; which is due to the presence of an element interfering with this wavelength of silica
- Only the spectral line corresponding to calcium in the sample is seen Figure 4.2c. This is because the amount of calcium present in the leachate is copious and the intensity of the line is still strong, even when the sample is already diluted by 100 times. The standard signal, corresponding to a concentration of 1 μgmL^{-1} is not seen in the Figure 4.2c. The high concentration of Ca in the leachate could be a result of an attack of carbonates during the extraction of the exchangeable fraction. The effectiveness of the carbonate extraction step is assessed in the following section

Leachate corresponding to the fraction of metals bound to carbonates extraction

This leachate corresponds to the extraction of the fraction bound to carbonates. The samples, blanks and standards are in a matrix of 1M sodium acetate at pH 5.

The spectral profiles for the standard, blank and sample at the optimum wavelength for Al (λ = 396 nm), Ca (λ = 393.366 nm) and Si (λ = 251.611 nm) are shown in Figures 4.3a, b and c, respectively.

Observations:

- Al is not attacked by the extraction of carbonates as shown in Figure 4.3a. Only some traces (less than 1 $\mu g\ g^{-1}$) of Al were found in the leachate. The standard signal shown in the figure corresponds to a concentration of 10 $\mu g\ mL^{-1}$
- The reagent contains Ca in a concentration of around 0.5 $\mu g\ mL^{-1}$, as seen in Figure 4.3b. The signal of the standard shown in this figure corresponds to a

concentration of 1 μg mL^{-1}. As it was expected, the quantities of Ca in the sample are copious

– Si was not attacked by the extraction of carbonates, as seen in Figure 4.3c

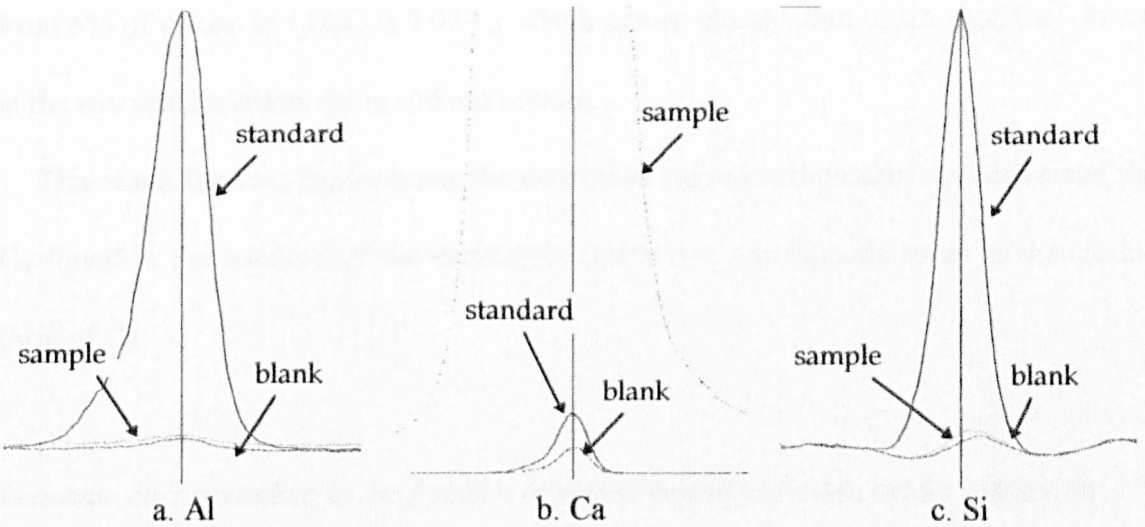


Figure 4.3. Spectral profiles of the standard, blank and sample of the leachate corresponding to the fraction bound to carbonates extraction.

Assessing the effectiveness of the extraction of Ca from carbonates using sodium acetate.

If the extraction of carbonates is effective, the mass of sodium acetate ($NaC_2H_3O_2$, m.w. = 82.03) needed to react with the calcite in one gram of Lower Oxford Clay (considering an average calcite content of 6 %) can be calculated using the following reaction:

$$CaCO_{3(s)} + 2NaC_2H_3O_2 \rightarrow Na_2CO_3 + Ca(C_2H_3O_2)_2$$

thus, the number of moles of calcite was 0.0006, and to balance the equation 0.0012 moles of sodium acetate were needed, representing a mass of 0.0984 g of sodium acetate. The Tessier *et al* (1979) method suggested to use 8 mL of 1M sodium acetate solution, that is, 0.656 g of sodium acetate. Thus the sodium acetate is in excess and should extract all the metals bound to carbonates. The sodium acetate was applied in

excess considering that the calcite concentrations could be as high as 33 % (Jackson and Fookes, 1974).

The amount of calcium in calcite was calculated from the formula and compared with the amount of calcium found in the extract using sodium acetate. The amount of Ca^{2+} from 6% of calcite in LOxC is 0.024 g which agrees closely with 0.025 g of Ca^{2+} found in the extracted solution using sodium acetate.

This result has two implications, the extraction step of carbonates is effective and the Ca found in the leachate of the exchangeable fraction corresponds to an exchangeable form of Ca.

Leachate corresponding to the fraction of metals bound to Fe-Mn oxides extraction

This leachate corresponds to the extraction of fraction bound to Fe-Mn oxides. Samples, blanks and standards are in a matrix of 0.04 M hydroxyl ammonium chloride in 25% HNO_3.

The spectral profiles for the standard, blank and sample at the best wavelength for Al (λ = 396 nm), Ca (λ = 393.366 nm) and Si (λ = 251.611 nm) are shown in Figures 4.4a, b and c respectively.

Observations:

- There is no aluminium in this reagent as shown Figure 4.4a; from this same figure it is seen that the extraction of Fe-Mn oxides is slightly attacking the Al in the clay and aluminium oxides. Around 2 µg mL^{-1} of Al were found, against the 10 µg mL^{-1} standard signal

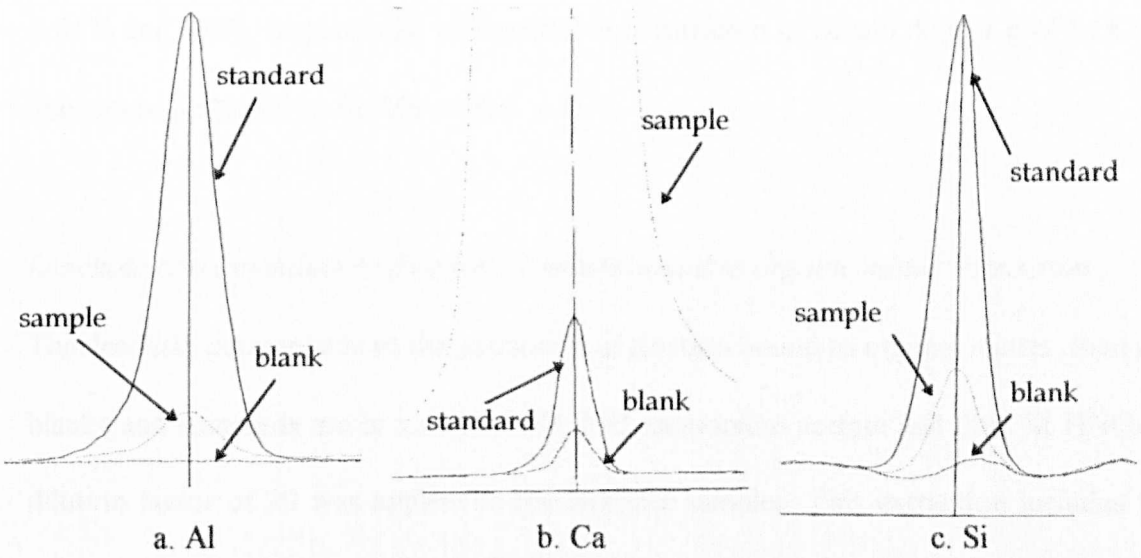


Figure 4.4. Spectral profiles of the standard, blank and sample of the leachate corresponding to the fraction bound to Fe-Mn oxides extraction.

- There is a copious presence of calcium as shown in Figure 4.3b, however this Ca does not correspond to carbonates. As seen in the previous section, the extraction of carbonates proposed by the method is achieved effectively. The Ca content of the reagents was < 0.05 μg mL^{-1}. The standard signal corresponds to a concentration of 1 μg mL^{-1}
- There is mild attack of Si in this extraction of Fe-Mn oxides as can be seen in Figure 4.3c, the traces found were around 3 μg mL^{-1}. There is no detectable presence of silica in the reagents
- The attack on Al and Si could be explained considering that this extraction is relatively violent compared to the previous ones; including heat at 96 ± 3 °C for 6 hours, and the use of an extracting solution with an acid pH

Conclusions

The extraction of metals bound to Fe-Mn oxides is also slightly attacking aluminosilicates and aluminium oxides. There were 43 μg of Si and 218 μg of Al, that is

0.01% and 0.4%, respectively, of the total concentration of Si and Al in 1 g of LOC. Ca appears to be bound to Fe-Mn oxides.

Leachate corresponding to fraction of metals bound to organic matter extraction ,

This leachate corresponds to the extraction of fraction bound to organic matter. Samples, blanks and standards are in a matrix of 3.2 M ammonium acetate and 0.02 M HNO_3. A dilution factor of 20 was applied to the leachate samples. This extraction includes two additions of 30% hydrogen peroxide, heating at 85 ± 2 °C and addition of an extracting solution with a pH 2.

The spectral profiles for the standard, sample and blank at the best wavelength for Al (λ = 396 nm), Ca (λ = 393.366 nm) and Si (λ = 251.611 nm) are shown in Figures 4.5a, b and c respectively.

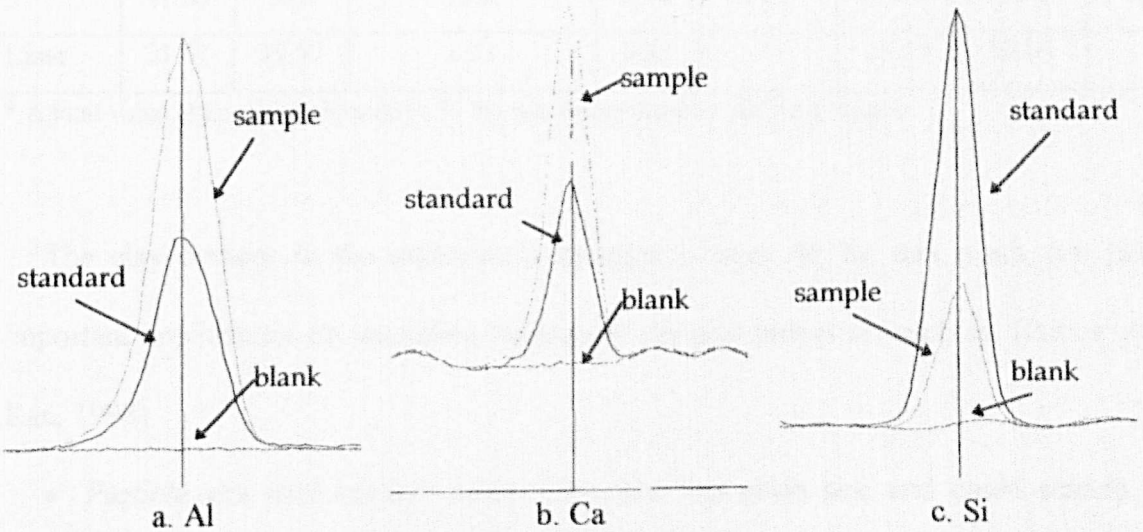


Figure 4.5. Spectral profiles of the standard, blank and sample of the leachate corresponding to the fraction bound to organic matter extraction.

Observations:

- There are no Al, Si or Ca in the reagents
- In the leachate, Al was detected at around seventeen µg mL^{-1}. Considering dilution factors, a total of 1942 µg of Al, were in the leachate, representing a 3.4% of the total

Al. In addition eight μg mL^{-1} of Ca and 20 μg mL^{-1} of Si were found. This is 323 μg of Si, represents 0.1% of the total concentration in the LOxC

4.4.4. Determination of the mineralogy composition

The exploratory samples were analysed on a Phillips P1830 diffractometer system using Cu K∝ radiation, fitted with a PW 1820 goniometer, an automatic divergence slit and a graphite monochromator. The samples were determined in both the whole rock and in the clay fractions. The results are given in Table 4.22.

Table 4.22. Mineralogical composition of bulk rock and clay fraction for exploratory samples of Oxford Clay samples from the L field site. Values given in % wt.

Sample	Whole rock		Other		Clay fraction			
	Quartz	Calcite	Albite-Paglioclase	Pyrite	Chlorite	Illite	Smectite	Kaolinite
1	46.55	6.00	1.47	3.35	0.85	17.48	21.32	2.98
2	42.96	5.29	2.27	3.63	0.92	19.72	22.01	3.21
3	41.80	5.62	1.62	2.90	1.92	25.96	14.42	5.77
Liner	31.47	19.57	1.23	4.42	*	23.39	13.00	*

* A joint value of kaolinite/chloride (4.33 %) was determined for the liner sample

The clay content in the exploratory samples is over 40 %; this result can have important implications on landfilling because of the clay properties such as: (Parker and Rae, 1998)

- ***Particle size and surface area***. Clays are fine grain size and could remain in suspension in aqueous solutions for relatively long periods of time; this increases the possibility of transport of pollutants sorbed by clays. Clays have a high ratio of surface area to volume, due to their fine grain size. Large surface areas sorb pollutants better than small surface areas

- ***Swelling*** is the clay expansion from the dry state up to several monolayers of adsorbed water molecules. This is relevant to landfilling because of the effective "seal" that clays present
- ***Surface charge*** determines the chemical activity of the clay surfaces. This negatively charged surface is a result of broken bonds, surface-growth defects and cation substitutions in the lattice. This property impacts on the adsorption and absorption of metals by the clay.

The properties of the clay minerals in the exploratory samples are given in Table 4.23.

Table 4.23. The properties of the clay minerals in the exploratory samples

Clay mineral	Layer structure	Layer thickness (nm)	Negative charge ($cmol_c kg^{-1}$)	Surface area ($m^2 g^{-1}$)	Swelling properties of crystals
Chlorite	2:2	1.4	10	10	none
Illite	2:1	1.0	25	20	none or very little
Smectite	2:1	1.0	100	800	extensive
Kaolinite	1:1	0.7	Up to 10	10	none

Smectite is one of the dominant clay minerals in the exploratory samples (13 - 22 %), this implies that the Lower Oxford Clay can be used as an effective seal and most importantly, smectite will influence the sorption processes of pollutants.

Observations:

– The mineralogical composition of the Lower Oxford Clay in this study differs from the study carried out in Stewartby, Bedfordshire; by Jackson and Fookes (1974); particularly for the quartz content. On the other hand, the clay content found in the exploratory samples (above 40 %) agreed well with the statement by Milodowski

et al (1986), that clay minerals generally make up the bulk of the shales and mudstones of the Lower Oxford Clay and clay mineral contents usually fall between 40 - 60 % of the bulk rock. They also reported that in the Midlands the clay mineralogy is dominated by illite and mixed-layer illite- smectite, which agrees with the results for illite and illite-smectite in the exploratory samples clay fraction

- There was no appreciable amount of kaolinite in the exploratory samples, although Milodowski *et al*, (1986) reported that samples collected in a surrounding area, had 20 - 30 % of kalonite in the clay fraction. Chlorite is present in all the exploratory samples but in low concentrations. This coincided with the result reported by Jackson and Flookes (1974) who indicated that chlorite is negligible or absent in some samples collected from Betchley, close to where the exploratory samples were taken
- The major non-clay minerals in the exploratory samples were quartz and calcite. Quartz is reported to be present as grains of detrital silt and fine sand and mixed with the clay (Morris, 1980; Milodowski and Wilmot, 1983) and comprises 10-25 % of the sediment. The Lower Oxford Clay is considered to be poorly calcareous by Morris (1980) with 2-8 % $CaCO_3$. However, $CaCO_3$ contents are variable and the occurrence of shell beds (Calloman, 1986; Duff, 1975) can result in high becaused calcite contents. Calcite contents of up to 33 % have been measured (Jackson & Fookes, 1974)
- Pyrite was ubiquitous and present in amounts less than 5%; this agreed with the results reported by Morris, 1980. However, Milodowski *et al* (1985) found that pyrite contents were as high as 15 % in some horizons within the LOxC. They also stated that pyrite occurs replacing calcareous shell debris, infilling fossils, coating

shells or disseminated through the clay matrix as framboidal aggregates, or small well-formed euhedral crystals

Conclusions:

The mineralogical composition of the Oxford Clay series in the L-field site, Stewartby, Bedfordshire is representative for the horizon. Differences in mineralogical composition percentages can be explained in terms of spatial variations during sampling and geological variations characteristic of the area as well as the weathering effect of the LOxC.

4.4.5. Measuring of soil pH

pH is the pre-eminent factor controlling the chemical behaviour of metals and many other important processes in the soil. However, these measurements will present some variability, because of the heterogeneity of the soil, the relatively small proportion of solution present in the pores of the solid soil and the adsorption of cationic H^+ ions on to soil surfaces.

The pH of the soil depends on the H^+ ion concentration in the solution present in the soil pores, which is in dynamical equilibrium with the negatively charge surfaces of the soil particles. Hydrogen ions are strongly attached to the surface negative charges, and they have the power to replace most other cations. Soil pH is affected by the changes in redox potential which occur in soils that become waterlogged periodically. Reducing conditions generally cause a pH increase, while oxidising conditions cause pH to decrease. (Hann *et al*, 1986).

Soil pH measurement in water was used to determine pH on the exploratory samples. A replicate was prepared for each sample. The results are shown in Table 4.24.

Table 4.24. Soil pH measurement in water for exploratory samples.

Sample	pH
S1	7.7 ± 0.1
S2	7.8 ± 0.1
S3	7.6 ± 0.1
Liner	7.8 ± 0.1

Observations:

No apparent variability on soil pH was found in the exploratory samples. The sample liner showed similarities with the other samples, contrary to all the analytical determinations carried out previously; where the parameters measured in the liner samples differed markedly.

4.5. Assessment of the sampling proposal

All the information revealed during the analytical determinations carried out on the exploratory samples, was taken into account when designing a new sampling protocol - that from now on, will be referred as the assessment sampling - to characterise a new cell in the L-field site.

The assessment sampling design

- The assessment sampling would be carried out on a regular grid, on the bottom of the cell, where the liner is already placed
- 30 samples would be taken with eight random replicates. This number was calculated (for a given level of precision) using the following equation (Carter, 1993):

$$n = \frac{t^2 s^2}{D^2}$$

where:

t is a value of student distribution given degrees of freedom

s^2 is the variance which is known beforehand from the exploratory sampling. It could be estimated by $s^2 = (R/4)^2$, where R is the estimated range likely to be encountered in sampling

D is the variability in mean estimation of the metal concentration.

The calculations were made, considering as starting points 10 samples and F = 0.975 of a t-distribution. Reiterations were calculated until a not significance difference was obtained. The values for the variance was the values for the smallest standard deviation of each element in case. The results are given in Table 4.25

- The depth at which samples would be taken, was restricted to the range 0 to 1-1.5 m; by Shanks and McEwan

Table 4.25. Number of samples to take during the assesment sampling.

Element	Number of samples
Cr	33.5
Ni	30.1
Cu	10.6
Zn	34.0
Pb	8.9

the standard deviations used for the calculations, are those of the total concentration of metal results, using ICP-AES

4.6. Conclusions

The detailed study carried out on the exploratory samples demonstrated that :

- ICP-AES would be a better analytical technique to use instead of ICP-MS, when applying extraction schemes that require the use of reagents containing carbon in their structures
- A sequential extraction scheme, rather than a single extraction, renders more information of a better quality. However, it is necessary to consider that the sequential extraction scheme developed by Tessier *et al* (1979) will slightly attack aluminosilicates during the extraction of metals bound to organic matter

- The stability of extractants in a sequential extraction is not longer than one week and the recommended time to determine the sample after it was extracted, is five days
- Cr, Cu and Zn could be determined in extractions from a sequential scheme with confidence by ICP-AES, in contrast to Ni and Pb, which have poor limits of detection
- If the liner is to be characterised, the samples must be taken from the liner already placed in the landfill site
- soil pH measured in water is satisfactory. However, another method could be tested for comparison

A sampling proposal was developed, taking into consideration the results of the analytical determinations carried out on the exploratory samples. This new sampling campaign would be carried out in the bottom of the landfill cell, using a regular grid design. The number of samples to be taken was 30, within a depth of 0 to 1.5 m. The strata to characterise will be the liner itself, already compacted and placed.

Chapter 5. The assessment campaign

5.1. Introduction

Once the geochemical parameters that affect attenuation in the Oxford Clay were identified, and the best methods and analytical techniques were chosen to characterise the Oxford clay, an assessment sampling was designed. The study was carried out using material from the engineered base of the L-field site north site. The samples were taken from the top of the clay liner in a newly constructed cell. This is an important zone in the landfill since the clay liner forms the last barrier for leachate as it migrates from the landfill.

In this chapter the sampling and analytical determinations applied to the assessment samples are detailed. The results from this study are given and discussed. The most relevant result of the assessment sample characterisation was the identification of a layer rich in pyrite (with an acid pH) beneath the compacted clay liner system. The causes of its acid pH and its influence on the liner systems are also discussed in this chapter.

5.2. The assessment sampling

The area to be sampled was 4800 m^2; the regular grid to cover this area had thirteen m intervals to the south-west and a ten m intervals to the north-east. 27 samples were taken in the regular grid, plus eight random samples were collected.

The sampling depth was 20 cm from the top, The location of this detailed sampling in the L-field site and the assessment sampling points are given in Figures 5.1 and 5.2, respectively.

The details of the assessment sampling are given in the Appendix 2. The assessment sampling report.



Figure 5.1. The assessment sampling location at L-field site landfill.

5.3. Sample pre-treatment

The samples were weighed and air-dried. Drying took three days to be completed. They were ground after dryness, passed through a stainless steal sieve of 2 mm and kept in sealed plastic bags at room temperature.

5.4. Analytical determinations on the assessment samples

A number of soil geochemical parameters were determined as follows:

- Clay content and iron and manganese hydrous-oxide content were calculated from the mineralogical composition using X-ray diffraction (Batchelder and Cressey, 1998)
- Organic carbon content was estimated by Weight Loss-on-Ignition method (Tan *et al*, 1996)

- Soil pH was determined by the 0.01 M $CaCl_2$ method and measurement in water (Carter, 1993)
- The Cation Exchange Capacity (CEC) and the exchangeable cations were determined using the method developed by Amrhein and Suarez (1990)

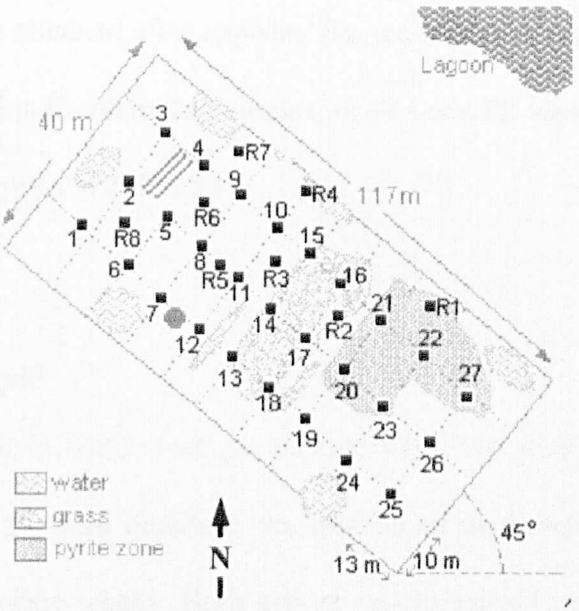


Figure 5.2. The assessment sampling points.

The effect of the geochemical parameters was identified by the localisation of selected heavy metals: Cd, Cu, Cr, Ni, Zn and Pb bound to solid phases, using:

- The sequential extraction method developed by Tessier et al (1979), using ICP-AES
- Total digestion using HF-$HClO_4$ method was applied to determine the total concentration of metals

5. 5. Result from the assessment sample characterisation

5.5.1. Total digestion using the HF-$HClO_4$ method and ICP-AES

This method was applied to determine the total concentration of Cd, Cr, Cu, Ni, Pb and Zn in the samples. This total concentration determination was used as a first control of the sequential extraction applied on the same samples, that is the sum of the concentrations in the fraction obtained after applying the sequential extraction, should be less than the total concentration found in the samples. In all cases Pb was below the limit of detection. The results are given in Table 5.1.

5.5.2. Determination of soil pH

The method of measurement in water was the applied first, but when the results of samples 22, 23, 24, 25 and 27 were obtained, the method of measurement in 0.01 M $CaCl_2$ was applied to corroborate results. Both sets of results agreed within a range of 10%, as shown in Table 5.2.

The pH measurement in 0.01 M $CaCl_2$ of 18 assessment samples was higher than those pH measurements in water, this was due to the increase of salt concentration. For acidic soils with a net positive charge the increase in salt concentration causes H^+ to be adsorbed on to reactive sites, this results in a solution pH increase by up to 0.5 units (Rowell, 1994). The reason why few samples rather than all showed salt increase could be due to spatial variability of salt in the field.

Table 5.1. Total concentration of heavy metals on assessment samples, values are given in mg kg^{-1}.

Sample	Zn	Ni	Cu	Cd	Cr
1	121 ± 24	57 ± 10	23 ± 1	< 11	101 ± 11
2	165 ± 6	74 ± 7	27 ± 1	"	102 ± 24
3	157 ± 19	65 ± 19	27 ± 1	11 ± 2	105 ± 2
4	157 ± 8	63 ± 8	26 ± 0.3	< 11	106 ± 6
5	132 ± 14	53 ± 6	25 ± 1	"	100 ± 4
6	152 ± 22	62 ± 7	24 ± 1	"	103 ± 7
7	123 ± 4	57 ± 9	20 ± 0.3	14 ± 2	106 ± 3
8	134 ± 6	55 ± 8	20 ± 0.4	15 ± 3	108 ± 3
9	127 ± 5	91 ± 7	30 ± 1	< 11	120 ± 5
10	116 ± 8	84 ± 7	22 ± 1	15 ± 2	113 ± 5
11	143 ± 29	54 ± 9	21 ± 1	12 ± 2	108 ± 6
12	134 ± 7	48 ± 9	20 ± 0.3	15 ± 3	115 ± 2
13	136 ± 8	< 9	22 ± 1	< 11	110 ± 9
14	124 ± 7	61 ± 4	19 ± 1	19 ± 7	115 ± 3
15	119 ± 6	< 9	22 ± 1	< 11	89 ± 4
16	126 ± 6	"	24 ± 1	"	100 ± 5
17	170 ± 27	53 ± 8	22 ± 1	10 ± 2	96 ± 3
18	110 ± 15	53 ± 8	22 ± 3	< 11	106 ± 21
19	114 ± 12	51 ± 5	18 ± 1	9 ± 2	73 ± 5
20	125 ± 25	< 9	29 ± 4	< 11	126 ± 5
21	110 ± 15	51 ± 3	22 ± 0.3	"	124 ± 4
22	44 ± 7	91 ± 7	8 ± 1	"	78 ± 3
23	70 ± 7	95 ± 11	9 ± 1	"	60 ± 4
24	103 ± 18	105 ± 11	6 ± 1	"	38 ± 4
25	78 ± 19	61 ± 8	7 ± 0.3	13 ± 2	81 ± 5
26	126 ± 9	52 ± 7	4 ± 0.2	21 ± 2	71 ± 8
27	54 ± 9	52 ± 8	11 ± 1	< 11	93 ± 3
R1	121 ± 7	53 ± 9	14 ± 0.4	"	98 ± 10
R2	111 ± 12	62 ± 10	18 ± 1	"	91 ± 4
R3	117 ± 9	< 9	21 ± 1	"	102 ± 2
R4	117 ± 9	46 ± 4	19 ± 1	"	95 ± 6
R5	**353 ± 43**	53 ± 6	19 ± 1	"	99 ± 4
R6	141 ± 18	43 ± 6	18 ± 2	"	99 ± 2
R7	122 ± 6	44 ± 7	17 ± 1	"	91 ± 6
R8	118 ± 16	50 ± 3	36 ± 1	"	106 ± 1

Table 5.2. Results for the soil pH measurement.

Sample	in water	in 0.01 M $CaCl_2$
1	7.2 ± 0.1	7.3 ± 0.2
2	7.4 ± 0.0_2	7.5 ± 0.0_4
3	7.6 ± 0.0_1	7.6 ± 0.0_3
4	7.8 ± 0.0_1	7.7 ± 0.0_1
5	7.4 ± 0.2	7.5 ± 0.0_1
6	7.4 ± 0.1	7.5 ± 0.0_2
7	7.2 ± 0.0_2	7.7 ± 0.0
8	7.6 ±0.0	7.6 ± 0.0_1
9	7.7 ± 0. 0_1	7.6 ± 0.0_1
10	7.8 ± 0.0_4	7.4 ± 0.0_3
11	7.8 ± 0.0_4	7.4 ± 0.0_4
12	7.4 ± 0.1	7.6 ± 0.0
13	7.6 ± 0.1	7.7 ± 0.0_1
14	7.4 ± 0.1	7.2 ± 0.1
15	7.3 ± 0.2	7.4 ± 0.0_2
16	7.7 ± 0.0_1	7.3 ± 0.1
17	7.7 ± 0.0_4	7.4 ± 0.0_1
18	7.6 ± 0.0_3	7.5 ± 0.0_1
19	6.5 ± 0.0	6.3 ± 0.1
20	7.7 ± 0.0_3	7.5 ± 0.0
21	7.2 ± 0.1	7.4 ± 0.0_4
22	**2.8** ± 0.1	**2.7** ± 0.0_1
23	**3.9** ± 0.0_4	**4.1** ± 0.1
24	**2.5** ± 0.0_1	**2.6** ± 0.0
25	**2.9** ± 0.1	**2.7** ± 0.0_1
26	6.9 ± 0.0_2	7.3 ± 0.1
27	**4.5** ± 0.0_1	**4.9** ± 0.1
R1	6.8 ± 0.1	7.0 ± 0.0_1
R2	7.2 ± 0.0_1	7.5 ± 0.0_1
R3	7.3 ± 0.3	7.6 ± 0.0_4
R4	7.6 ± 0.0_1	7.7 ± 0.0
R5	7.8 ± 0.0_2	7.5 ± 0.0
R6	7.2 ± 0.1	7.6 ± 0.1
R7	7.8 ± 0.1	7.5 ± 0.0
R8	7.3 ± 0.0_1	7.2 ± 0.2

5.5.3. The mineralogical composition

A mineralogical composition determination was carried out on samples from the acid pH zone and neutral-alkaline zone to explain the differences in pH measured across the base of the exposed landfill cell. The results are shown in Table 5.3.

Table 5.3. Mineralogical composition of the two pH zones.

	neutral-alkaline, wt %	acid, wt %
quartz	26-29	23-32
plagioclase	1-2	0-3
calcite	1	0-1
dolomite	0-1	0
gypsum	3	17-24
amorphous Fe oxide	1-3	8-9
natrojarosite	0	trace
pyrite	2-3	1-5
anatase	1	0-1
muscovite	0-2	0-1
chamosite	1	trace
kaolinite	16-17	6-9
near-illite	20-27	17-19
illite-smectite	16-18	8-12

It can be seen that the two zones vary in composition. Samples in the neutral alkaline zone (pH 7-7.7) belong to the compacted liner. There is a layer underneath rich in pyrite (pH 2.6- 6.5).

The neutral-alkaline zone shows fairly continuous pH values. This is not the case for the acid zone. The natural acidification in the acid region is a result of the oxidation of iron pyrites (FeS_2). This produces hydrogen ions (H^+) in abundance. The overall oxidation of pyrite may be represented by the following reaction (Milodowski *et al*, 1986):

$$4FeS_2 + 15O_2 + 14\,H_2O \rightarrow 4Fe(OH)_3 + 16H^+ + 8SO_4^{2-} \qquad (1)$$

The pyrite content in samples varies from 1- 5 wt %. When all the pyrite in one g of the average clay is oxidised, the molar concentration of H^+ produced by reaction (1) will be 0.0011, representing a pH of 2.96.

Pyrite can be oxidised directly by oxygenated water or by the reduction of ferric iron (Fe^{3+}) in aqueous solution. In surface or near-surface environments, the oxidation of the

ferrous (Fe^{2+}) to ferric (Fe^{3+}) ion is thermodynamically favourable and is probably controlled by bacteria such as *Thiobacillus ferroxidans*, which uses the energy released by this reaction (Milodowski *et al*, 1986).

From Table 5.3, it can be seen that the content of amorphous iron oxide in the acid region (via reaction (2)) is higher than in the neutral-slightly alkaline one. This suggests that originally there was more pyrite present than has been degraded and neutralised with calcite resulting in the precipitation of large quantities of gypsum, (via reaction (3)).

$$2Fe^{3+} + 6H_2O \rightarrow Fe_2O_3 \bullet 3H_2O + 6H^+ \qquad (2)$$

$$CaCO_3 + SO_4^{2-} + 2H^{2+} \rightarrow CaSO_4 \bullet 2H_2O + CO_2 \qquad (3)$$

It can be seen that, the most redox sensitive parameters are pyrite and iron oxides.

Conclusions:

When comparing the mineralogical composition for the two zones it can be concluded that:

- The layer rich in pyrite is still undergoing a weathering process, with pyrite as the most redox sensitive component. Oxidation of pyrite produces sulphuric acid, leaching of carbonate minerals, and increases of gypsum and amorphous Fe oxides. Gypsum may cause expansion and disruption of the clay or concrete fabric. However, the increase of the amorphous Fe oxides will increase the sorption and cation exchange properties of the clay
- On the other hand, the compacted clay liner offers a more stable zone, where pyrite has not been oxidised and gypsum has not been generated. The clay mineral concentration in the compacted clay liner is high; this will increase the cation exchange properties of the clay. From the clay minerals, smectite (for its swelling properties) will give the effective "seal" character to the clay.

5.5.4. Determination of organic carbon content by the Loss-On-Ignition method

The organic matter content influences many soil properties such as: content of N, P and S, infiltration and retention of water, degree of aggregation and overall structure that affect the relationship air-water, cation exchange capacity, soil colour (that impact on the temperature relationships), adsorption of agricultural chemicals (Tan *et al*, 1996). The results of the determination of organic carbon content by Loss-On-Ignition (LOI) method are given in Table 5.4.

Observations:

Results coincide with the lowest organic contents (1-2.3 %) reported previously, to be found in the silts and silty clays near the top of the sequence and shell beds (Milodowski *et al*, 1986).

5.5.5. The cation exchange capacity and the exchangeable cations

The cation exchange capacity (CEC) is the capacity of the soil to hold and exchange cations (Tan, 1996b). It has its origins on the negatively charged soil particles, such as clay, organic matter and sesquioxides. CEC can only be determined in an operational way because the charge of the soil components depends strongly on the conditions in the ambient solution. Variations in soil can affect cation selectivity of soil clays; it is then recommended to avoid determination on soil samples with pH levels below 4.5 to 5 (Tan, 1996a).

The method of Amrhein and Suarez (1990) was selected to determine CEC and exchangeable cations on the assessment samples, because this method determines these parameters in soils containing carbonates. As seen before, the assessment samples have gypsum and carbonates in their mineralogical composition. Five samples with acid pH were not analysed for their CEC and exchangeable cation content. From the other

remaining 30 samples, only 24 were determined because of analytical complications. The results for the CEC and exchangeable cations are given in Table 5.5.

Table 5.4. Organic matter content determined by the LOI method.

Sample	LOI, %
1	2.6
2	3.1
3	2.2
4	2.7
5	2.3
6	2.7
7	3.0
8	2.9
9	2.0
10	2.3
11	2.8
12	2.8
13	2.2
14	2.0
15	1.8
16	2.7
17	2.8
18	2.4
19	2.6
20	2.7
21	2.4
22	1.0
23	1.7
24	1.4
25	2.4
26	1.1
27	1.5
R1	1.6
R2	2.7
R3	2.6
R4	2.5
R5	1.8
R6	2.4
R7	2.1
R8	2.2

Observations

- CEC values are between 19-71 $cmol_c\ kg^{-1}$, this agrees well with the CEC values reported as commonly found in clay, which is in the range 4-60 $cmol_c\ kg^{-1}$ (Rowell, 1994)
- Ca^{2+} dominates the CEC in the assessment samples. It varies from 63-84 % of the CEC
- Mg^{2+} is the second most important exchangeable cation, and it is 11-29 % of the CEC
- The Ca^{2+}:Mg^{2+} ratios vary from 1:2 to 1:7, these values agree with those previously reported - between 5:1 and 1:2- by Rowell (1994)
- Na^{+} and K^{+} are 1-12 % and 0-4 %, respectively, of the CEC. It had been reported that K^{+} may be up to 5 % of the CEC (Rowell, 1994)

5.5.6. The fractionation of Ni, Cu, Zn, and Cd in solid phases using a sequential extraction method and ICP-AES

The fractionation of Cd, Cr, Cu, Ni, Pb and Zn as natural components in solid phases by sequential extractions was determined by the ICP-AES system, Jobin Yvon JY24, (power 1.1 kW, cooling gas: 16 L/min, sheating gas: 0.18 L/min, nebulizer pressure 40 psi, aerosol flow rate: 0.69 L/min, nebulizer gas: 0.3 L/min).

"Spectral profiles" of sample, blank and matrix matched standards were obtained for each element in every extraction step, in order to choose the most suitable wavelength that did not show any interference. The wavelengths used are those shown in Table 4.6.

Table 5.5. CEC and exchangeable cations in the assessment samples, values are given in centimoles of cation charge per kilogram ($cmol_c\,kg^{-1}$).

Sample	Mg^{2+}	Na^{+}	K^{+}	Ca^{2+}	CEC
1	10.9 ± 0.6	4.5 ± 0.1	1.13 ± 0.02	38 ± 2	55 ± 2
2	19.4 ± 0.4	5.0 ± 0.2	1.28 ± 0.04	45 ± 1	71 ± 1
3	11.2 ± 1.1	4.2 ± 0.1	1.18 ± 0.03	43 ± 1	60 ± 1
4	8.6 ± 0.4	4.3 ± 0.0	1.18 ± 0.05	40 ± 1	54 ± 1
9	6.1 ± 0.2	1.9 ± 0.1	1.28 ± 0.02	27 ± 1	36 ± 1
10	5.9 ± 0.2	2.5 ± 0.1	1.33 ± 0.01	42 ± 2	52 ± 2
11	6.9 ± 0.2	5.4 ± 0.1	1.28 ± 0.07	36 ± 1	50 ± 1
12	6.7 ± 0.1	2.9 ± 0.0	1.28 ± 0.01	21 ± 2	32 ± 2
13	7.2 ± 0.1	3.6 ± 0.1	1.33 ± 0.05	26 ± 3	38 ± 3
14	6.9 ± 0.2	2.3 ± 0.1	1.23 ± 0.03	23 ± 2	33 ± 2
15	7.7 ± 0.1	5.2 ± 0.2	1.48 ± 0.04	28 ± 1	42 ± 1
16	6.9 ± 0.1	1.4 ± 0.1	1.13 ± 0.03	48 ± 2	57 ± 2
17	4.4 ± 0.1	2.5 ± 0.0	0.72 ± 0.05	28 ± 3	36 ± 3
18	4.8 ± 0.5	3.5 ± 0.3	0.66 ± 0.05	23 ± 1	32 ± 1
19	6.6 ± 0.3	1.0 ± 0.0	0.20 ± 0.01	42 ± 1	50 ± 1
20	5.4 ± 0.4	2.4 ± 0.0	0.77 ± 0.02	25 ± 1	34 ± 1
21	5.6 ± 0.0	1.9 ± 0.1	0.66 ± 0.04	19 ± 1	27 ± 1
26	6.7 ± 0.0	1.8 ± 0.0	0.20 ± 0.04	38 ± 1	47 ± 1
R1	8.6 ± 0.1	0.3 ± 0.0	0.41 ± 0.03	21 ± 1	30 ± 1
R2	6.3 ± 0.2	1.2 ± 0.0	0.56 ± 0.02	16 ± 1	24 ± 1
R3	5.1 ± 0.1	2.3 ± 0.0	0.72 ± 0.05	24 ± 1	32 ± 1
R4	3.0 ± 0.2	1.0 ± 0.1	0.56 ± 0.01	14 ± 1	19 ± 1
R5	4.6 ± 0.3	2.9 ± 0.1	0.61 ± 0.06	23 ± 2	31 ± 2
R6	4.4 ± 0.2	2.4 ± 0.2	0.77 ± 0.01	18 ± 1	26 ± 1

The sequential extraction method of Tessier *et al* (1979) was applied and a total of 1750 determinations were carried out using ICP-AES. Four batches of 9 samples (each with a respective replicate) and two blanks were prepared for easier handling and treatment of samples. Each extraction was centrifuged at 2000 rpm for 30 min. The extracted solution was kept for analysis at 4-5 °C, a water wash was applied for 10 min in the sample, after that the sample was centrifuged again and the supernatant was thrown away, before start the next extraction.

All measurements were completed in a period of one week because in previous experiments the extract stability was no longer reliable after this period.

The results from the sequential extraction on liner samples are given from Tables 5.6 to 5.10.

Table 5.6. Results for the fraction of heavy metals as exchangeable forms, values are given in mg kg^{-1}.

Sample	Zn	Ni	Cu	Cd	Cr
1	< 0.13	< 2.41	< 0.13	< 1.67	< 1.17
2	"	"	"	"	"
3	"	"	"	"	"
4	"	"	"	"	"
5	"	"	"	"	"
6	"	"	"	"	"
7	"	"	"	"	"
8	"	"	"	"	"
9	"	"	"	"	"
10	"	"	"	"	"
11	"	"	"	"	"
12	"	"	"	"	"
13	"	"	"	"	"
14	"	"	"	"	"
15	"	"	"	"	"
16	"	"	"	"	"
17	"	"	"	"	"
18	"	"	"	"	"
19	7 ± 0.4	"	"	"	"
20	< 0.13	"	"	"	"
21	"	"	"	"	"
22	8 ± 0.1	"	1.4 ± 0.1	"	"
23	5 ± 0.2	"	< 0.13	"	"
24	53 ± 3	"	0.9 ± 0.04	"	"
25	10 ± 1	"	1.2 ± 0.1	13.7 ± 1.7	19.5 ± 1.4
26	< 0.13	"	< 0.13	< 1.67	19.7 ± 2.2
27	5 ± 0.3	"	"	"	14.1 ± 1.1
R1	< 0.13	"	"	"	17.0 ± 1.0
R2	"	"	"	"	< 1.17
R3	"	"	"	"	"
R4	"	"	"	"	"
R5	"	"	"	"	"
R6	"	"	"	"	"
R7	"	"	"	"	"
R8	"	"	"	"	"

Observations:

- In general there was a lower concentration of metals in the samples from the acid zone, suggesting that those metals were solubilised.

Table 5.7. Results for the heavy metal fraction bound to carbonates, values are given in mg kg^{-1}.

Sample	Zn	Ni	Cu	Cd	Cr
1	7.5 ± 0.6	< 0.20	< 0.02	< 0.91	< 0.30
2	10.0 ± 0.8	"	"	"	"
3	10.2 ± 1.7	"	"	"	"
4	6.6 ± 1.5	"	"	"	"
5	11.2 ± 1.0	"	2.89 ± 0.18	"	"
6	< 0.29	"	< 0.02	"	"
7	8.5 ± 1.2	"	2.54 ± 0.18	"	"
8	9.3 ± 1.1	"	2.42 ± 0.15	"	"
9	8.6 ± 1.1	"	2.97 ± 0.60	"	"
10	10.1 ± 2.2	"	< 0.02	"	"
11	10.6 ± 2.0	"	"	"	"
12	< 0.29	"	"	"	"
13	"	"	"	"	"
14	"	"	"	"	"
15	"	"	"	"	"
16	"	"	"	"	"
17	"	"	"	"	"
18	"	"	2.97 ± 0.67	"	"
19	"	"	2.23 ± 0.22	"	"
20	"	"	3.50 ± 0.16	"	"
21	8.8 ± 1.5	"	< 0.02	"	"
22	< 0.29	"	"	"	"
23	"	"	"	"	"
24	"	"	"	"	"
25	"	"	"	5.8 ± 1.2	"
26	"	"	"	< 0.91	"
27	"	"	"	"	"
R1	12.1 ± 1.6	"	"	"	"
R2	< 0.29	"	"	"	"
R3	9.3 ± 1.1	"	"	"	"
R4	< 0.29	"	"	"	"
R5	14.4 ± 0.9	"	"	"	"
R6	13.6 ± 1.1	"	"	"	"
R7	10.6 ± 0.1	"	"	"	"
R8	12.3 ± 0.7	"	"	"	"

- The measurements of Cd and Ni are not reliable by ICP-AES. All Ni is presumably bound to Fe-Mn oxides, however the concentration in that fraction exceeded the Ni total concentrations.

Table 5.8. Results for the heavy metal fraction bound to Fe-Mn oxides, values are given in mg kg^{-1}.

Sample	Zn	Ni	Cu	Cd	Cr
1	29 ± 5	76 ± 13	< 0.08	< 0.48	< 0.29
2	39 ± 4	63 ± 11	"	"	"
3	41 ± 4	46 ± 8	"	"	"
4	38 ± 1	72 ± 7	"	"	"
5	42 ± 6	68 ± 11	"	"	"
6	47 ± 3	130 ± 16	"	"	"
7	39 ± 3	69 ± 9	"	"	"
8	26 ± 3	87 ± 9	"	"	"
9	40 ± 3	89 ± 7	"	"	"
10	36 ± 3	142 ± 12	"	"	"
11	35 ± 3	132 ± 12	"	"	"
12	36 ± 4	146 ± 7	"	"	"
13	39 ± 4	147 ± 5	"	"	"
14	34 ± 2	147 ± 16	"	"	"
15	35 ± 5	128 ±11	"	"	"
16	23 ± 3	104 ± 13	"	"	"
17	31 ± 4	120 ±23	"	"	"
18	30 ± 4	69 ± 11	"	"	"
19	48 ± 4	81 ± 5	"	"	"
20	29 ± 3	76 ± 13	"	"	"
21	29 ± 3	90 ± 11	"	"	"
22	$3 \pm 0_{.4}$	85 ± 11	"	"	"
23	10 ± 1	62 ± 4	"	"	"
24	9 ± 1	71 ± 10	"	"	"
25	8 ± 1	79 ± 6	"	"	"
26	9 ± 1	61 ± 3	"	"	"
27	7 ± 1	60 ± 7	"	"	"
R1	37 ± 3	58 ± 10	"	"	"
R2	34 ± 4	65 ± 9	"	"	"
R3	46 ± 3	94 ± 8	"	"	"
R4	30 ± 2	102 ± 9	"	"	"
R5	47 ± 5	89 ± 9	"	"	"
R6	47 ± 6	105 ± 9	"	"	"
R7	30 ± 3	77 ± 6	"	"	"
R8	38 ±4	70 ± 7	"	"	"

- The fraction bound to carbonates was affected by pH changes to a lesser extent, this is because the carbonate itself was involved in neutralisation of the acid component of the system.

Table 5.9. Results for the heavy metal fraction bound to organic matter, values are given in mg kg^{-1}.

Sample	Zn	Ni	Cu	Cd	Cr
1	33 ± 2	< 0.02	18.0 ± 1.1	< 0.18	4.3 ± 0.4
2	38 ± 2	"	18.4 ± 1.2	"	4.1 ± 0.4
3	40 ± 2	"	18.9 ± 1.0	"	4.1 ± 0.4
4	39 ± 2	"	17.8 ± 0.6	"	4.0 ± 0.3
5	44 ± 2	"	20.7 ± 0.9	3.8 ± 0.5	5.1 ± 0.2
6	38 ± 1	"	16.5 ± 0.6	< 0.18	5.0 ± 0.5
7	33 ± 2	"	16.2 ± 0.7	"	3.1 ± 0.1
8	40 ± 2	"	19.1 ± 0.8	"	4.4 ± 0.2
9	43 ± 2	"	16.4 ± 0.7	"	5.5 ± 0.3
10	44 ± 2	"	18.6 ± 0.8	"	5.4 ± 0.3
11	36 ± 1	"	15.0 ± 0.9	"	5.0 ± 0.2
12	50 ± 4	"	16.4 ± 1.2	"	4.1 ± 0.6
13	39 ± 2	"	16.7 ± 1.0	4.44 ±0.7	4.6 ± 0.3
14	39 ± 2	"	16.4 ± 0.9	< 0.18	4.5 ± 0.3
15	36 ± 1	"	14.8 ± 1.0	"	3.9 ± 0.3
16	34 ± 2	"	18.1 ± 1.3	"	5.5 ± 0.1
17	28 ± 2	"	11.6 ± 1.1	"	3.8 ± 0.4
18	42 ± 3	"	16.2 ± 1.1	"	6.4 ± 0.4
19	34 ± 3	"	8.6 ± 0.5	"	3.5 ± 0.3
20	48 ± 3	"	11.7 ± 0.7	"	4.6 ± 0.1
21	38 ± 2	"	11.3 ± 0.8	"	4.5 ± 0.1
22	$4 \pm 0_{.3}$	"	7.0 ± 0.9	"	$1.2 \pm 0.0_4$
23	$6 \pm 0_{.4}$	"	7.3 ± 0.8	"	3.0 ± 0.2
24	9 ± 1	"	5.9 ± 0.5	"	$1.2 \pm 0.0_4$
25	8 ± 1	"	5.5 ± 0.4	"	$1.5 \pm 0.0_3$
26	38 ± 1	"	15.6 ± 0.9	"	4.4 ± 0.2
27	7 ± 1	"	10.3 ± 0.6	"	2.9 ± 0.1
R1	20 ± 1	"	15.0 ± 0.9	"	4.3 ± 0.1
R2	36 ± 1	"	16.1 ± 0.9	"	4.6 ± 0.3
R3	39 ± 2	"	16.4 ± 0.5	"	4.7 ± 0.3
R4	40 ± 2	"	16.5 ± 0.4	"	4.7 ± 0.3
R5	41 ± 2	"	16.1 ± 0.9	"	4.6 ± 0.2
R6	39 ± 2	"	16.4 ± 1.1	"	4.7 ± 0.3
R7	40 ± 2	"	16.0 ± 0.9	"	4.6 ± 0.2
R8	39 ± 2	"	15.4 ± 0.9	"	4.4 ± 0.2

Table 5.10. Results for the heavy metals in the residuals, values are given in mg kg^{-1}.

Sample	Zn	Ni	Cu	Cd	Cr
1	49 ± 4	< 0.09	3.1 ± 0.4	< 0.18	91 ± 7
2	75 ± 8	"	5.3 ± 0.4	"	94 ± 7
3	62 ± 7	"	5.0 ± 0.4	9.0 ± 2	96 ± 6
4	71 ± 7	"	4.9 ± 0.4	< 0.18	100 ± 7
5	32 ± 3	"	< 0.06	"	91 ± 8
6	64 ± 7	"	4.5 ± 0.4	"	94 ± 7
7	40 ± 5	"	< 0.06	11 ± 2	100 ± 6
8	55 ± 8	"	"	11 ± 2	100 ± 7
9	30 ± 4	"	7.6 ± 0.6	< 0.18	110 ± 6
10	21 ± 3	"	< 0.06	"	102 ± 5
11	57 ± 8	"	3.0 ± 0.4	11 ± 2	103 ± 5
12	44 ± 5	"	< 0.06	11 ± 2	107 ± 6
13	54 ± 8	"	2.9 ± 0.4	< 0.18	101 ± 5
14	48 ± 5	"	< 0.06	15 ± 2	106 ± 6
15	44 ± 5	"	3.2 ± 0.4	< 0.18	81 ± 5
16	65 ± 8	"	2.8 ± 0.4	"	101 ± 5
17	105 ± 9	"	7.4 ± 0.5	9 ± 2	88 ± 5
18	34 ± 4	"	< 0.06	< 0.18	96 ± 5
19	25 ± 3	"	3.1 ± 0.4	"	66 ± 4
20	44 ± 5	"	10.5 ± 0.5	"	117 ± 6
21	30 ± 4	"	7.7 ± 0.6	"	116 ± 6
22	25 ± 3	"	< 0.06	"	74 ± 4
23	44 ± 5	"	"	"	54 ± 4
24	26 ± 3	"	"	"	33 ± 3
25	44 ± 5	"	"	"	56 ± 4
26	75 ± 8	"	"	19 ± 2	44 ± 4
27	30 ± 4	"	"	< 0.18	72 ± 5
R1	47 ± 3	"	"	"	73 ± 4
R2	36 ± 4	"	"	"	84 ± 4
R3	18 ± 2	"	"	"	94 ± 6
R4	42 ± 4	"	"	"	87 ± 4
R5	108 ± 9	"	"	"	91 ± 6
R6	36 ± 4	"	"	"	91 ± 4
R7	36 ± 4	"	"	"	83 ± 4
R8	22 ± 3	"	15.5 ± 0.5	"	97 ± 7

As mentioned previously, the total concentration determination can be used to check the sequential extraction applied to the same samples. The sum of the concentrations in the fraction obtained after applying the sequential extraction, should be less than the total concentration found in the samples. A comparison between the sum of concentration of Zn, Cr and Cu in the fractions obtained using the sequential extraction method versus the

total concentration obtained using the $HF\text{-}HClO_4$ method is given in Tables 5.11 to 5.13. Only Zn, Cu and Cr are shown because the determination of Ni and Cd were not reliable, as previously described. The standards devations reported next to the mean under the Σ symbol were calculated as described in page 78.

Table 5.11. Comparison between the total concentration of Zn versus the sum of concentration of Zn in solid fractions, values are given in mg kg^{-1}.

Sample	Zn						Zn_{total}
	exchangeable	bound to carbonates	bound to Fe-Mn oxides	bound to organic matter	in the residuals	Σ	$HF\text{-}HCl_4$
1	< 0.13	7.5 ± 0.6	29 ± 5	33 ± 2	49 ± 4	119 ± 7	121 ± 24
2	"	10.0 ± 0.8	39 ± 4	38 ± 2	75 ± 8	163 ± 9	165 ± 6
3	"	10.2 ± 1.7	41 ± 4	40 ± 2	62 ± 7	153 ± 9	157 ± 19
4	"	6.6 ± 1.5	38 ± 1	39 ± 2	71 ± 7	155 ± 8	157 ± 8
5	"	11.2 ± 1.0	42 ± 6	44 ± 2	32 ± 3	129 ± 7	132 ± 14
6	"	< 0.29	47 ± 3	38 ± 1	64 ± 7	149 ± 8	152 ± 22
7	"	8.5 ± 1.2	39 ± 3	33 ± 2	40 ± 5	121 ± 6	123 ± 4
8	"	9.3 ± 1.1	26 ± 3	40 ± 2	55 ± 8	130 ± 9	134 ± 6
9	"	8.6 ± 1.1	40 ± 3	43 ± 2	30 ± 4	122 ± 6	127 ± 5
10	"	10.1 ± 2.2	36 ± 3	44 ± 2	21 ± 3	111 ± 5	116 ± 8
11	"	10.6 ± 2.0	35 ± 3	36 ± 1	57 ± 8	139 ± 9	143 ± 29
12	"	< 0.29	36 ± 4	50 ± 4	44 ± 5	130 ± 8	134 ± 7
13	"	"	39 ± 4	39 ± 2	54 ± 8	132 ± 9	136 ± 8
14	"	"	34 ± 2	39 ± 2	48 ± 5	121 ± 6	124 ± 7
15	"	"	35 ± 5	36 ± 1	44 ± 5	115 ± 7	119 ± 6
16	"	"	23 ± 3	34 ± 2	65 ± 8	122 ± 9	126 ± 6
17	"	"	31 ± 4	28 ± 2	105 ± 9	164 ± 10	170 ± 27
18	"	"	30 ± 4	42 ± 3	34 ± 4	106 ± 6	110 ± 15
19	$7 \pm 0_{.4}$	"	48 ± 4	34 ± 3	25 ± 3	114 ± 6	114 ± 12
20	< 0.13	"	29 ± 3	48 ± 3	44 ± 5	121 ± 7	125 ± 25
21	"	8.8 ± 1.5	29 ± 3	38 ± 2	30 ± 4	106 ± 6	110 ± 15
22	$8 \pm 0_{.1}$	< 0.29	$3 \pm 0_{.4}$	$4 \pm 0_{.3}$	25 ± 3	40 ± 3	44 ± 7
23	$5 \pm 0_{.2}$	"	10 ± 1	$6 \pm 0_{.4}$	44 ± 5	65 ± 5	70 ± 7
24	53 ± 3	"	9 ± 1	9 ± 1	26 ± 3	97 ± 5	103 ± 18
25	10 ± 1	"	8 ± 1	8 ± 1	44 ± 5	70 ± 5	78 ± 19
26	< 0.13	"	9 ± 1	38 ± 1	75 ± 8	122 ± 8	126 ± 9
27	$5 \pm 0_{.3}$	"	7 ± 1	7 ± 1	30 ± 4	49 ± 4	54 ± 9
R1	< 0.13	12.1 ± 1.6	37 ± 3	20 ± 1	47 ± 3	116 ± 5	121 ± 7
R2	"	< 0.29	34 ± 4	36 ± 1	36 ± 4	106 ± 6	111 ± 12
R3	"	9.3 ± 1.1	46 ± 3	39 ± 2	18 ± 2	112 ± 4	117 ± 9
R4	"	< 0.29	30 ± 2	40 ± 2	42 ± 4	112 ± 5	117 ± 9
R5	"	14.4 ± 0.9	47 ± 5	41 ± 2	108 ± 9	210 ± 11	**353 ± 43**
R6	"	13.6 ± 1.1	47 ± 6	39 ± 2	36 ± 4	136 ± 8	141 ± 18
R7	"	10.6 ± 0.1	30 ± 3	40 ± 2	36 ± 4	117 ± 5	122 ± 6
R8	"	12.3 ± 0.7	38 ± 4	39 ± 2	22 ± 3	111 ± 5	118 ± 16

Table 5.12. Comparison between the total concentration of Cu versus the sum of concentration of Cu in solid fractions, values are given in mg kg^{-1}.

Sample	Cu						Cu_{total}
	exchangeable	bound to carbonates	bound to Fe-Mn oxides	bound to organic matter	in the residuals	Σ	$HF-HCl_4$
1	< 0.13	< 0.02	< 0.08	18.0 ± 1.1	3.1 ± 0.4	21.1 ± 1.2	23 ± 1
2	"	"	"	18.4 ± 1.2	5.3 ± 0.4	23.7 ± 1.3	27 ± 1
3	"	"	"	18.9 ± 1.0	5.0 ± 0.4	23.9 ± 1.1	27 ± 1
4	"	"	"	17.8 ± 0.6	4.9 ± 0.4	22.7 ± 0.7	$26 \pm 0_3$
5	"	2.89 ± 0.18	"	20.7 ± 0.9	< 0.06	23.6 ± 0.9	25 ± 1
6	"	< 0.02	"	16.5 ± 0.6	4.5 ± 0.4	21.0 ± 0.7	24 ± 1
7	"	2.54 ± 0.18	"	16.2 ± 0.7	< 0.06	18.7 ± 0.7	$20 \pm 0_3$
8	"	2.42 ± 0.15	"	19.1 ± 0.8	"	21.5 ± 0.8	$20 \pm 0_4$
9	"	2.97 ± 0.60	"	16.4 ± 0.7	7.6 ± 0.6	27.0 ± 1.1	30 ± 1
10	"	< 0.02	"	18.6 ± 0.8	< 0.06	18.6 ± 0.8	22 ± 1
11	"	"	"	15.0 ± 0.9	3.0 ± 0.4	18.0 ± 1.0	21 ± 1
12	"	"	"	16.4 ± 1.2	< 0.06	16.4 ± 1.2	$20 \pm 0_3$
13	"	"	"	16.7 ± 1.0	2.9 ± 0.4	19.6 ± 1.1	22 ± 1
14	"	"	"	16.4 ± 0.9	< 0.06	16.4 ± 0.9	19 ± 1
15	"	"	"	14.8 ± 1.0	3.2 ± 0.4	18.0 ± 1.1	22 ± 1
16	"	"	"	18.1 ± 1.3	2.8 ± 0.4	20.9 ± 1.4	24 ± 1
17	"	"	"	11.6 ± 1.1	7.4 ± 0.5	19.0 ± 1.2	22 ± 1
18	"	2.97 ± 0.67	"	16.2 ± 1.1	< 0.06	19.2 ± 1.3	22 ± 3
19	"	2.23 ± 0.22	"	8.6 ± 0.5	3.1 ± 0.4	13.9 ± 0.7	18 ± 1
20	"	3.50 ± 0.16	"	11.7 ± 0.7	10.5 ± 0.5	25.7 ± 0.9	29 ± 4
21	"	< 0.02	"	11.3 ± 0.8	7.7 ± 0.6	19.0 ± 1.0	$22 \pm 0_3$
22	1.4 ± 0.1	"	"	7.0 ± 0.9	< 0.06	8.4 ± 0.9	8 ± 1
23	< 0.13	"	"	7.3 ± 0.8	"	7.3 ± 0.8	9 ± 1
24	$0.9 \pm 0.0_4$	"	"	5.9 ± 0.5	"	6.8 ± 0.5	6 ± 1
25	1.2 ± 0.1	"	"	5.5 ± 0.4	"	6.7 ± 0.4	$7 \pm 0_3$
26	< 0.13	"	"	15.6 ± 0.9	"	15.6 ± 0.9	$4 \pm 0_2$
27	"	"	"	10.3 ± 0.6	"	10.3 ± 0.6	11 ± 1
R1	"	"	"	15.0 ± 0.9	"	15.0 ± 0.9	$14 \pm 0_4$
R2	"	"	"	16.1 ± 0.9	"	16.1 ± 0.9	18 ± 1
R3	"	"	"	16.4 ± 0.5	"	16.4 ± 0.5	21 ± 1
R4	"	"	"	16.5 ± 0.4	"	16.5 ± 0.4	19 ± 1
R5	"	"	"	16.1 ± 0.9	"	16.1 ± 0.9	19 ± 1
R6	"	"	"	16.4 ± 1.1	"	16.4 ± 1.1	18 ± 2
R7	"	"	"	16.0 ± 0.9	"	16.0 ± 0.9	17 ± 1
R8	"	"	"	15.4 ± 0.9	15.5 ± 0.5	30.9 ± 1.0	36 ± 1

Observations:

- The total concentration determination is a useful and simple tool to check the performance of the sequential extraction. The sum of the concentrations in the

fraction obtained after applying the sequential extraction, was less than the total concentration found in the same samples for Zn, Cu and Cr.

Table 5.13. Comparison between the total concentration of Cr versus the sum of concentration of Cr in solid fractions, values are given in mg kg^{-1}.

Sample	Cr						Cr_{total}
	exchangeable	bound to carbonates	bound to Fe-Mn oxides	bound to organic matter	in the residuals	Σ	HF-HCl_4
1	< 1.17	< 0.30	< 0.29	4.3 ± 0.4	91 ± 7	95 ± 7	101 ± 11
2	"	"	"	4.1 ± 0.4	94 ± 7	98 ± 7	102 ± 24
3	"	"	"	4.1 ± 0.4	96 ± 6	110 ± 6	105 ± 2
4	"	"	"	4.0 ± 0.3	100 ± 7	104 ± 7	106 ± 6
5	"	"	"	5.1 ± 0.2	91 ± 8	96 ± 8	100 ± 4
6	"	"	"	5.0 ± 0.5	94 ± 7	99 ± 7	103 ± 7
7	"	"	"	3.1 ± 0.1	100 ± 6	103 ± 6	106 ± 3
8	"	"	"	4.4 ± 0.2	100 ± 7	104 ± 7	108 ± 3
9	"	"	"	5.5 ± 0.3	110 ± 6	116 ± 6	120 ± 5
10	"	"	"	5.4 ± 0.3	102 ± 5	107 ± 5	113 ± 5
11	"	"	"	5.0 ± 0.2	103 ± 5	108 ± 5	108 ± 6
12	"	"	"	4.1 ± 0.6	107 ± 6	111 ± 6	115 ± 2
13	"	"	"	4.6 ± 0.3	101 ± 5	106 ± 5	110 ± 9
14	"	"	"	4.5 ± 0.3	106 ± 6	111 ± 6	115 ± 3
15	"	"	"	3.9 ± 0.3	81 ± 5	85 ± 5	89 ± 4
16	"	"	"	5.5 ± 0.1	101 ± 5	107 ± 5	100 ± 5
17	"	"	"	3.8 ± 0.4	88 ± 5	92 ± 5	96 ± 3
18	"	"	"	6.4 ± 0.4	96 ± 5	100 ± 5	106 ± 21
19	"	"	"	3.5 ± 0.3	66 ± 4	100 ± 4	73 ± 5
20	"	"	"	4.6 ± 0.1	117 ± 6	122 ± 6	126 ± 5
21	"	"	"	4.5 ± 0.1	116 ± 6	121 ± 6	124 ± 4
22	"	"	"	1.2 ± 0.0_4	74 ± 4	75 ± 4	78 ± 3
23	"	"	"	3.0 ± 0.2	54 ± 4	57 ± 4	60 ± 4
24	"	"	"	1.2 ± 0.0_4	33 ± 3	34 ± 3	38 ± 4
25	19.5 ± 1.4	"	"	1.5 ± 0.0_3	56 ± 4	77 ± 4	81 ± 5
26	19.7 ± 2.2	"	"	4.4 ± 0.2	44 ± 4	68 ± 5	71 ± 8
27	14.1 ± 1.1	"	"	2.9 ± 0.1	72 ± 5	89 ± 5	93 ± 3
R1	17.0 ± 1.0	"	"	4.3 ± 0.1	73 ± 4	94 ± 4	98 ± 10
R2	< 1.17	"	"	4.6 ± 0.3	84 ± 4	89 ± 4	91 ± 4
R3	"	"	"	4.7 ± 0.3	94 ± 6	99 ± 6	102 ± 2
R4	"	"	"	4.7 ± 0.3	87 ± 4	92 ± 4	95 ± 6
R5	"	"	"	4.6 ± 0.2	91 ± 6	96 ± 6	99 ± 4
R6	"	"	"	4.7 ± 0.3	91 ± 4	96 ± 4	99 ± 2
R7	"	"	"	4.6 ± 0.2	83 ± 4	88 ± 4	91 ± 6
R8	"	"	"	4.4 ± 0.2	97 ± 7	101 ± 7	106 ± 1

5.5.7. Characterisation of the soil solution

A soil solution concentration determination experiment was carried out on the compacted clay liner samples with the objective of characterising the available fraction of chemicals occurring in the soil environment. The soil solution was obtained using the saturation extract method developed by United States Salinity Laboratory Staff (1969) and operationally defined by its cation content using the ICP-AES technique, and its anion content using spectrocolorimetry methods and ion chromatography. Adaptations were applied to several reference methodologies as described below.

5.5.7.1. The saturation extract

This technique was developed by the United States Salinity Laboratory Staff (1969) and it is still one of the simplest and most commonly applied on soil solution studies.

The saturation paste was prepared as recommended by the method, but because the amount of sample was small, the air-died soil sample weight was modified, instead of using 250 g, 50 g were used. The saturation criteria for 50 g was reached at around 40 mL of deionised water.

5.5.7.2. The soil-water extract

The filtration step using Buechner funnel was changed to a centrifugation one. The filtration involved a lot of manipulation, sample was lost during the process and very little soil solution was recovered; around 5 mL from 100 g. Around 15 mL of soil solution were obtained from 50 g of soil, when using centrifugation.

To avoid excessive manipulation of the sample, the saturation paste was prepared in high density polyethylene centrifuge tubes of 70 mL, with an internal diameter of 3.5 cm. The centrifugation was done at 2000 rpm, then the applied pressure was:

$$P = \frac{F}{A},$$

but $F = m * a$

then $P = \frac{m * a}{A}$

where:

F = force $[N.m^{2-}]$

A = area $[m^2]$

a = acceleration $[msec^{2-}]$

m = mass [kg]

using a sample of 50 grams:

$m = 50\ g = 0.05\ kg$

the centrifugation was carried out at 2000 rpm, that expressed in second is

$$\frac{2000}{60} = 33.3\ rps$$

The angular velocity (ω) is

$\omega = 33.3 * 2\pi = 209.44$ radians sec^{1-}

The angular accelaration $= \omega^2 r = (209.44)^2 * 0.00175\ m = 76.76\ msec^{2-}$

The force is

$F = 0.05\ kg * 76.76\ msec^{2-} = 3.84\ N$

The area is

$A = \pi * r^2 = \pi * (0.00175\ m)^2 = 9.62 \times 10^{-6}\ m^2$

Pressure

$$P = \frac{F}{A} = \frac{3.84\ N}{9.62 \times 10^{-6}\ m^2} = 399168.4\ Pa \text{ or } 400\ kPa$$

Centrifugations carried out under pressure below 500 kPa are denominated Low-Pressure Centrifugation Displacement (Wolt, 1994).

The duration of the displacement was set to 30 mins after various trials. Changes in the anion and cation composition of the soil solution had been reported when the time varied from 20 to 240 mins (Wolt, 1994).

One more modification to the method to displace soil solution, was to extract two soil solution samples from one soil sample. One was used to determine cations, to this solution few drops of a solution 10 % of HNO_3 were added. The other was used to determine anions, to that, a drop of 1,000 mg L^{-1} of sodium hexametaphosphate solution was added (it should be added at a rate of one drop per 25 ml of extract) prior to stoppering and storing, this prevents the precipitation of calcium carbonate on standing.

The saturated paste preparation takes 24 h to be ready before extraction.

5.5.7.3. Determination of the cation content using ICP-AES

The cation content found in the soil solution, the wavelength used for the ICP-AES determination, the factor dilution applied and the calibration curve recommended to cover the cation range presented in the soil solution, are given in Table 5.14.

Observations:

- Around 15 mL of sample were needed to determine all the cations listed in Table 5.14
- The cations to be determined simultaneously in the ICP-AES can be grouped, as follows:

  1. Ca, Mg, Na
  2. K, Si
  3. Al, Fe, Pb, Zn
  4. Cd, Cr, Cu, Ni

Cations were classified according to their concentration ranges. Thus, when applying a dilution factor, all cations in a specific group can be taken to similar detectable levels. Wavelengths used to determine a specific cation were considerd too when grouping the elements listed above. The wavelengths chosen must not interfere with the rest of wavelength used to determine the others.

Table 5.14. Analytical details for the determination of cations in the ICP-AES system and the cation content in soil solution.

Cation	λ, nm	Concentration in sample, μg mL	Dilution factor to apply	Calibration curve points suggested, μg mL^{-1}
Si	251.611	9	5	1, 2, 5
Mg	279.553	99	100	0.1, 0.5, 1.0
Ca	393.366	115	100	0.1, 0.5, 1.0
Na	589.592	288	100	0.1, 0.5, 1.0
K	766.490	83	5	5, 15, 20
Al	769.896	0.51	none	1, 2, 5
Fe	238.204	1.4	none	1, 2, 5
Zn	481.053	2.4	none	1, 2, 5
Pb	220.353	0.83	none	5, 10, 20
Cd	214.438	~0.18	none	1, 2, 3
Cr	205.552	~0.13	none	1, 2, 3
Cu	324.754	~0.13	none	1, 2, 3
Ni	227.021	not detected	none	1, 2, 3

5.5.7.4. Determination of the anion content

The anions and colorimetric methods used to determine them are listed below:

- Cl^- by mercury (II) thiocyanate method (Tan *et al*, 1996)
- F^- determination using sodium 2-(parasulfophenylazo)-1,8- dihydroxy-3,6-Naphtalene bisulphate method (Tan *et al*, 1996)
- NH_4^+-N by colorimetry salicylate method (Tan *et al*, 1996)
- $H_2PO_4^-$ by spectrometry (Rowell, 1994)
- NO_2^- by a modification of the Griess-Ilosvay method (Tan *et al*, 1996)

- Alkalinity (CO_3^{2-} plus HCO_3^- concentrations) by titration method using methyl orange indicator and hydrochloric acid, 0.01 M (Rowell, 1994)

The determination of Cl^-, F^-, NH_4^+-N and $H_2PO_4^-$ were carried out in an UV/visible spectrophotometer Ultrospec III Pharmacia LKB.

The anion content found in the soil solution, the wavelength used for the determination using the UV/visible spectrophotometer mentioned above, the limits of detection for each anion and the calibration curve recommended to cover the cation range presented in the soil solution, are given in Table 5.15.

Table 5.15. Analytical details for the determination of anions in soil solution using the UV/visible spectrophotometer Ultrospec III Pharmacia LKB.

Anion	**λ, nm**	**Concentration in sample, μg mL^{-1}**	**Limit of Detection, μg mL^{-1}**	**Calibration curve points suggested, μg mL^{-1}**
NH_4^+-N	667	---	2.7	0.08, 0.16, 0.24, 0.4, 0.8
$H_2PO_4^-$	880	20.15	0.13	0, 5, 10, 15
NO_2^-	540	2.87	0.02	0, 1, 2, 3, 4, 5, 6
Cl^-	460	3.73	0.12	0, 2, 4, 6

HCO_3^-, CO_3^{2-} were determined together as alkalinity, the concentration in the soil solution was 0.04 mmol. Assuming that alkalinity can be express in terms of a mass concentration of CaCO3 (mg/L), the concentrations of bicarbonate and carbonate in the soil solution can be calculated using the two following formulas (Deutsch, 1997):

$$HCO_3^- \left(\frac{mg}{L}\right) = \frac{Alkalinity\left(\frac{mg}{L} CaCO_3\right)}{\left(1+\frac{2x10^{-10.3}}{10^{-pH}}\right)x50} x61$$

$$CO_3^{2-} \left(\frac{mg}{L}\right) = \frac{Alkalinity\left(\frac{mg}{L} CaCO_3\right)}{\left(1+\frac{10^{-pH}}{10^{-10.3}}\right)x50} x60$$

results are given in Table 5.16.

Table 5.16. Concentrations of bicarbonate and carbonate calculated from the alkalinity expressed in terms of $CaCO_3$.

Anion	Concentration in sample, μg mL^{-1}
HCO_3^-	4.87
CO_3^{2-}	$7.59x10^{-3}$

Observations:

- F^- ions were absorbed on the glassware, and so a plastic volumetric flask will be needed if the determination is to be carried out. The determination of F^- is interfered with Cl^- and $H_2PO_4^-$
- Colorimetric methods are quite time consuming and suffer from interferences in a complex multianion sample, such as a soil solution sample

Ion chromatography was proposed as an analytical option for determining anions in soil solution. Anion content was determined with a Dionex ion chromatograph system, using an eluent of 3.5 mM Na_2CO_3/ 1.0 mM $NaHCO_3$ at a flow rate of 0.3 mL/min, with

guard and separator columns of a strong basic anion exchanger. The system has a micromembrane suppressor batched in continuously flowing strongly acid solution (regenerant solution). The separated anions, in their acid forms, were measured by conductivity, and were identified on the basis of retention time compared to standards. Peak areas were used to quantify the concentration of anions in solution. Calibration curves were prepared from a Dionex certified standard for five anions.

Resolution and limits of detection were calculated for the anions in the standard. The results for retention time in the IC system, the limits of detection for the standard, the resolution per anion and the anion concentration the sample are shown in Table 5.17.

Observations:

– The use of IC radically improves the determination of anion content in soil solution, the limit of detection and the time of analysis

Table 5.17. Retention time, resolution and limit of detection for 5 anions and the anion concentration in the sample.

Anion	**Concentration in sample, μg mL^{-1}**	**Retention time, min**	**Resolution**	**Limit of detection, μg mL^{-1}**
F^-	3	2.87	1.7	0.0029
Cl^-	52	4.28	4.0	0.0168
NO_3^-	----	8.15	1.5	0.0449
HPO_4^{2-}	----	10.08	1.4	-
SO_4^{2-}	2300	12.32	0.0	0.1371

– The resolution is good enough to give complete separation and values agreed well with those certified for the five anion standard Dionex, with the exception of nitrate

– The limits of detection quoted are in reagent water (deionised water of 18 megaohm-cm resistivity containing no particles larger than 0.20 mm) and agree well

with those reported in the standard methods for the examination of water and wastewater, ed. 18th, 1992. APHA, AWWA, WEF

– Filtration of the sample to be injected in the system is strongly recommended. Filtration through a Millipore membrane filter (HAWP, 0.45 μm) is cited as optimum to separate low-molecule-weight organic acids from the sample. The filtration has two objectives: to preserve the life of the column and to eliminate interferences

– When soil solution samples with a high anion concentration were injected, three washes with deionised water injections were necessary to clean the injection system

– The degassing of eluent was shown to be crucial in the performance of the system. The eluents were degassed following the steps given below:

1. The eluent was poured into a vacuum flask, tapped and connected to a vacuum pump
2. The flask was put into the ultrasonic bath
3. Sonification and vacuum were applied for 10 minutes
4. The degassed eluent was poured carefully in the eluent reservoir without shaking

– Cl^- was the only anion determined by the two methods, which gave different results for the same sample. The concentration of Cl^- determined using the mercury(II) thiocyanate method (Table 5.15) was smaller than that determined using IC (Table 5.16). This could be explained on the basis that nitrite and sulphite can interfere with the mercury (II) thiocyanate determination.

5.5.6. Conclusions

Through the detailed study carried out on assessment samples was possible to:

- Determine operationally the reactivity of Cr, Cu and Zn as natural components, using the Tessier *et al* (1979) sequential extraction method

- Identify the high influence of geochemical parameters on heavy metal reactivity, such as: soil pH, organic matter content and mineralogical composition (clay content and iron and manganese hydrous-oxide content)
- Identify the determination of the total concentration of metals as an important control parameter of the sequential extraction scheme
- Confirm that the determination of Ni, Pb and Cd is not adequate when using ICP-AES
- Determine the main cations and anion in the soil solution of the assessment samples
- Identify ion chromatography as the best technique to determine anions, with the exception of phosphates, when a colorimetric is proposed

Chapter 6. Inorganic metal species in solution

6.1. Introduction

In this chapter the possible inorganic species of Cr, Cu, and Zn in the liner soil solution were estimated in a qualitative way using stability diagrams as a function of pH and in a uantitative way using the geochemical equilibrium model Geochem-PC. The anion or cation concentrations used for the estimation were those from the soil solution experiments shown in Chapter 5. It is important to remark that the contribution of dissolve organic matter (DOM) to the soil solution was not considered in the metal speciation estimation carried out in this chapter.

Stability diagrams were prepared for all the mineral components of the liner, because stability diagrams can be used to predict the stability, formation and weathering of the components that influence on the metal speciation in solution. The equilibrium constants were taken from Lindsay (1979). For simplicity the water molecules of all the species in solution were omitted, and the hydronium ion is solely considered as proton (Appendix 3).

The use of a geochemical equilibrium model can solve in a more efficient way, the large array of equations required to describe the soil systems. However the capacity to predict of such models is largely based on the enclosed thermochemical database and the capability to model important reactions such as: hydrolysis, complexation, dissolution/precipitation, oxidation/reduction, ion exchange and adsorption (Loeppert *et al*, 1995). Geochem-PC is an example of a computational code, which includes both features to make it reliable. Nevertheless, the features of any numerical model should be verified and its limitations established for its assessment of accuracy.

Geochem-PC was used to quantify the inorganic species in the soil solution. Previous to this use, the model was verified in its algorithms and the database content, and was checked analytically for a simple system.

6.2. Stability diagrams

The anion or cation concentrations used for the estimation are summarised in Table 6.1. For the calculation of the chemical species shown in the stability diagrams it was assumed that the phases (mineral that dissolves and chemical species in the solution) are in thermodynamic equilibrium. Thus, for example for the reaction:

$$A + B \Leftrightarrow AB \qquad 1$$

the thermodynamic equilibrium constant (K^0), was calculated as follows:

$$K^0 = \frac{\{AB\}}{\{A\}\{B\}} \qquad 2$$

where: {} means activities, ^{0} referes to the standard state (T=298.15 °K and p=1 atm)

The thermodynamic equilibrium constant relates to the Gibbs free energy of the reaction (ΔG^0_r), as follows:

$$\Delta G_r^0 = -RT \ln K^0 \qquad 3$$

where: R is the universal gas constant and T is the absolute temperature in Kelvin degrees

The Gibbs free energy of the reaction can be calculated from the Gibbs free energy of products and reactants, using the following reaction:

$$\Delta G_r^0 = \sum \Delta G^0_{fproducts} - \sum \Delta G^0_{freactants} \qquad 4$$

where: $\Sigma\Delta G$ is the sum of the free energies of formation of products or reactants

Table 6.1. Measured concentrations of chemical species in soil solution extracted from compacted virgin Lower Oxford Clay.

Chemical species	Concentration, mg/l	Atomic masses	Molar	Concentration
			$x10^{3-}$	-log
Si^{4+}	9	28.09	$3.2x10^{-4}$	3.49
Mg^{2+}	99	24.31	4.1	2.39
Ca^{2+}	115	40.08	2.8	2.54
Na^{+}	288	22.99	12.5	1.90
K^{+}	83	39.10	2.1	2.67
Al^{3+}	0.5	26.98	$1.8x10^{-5}$	4.73
Fe^{3+}	1.4	55.85	$2.5x10^{-5}$	4.60
Zn^{2+}	2.4	65.39	$3.7x10^{-5}$	4.44
$H_2PO_4^{-}$	20	96.97	$2.1x10^{-4}$	3.69
F^{-}	3	19.00	$1.6x10^{-4}$	3.80
Cl^{-}	52	35.45	1.5	2.83
SO_4^{2-}	2300	96.00	24	1.62

The activity of ions rather than their concentrations are used in equation 2. The activity of A species $\{A_i\}$ is related to the total concentration $[C_i]$ by the activity coefficient, (γ_i) according to the following reaction:

$$A_i = \gamma_i * C_i \qquad 5$$

The activity coefficient will be one at infinitely dilute solutions and then concentrations and activities are equal. This criteria was assumed for the calculation of chemical species in solution.

6.2.1. Stability diagram of the major mineral components of the liner

6.2.1.1. Clay fraction

The solubilities of clay fraction minerals can be expressed in terms of the activities{} of Al^{3+}, H^+, K^+, $H_4SiO_4^0$. Stabilities for the clay fraction components are plotted in Figure 6.1. An example of how these lines were developed is shown for chloride:

	$\log K^o$
$Mg_5Al_2Si_3O_{10}(OH)_8$ (chlorite) + $16H^+ \Leftrightarrow 5Mg^{2+} + 2Al^{3+} + 3H_4SiO_4^0 + 6H_2O$	60.30
$3H_4SiO_4^0 \Leftrightarrow 3SiO_2$ (quartz) $+ 6H_2O$	12.00
$Mg_5Al_2Si_3O_{10}(OH)_8$(chlorite)$+16H^+ \Leftrightarrow 5Mg^{2+} + 2Al^{3+} + 3SiO$(quartz)$+ 12H_2O$	72.30

the activity of $H_4SiO_4^0$ was considered to be controlled exclusively by α-SiO_2(quartz), activities for pure components (among them water) is 1, thus:

$$\frac{\{Al^{3+}\}^2\{Mg^{2+}\}^5}{\{H^+\}^{16}} = 10^{72.3}$$

$$\log\left[\{Al^{3+}\}^2\{Mg^{2+}\}^5\right] - \log\{H^+\}^{16} = 72.3$$

$$2\log\{Al^{3+}\} + 5\log\{Mg^{2+}\} + 16pH = 72.3$$

$$2\log\{Al^{3+}\} = 72.3 - 16pH - 5\log\{Mg^{2+}\}$$

$$\log\{Al^{3+}\} = 36.15 - 8pH - 2.5\log\{Mg^{2+}\}$$

$$\text{but } \log\{Mg^{2+}\} = -2.39$$

$$\log\{Al^{3+}\} = 42.125 - 8pH$$

The solubility of the clay fraction minerals decreases in the order chlorite>Mg-montmorillonite (smectite)>illite>kaolinite in the pH range 2 to 5.5. Chlorite is highly pH dependent going from quite soluble in acid to stable in alkaline environments, above pH 7.5. Mg-montmorillite will be the most soluble clay mineral above pH 5.7. Release of cations into solution (Mg^{2+}, Al^{3+} and Fe^{3+}), would be expected to influence shear-strength and speciation in the soil solution at acid pH. At an alkaline pH, K^+ will be released.

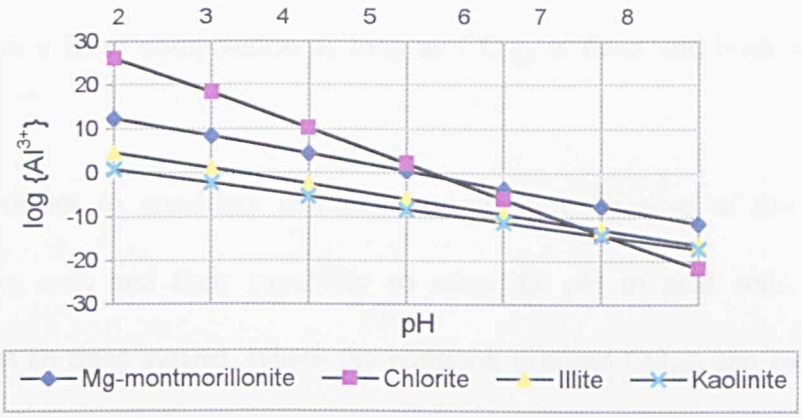


Figure 6.1. Stability diagram of the liner clay fraction.

It is quite possible that chlorite was the most affected mineral during the attack of aluminosilicates by the sequential extraction.

6.2.1.2. Carbonates

There are two sources of carbonates in the site, calcite and gypsum. The stability diagram for the system calcite-gypsum is shown in Figure 6.2. Two assumptions were taken to calculate this diagram 1) Ca^{2+} is controlled by calcite and 2) the level of $CO_{2(g)}$ is 0.003 atm.

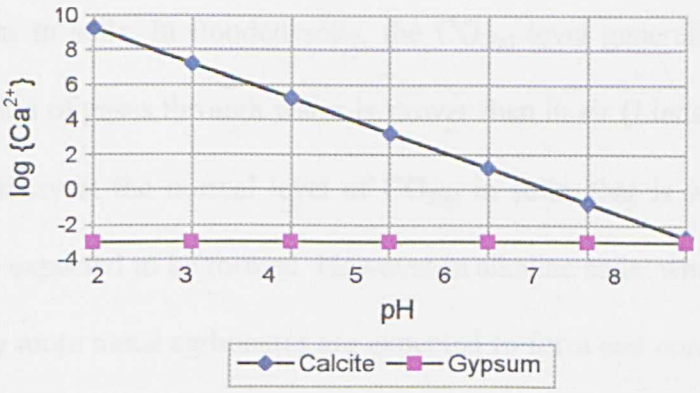


Figure 6.2. Stability diagram for the system calcite-gypsum.

Calcite and gypsum can coexist at around pH 8. If both calcite and gypsum are present, the system will have a unique composition, and the addition of a component such as water, dissolves calcite and precipitates gypsum and the composition of the

solution remains fixed. It is possible to calculate the composition of the solution phase that will have a fixed composition as long as $CO_{2(g)}$ is fixed and both solid phases are present.

It is important to considere carbonate equilibrium, because of the importance of carbonates in soils and their capability to raise the pH in acid soils. However this equilibrium is an open system, where the common product $CO_{2(g)}$ can escape from soils to the atmosphere and return as carbonate mineral precipitates.

Total carbonates in solution are given by:

$$H_2CO^0_3 + HCO^-_3 + CO^{2-}_3$$

Where the mole fraction, for example of CO^{2-}_3, will be given by:

$$MF_{CO_3^{2-}} = \frac{CO_3^{2-}}{H_2CO_3^0 + HCO_3^- + CO_3^{2-}}$$

If reactions are expressed in terms of pH and $CO_{2(g)}$, the latter be eliminated and this equation will be a function of formation constant and pH.

In most soils the partial pressure of $CO_{2(g)}$ is expected to be slightly higher than in the air because it is continually being released by the respiration of plant roots and microorganisms in soils. In flooded soils, the $CO_{2(g)}$ level generally goes much higher because diffusion of gases through water is slower than in air (Lindsay, 1979). CO^{2-}_3 has a very low activity at the normal level of $CO_{2(g)}$ in soils, that is why just a few metal carbonates are expected to be formed. However in alkaline soils, where the level of CO^{2-}_3 is higher, many more metal carbonates are expected to form and control the behaviour of metal cations.

6.2.1.3. Pyrite

Release of Fe^{2+} from pyrite and its subsequent oxidation to Fe^{3+} favours jarosite formation (Table 5.3). Potassium ions are also needed to precipitate jarosite formation, K^+ can be replaced to some extent by Na^+ or other cations in the jarosite generation. Jarosite crystallisation, like gypsum, can disrupt the clay fabric, opening up discontinuities.

The stability diagram for jarosite expressed in terms of Fe^{3+} is given in Figure 6.3. The activity of Fe^{3+} is shown to be controlled by either soil-Fe or geothite.

Only below pH 4 (or slightly higher depending on SO_4^{2-} and K^+ activities) can jarosite form. In acid soils jarosite can form from $Fe(OH)_3$ soil but not from geothite.

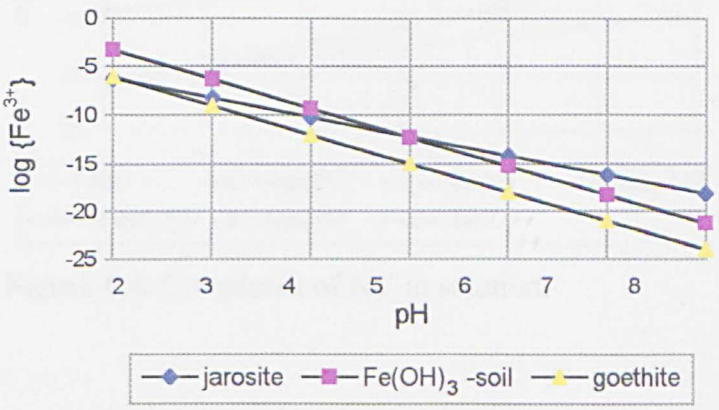


Figure 6.3. Stability diagram for jarosite.

6.2.2. Stability diagrams for the inorganic species in solution

From the stability diagrams prepared for the major components of the Oxford Clay, it was possible to identify which species will be in solution. Stability diagrams were calculated for each of the elements listed in Table 6.1. The objective was to predict the predominant inorganic species in a specific pH range for each element.

6.2.2.1. Sodium

Apparently there are no minerals controlling Na solubility in the Oxford Clay, however sodium aluminosilicates minerals are too soluble to persist in soils. A reference concentration of 10^{-3} M of Na^+ is given for well-drained soils (Lindsay, 1979). The concentration of Na^+ found in the liner was estimated to be $10^{-1.90}$ M, this means than Lower Oxford Clay is poorly drained and sodium salts can accumulate there.

The expected complexes of sodium in solution are plotted in Figure 6.4, from there it can be seen that the sodium in solution will be exclusively as Na^+.

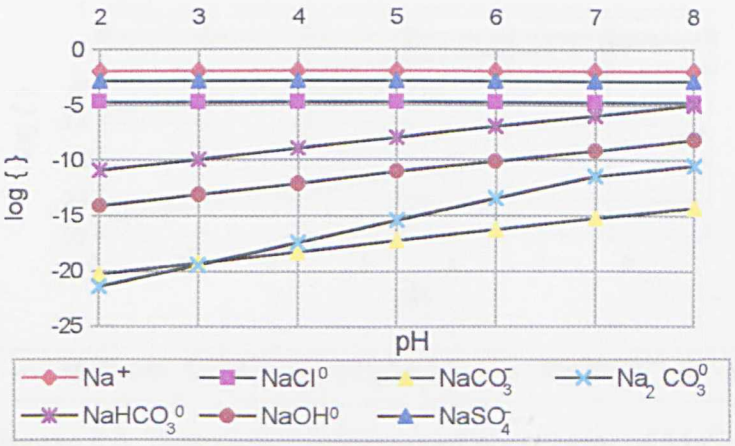


Figure 6.4. Complexes of Na^+ in solution.

6.2.2.2. Magnesium

The stability of various Mg^{2+} complexes are plotted in Figures 6.5 and 6.6. There is strong competition between Mg^{2+} and $MgSO^0_4$ to control the solubility of the total magnesium in solution. $MgHPO^0_4$ will contribute significantly to the total magnesium in solution above pH 6; however magnesium ion and magnesium sulphate will still contribute to the total magnesium in soil solution. Magnesium carbonates will become important above pH 7. Chloride and hydrolysis species are insignificant and will not contribute to the total magnesium in solution.

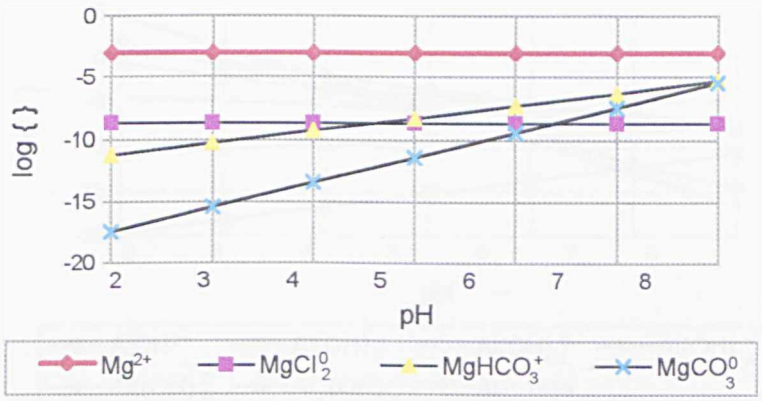


Figure 6.5. Chloride and carbonates of Mg^{2+} in solution.

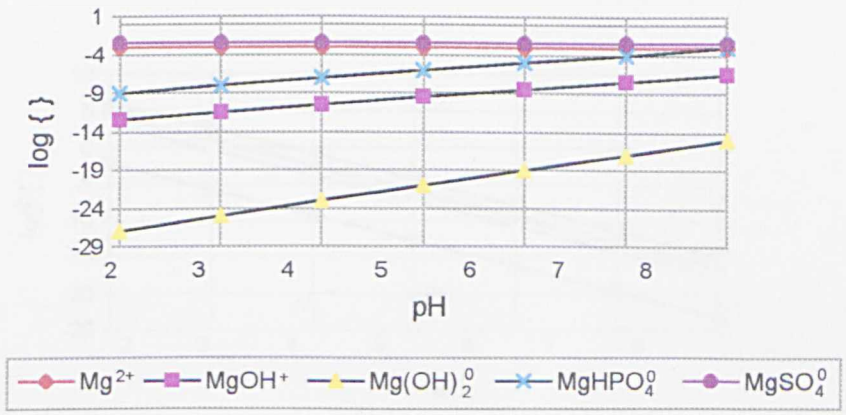


Figure 6.6. Hydrolysis, sulphate and phosphates of Mg^{2+} in solution.

6.2.2.3. Aluminium

In the case of Al^{3+} (Figures 6.7 and 6.8), $AlSO^{2+}{}_4$ will be the predominant specie below pH 3.8, $Al(OH)^{4+}{}_2$ will contribute the most to total aluminium in solution from pH 3.8 to 5, $Al(OH)^{4+}{}_2$ and $Al(OH)^{+}{}_2$ will be two main species from pH 5 to 6.8, $Al(OH)^{+}{}_2$ will be the most important until pH 7.7, Above pH 7.7 $Al(OH)^{+}{}_2$, $Al(OH)^{0}{}_3$, $Al(OH)^{-}{}_4$ and $Al((OH)^{4+}{}_2$ will contribute to the total aluminium in solution.

6.2.2.4. Potassium

The most probable species of potassium are shown in Figure 6.9.; from this figure it can be seen that potassium is exclusively an exchangeable cation in the liner soil solution.

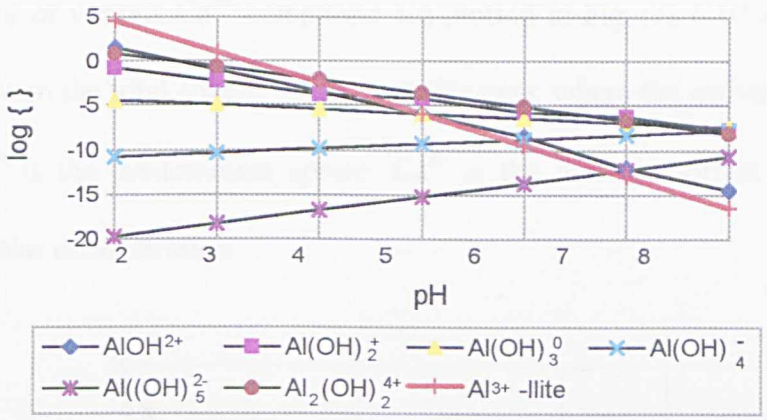


Figure 6.7. Hydrolysis species of Al^{3+} in equilibrium with Illite.

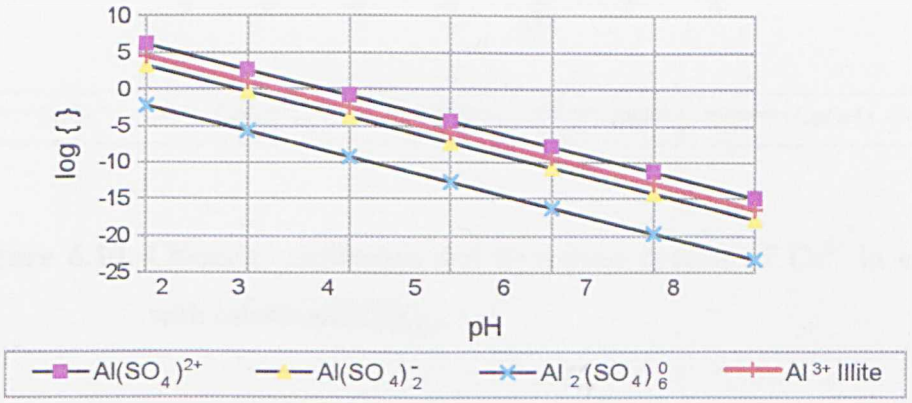


Figure 6.8. Sulphate species of Al^{3+} in equilibrium with Illite.

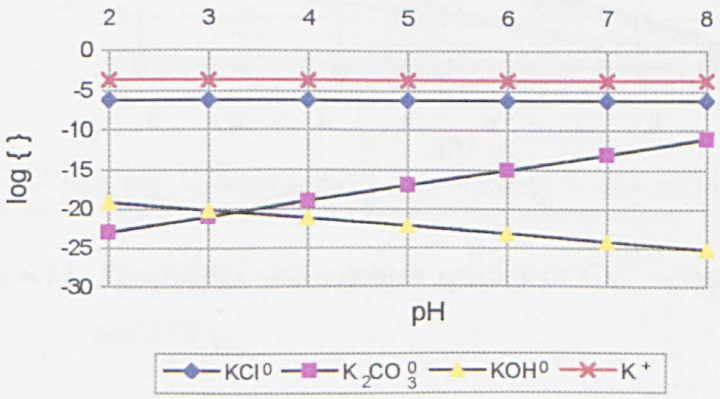


Figure 6.9. Species of K^{+}.

6.2.2.5. Calcium

The stability of various Ca^{2+} complexes are plotted in Figures 6.10 and 6.11. Ca^{2+} and $CaSO_4^0$ govern the total soluble calcium, in this case, where the activity of SO_4^{2-} is $10^{-1.62}$ M, $CaSO_4^0$ is the predominant specie. Ca^{2+} is the more important specie below this sulphate molar concentration.

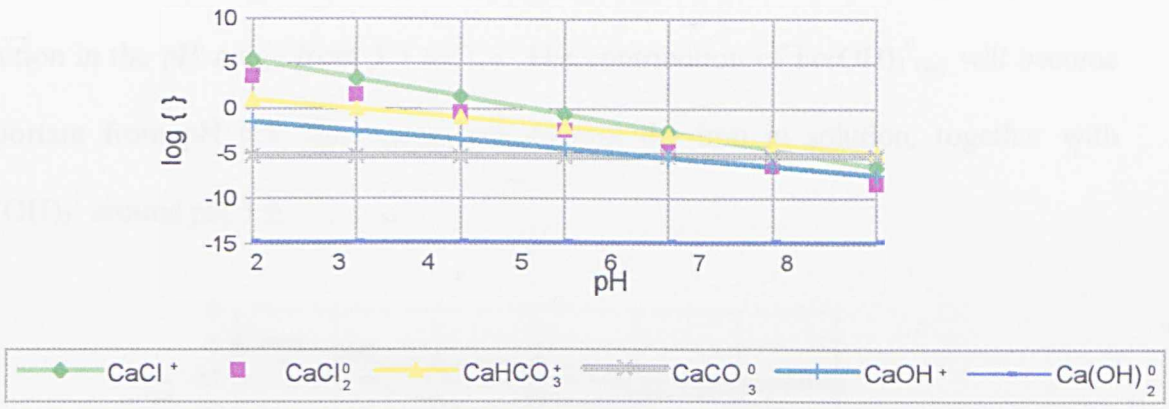


Figure 6.10. Chloride, carbonates and hydrolysis species of Ca^{2+} in equilibrium with calcite and $CO_{2(g)}$.

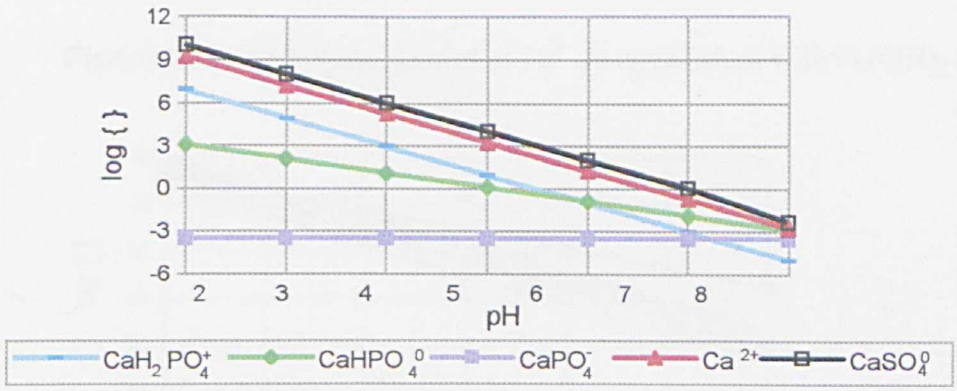


Figure 6.11. Phosphates and sulphate species of Ca^{2+} in equilibrium with calcite and $CO_{2(g)}$.

6.2.2.6. Iron

Fe^{3+} in solution can form both hydrolysis species (Figure 6.12) and complexes (Figure 6.13). $FeSO_4^+$, $FeH_2PO_4^{2+}$ and $FeHPO_4^+$, in particular the last one, will control the total iron in solution, in the pH range between 2 and 3. From pH 3.3 to 5 $FeHPO_4^+$ will control almost absolutely the iron in solution, while $Fe(OH)_2^+$ will contribute to a lesser extent. However this specie will dominate the rest of the species in controlling iron in solution in the pH range from 5.5 to 7.4. The contribution of $Fe(OH)_3^0{}_{(aq)}$ will become important from pH 6.5; this specie will control the iron in solution, together with $Fe(OH)_2^+$ around pH 7.5.

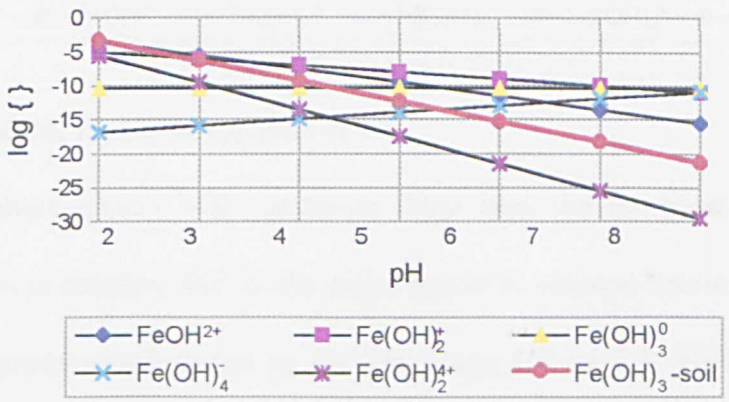


Figure 6.12. Hydrolysis species of Fe^{3+} in equilibrium with $Fe(OH)_3$-soil.

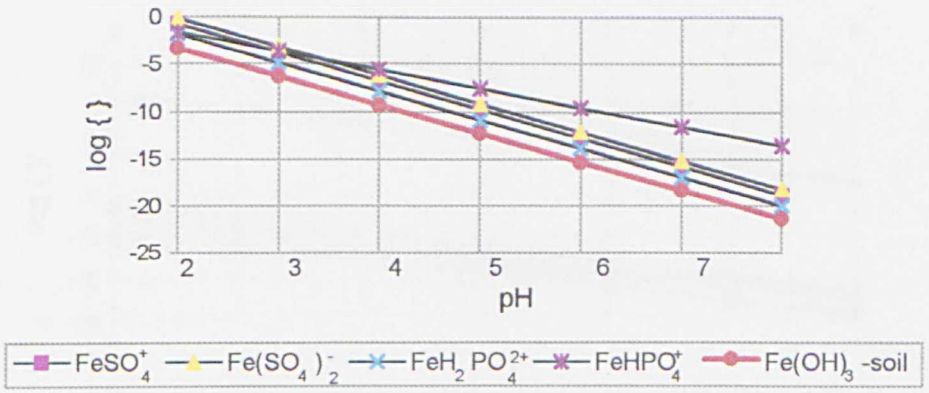


Figure 6.13. Sulphate and phosphates species of Fe^{3+} in equilibrium with $Fe(OH)_3$-soil.

Hydrolysis and inorganic complexes of Fe^{2+}

The stability diagrams for the hydrolysis species and inorganic complexes of Fe^{2+} are given in Figures 6.14 and 6.15, respectively. It was assumed that (pe+pH) is 4.00; this means that pyrite and Fe-soil were in equilibrium.

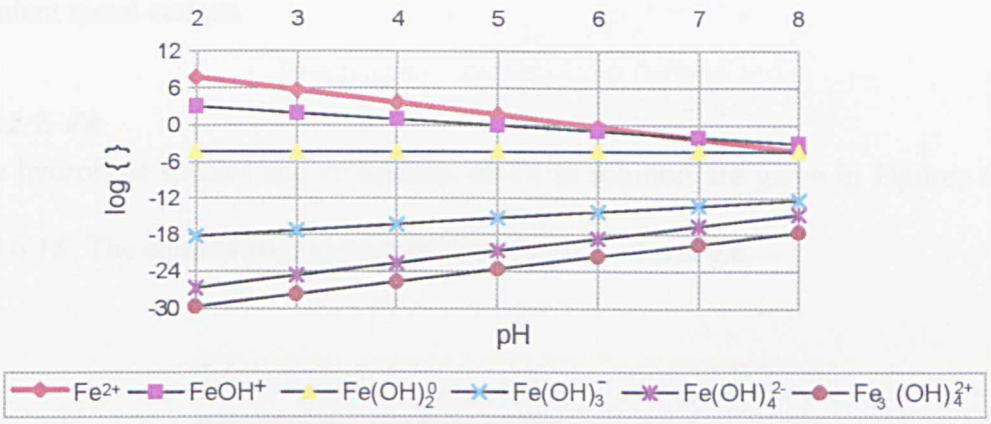


Figure 6.14. Hydrolysis species of Fe^{2+}.

The hydrolysis species will contribute more than the inorganic complexes to the ferrous species in solution. Fe^{2+} is the major specie in solution below pH 6.5, FeOH will become the predominant specie in the pH range 6.6 to 7.8, $Fe(OH)^0_2$ will become important around pH 8.

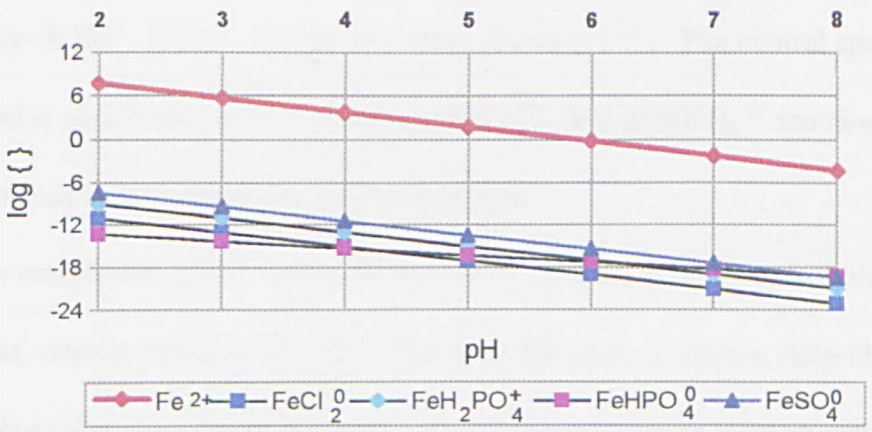


Figure 6.15. Complexes of Fe^{2+} in solution.

Observations:

Since iron is present in soils in much greater quantities that many of the divalent metals such as zinc and copper, it is highly unlikely that ferrite minerals will control iron solubility, but iron is expected to have an important influence on the solubility of many divalent metal cations.

6.2.2.7. Zn

The hydrolysis species and complexes of Zn in solution are given in Figures 6.16, 6.17 and 6.18. The equilibrium was established in terms of soil-Zn.

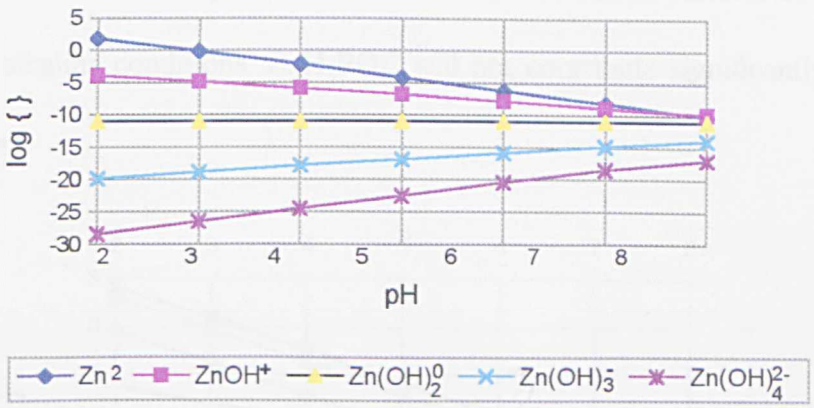


Figure 6.16. The hydrolysis species of Zn^{2+} in equilibrium with Zn-soil.

The predominant specie of Zn in solution below pH 7.7 -the pH range of interest in this study- is Zn^{2+}. $ZnOH^{+}$ is more prevalent above pH 7.7. The neutral specie $Zn(OH)_2{}^{0}$ is the major specie above 9.11, whereas $Zn(OH)_3^{-}$ and $Zn(OH)_4{}^{2-}$ are never going to be major species in solution in the pH range of soils.

Other complexes of Zn^{2+} could be present in solution, besides hydrolysis species, such as halides, nitrate, sulphate and phosphates. In the case of halides, only chloride species of Zn were calculated, this is because it was the only halide in a detectable concentration in the soil solution obtained from the liner. Only the specie $ZnCl^{+}$ seems a candidate to contribute slightly at acid conditions, however it will not contribute in a significant way to the total Zn in solution in comparison with the other predominant species.

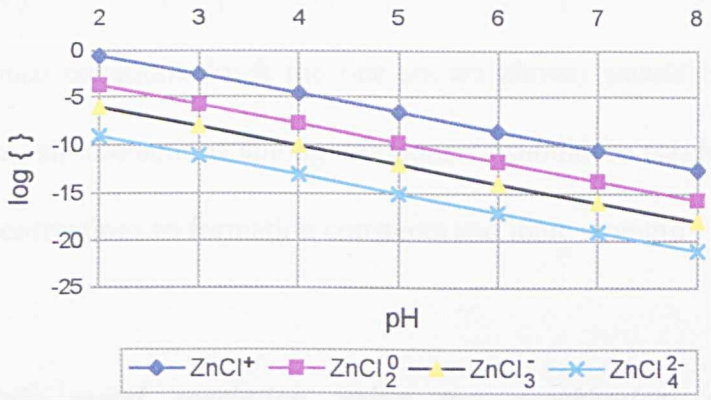


Figure 6.17. Chloride complexes of Zn^{2+} in solution.

Zn^{2+} will be almost entirely as $ZnSO_4^0$ under acid conditions; $ZnH_2PO_4^0$ will become important at alkaline conditions. $ZnH_2PO_4^+$ will not contribute significantly to the total Zn in solution.

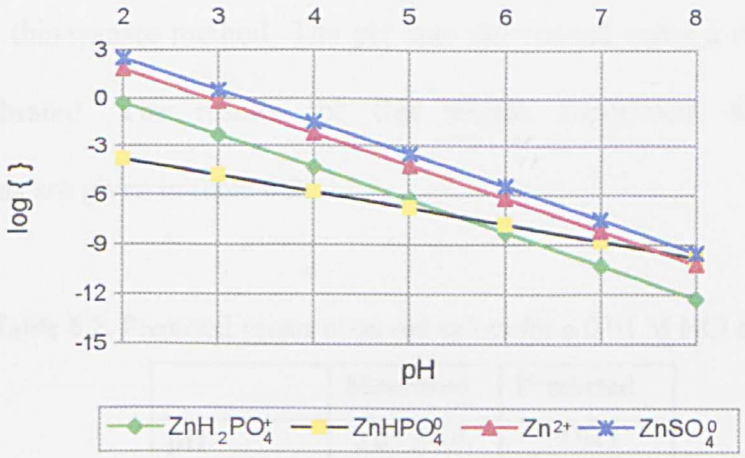


Figure 6.18. Sulphate and phosphates of Zn in solution.

6.2.3. Final remarks on the use of stability diagrams for chemical speciation

The information revealed by stability diagrams can be used to quantify the chemical species in solution, provided that the number of equations needed to defined the system are known.

The total concentration of an element in solution will be given by the sum of the concentrations of individual species. Thus, for example, the total concentration of Zn in solution will be given by:

$$\left[Zn_{inorg}\right] = \left[Zn^{2+}\right] + \left[ZnSO_4^0\right] + \left[ZnOH^+\right] + \left[Zn(OH)_2^0\right] + \left[ZnHPO_4^0\right]$$

Mass balance equations (such the one shown above) should be prepared for each element. Then, all interactions among components should be carefully described, taking into account corrections to formation constants and ionic strength.

6.3. Inorganic metal speciation using the geochemical equilibrium model: GEOCHEM-PC

6.3.1. Analytical scheme for the geochemical equilibrium model confirmation

Prior calculation of the chemical species in the soil solution, the calculation of pH and species of a 0.01 M HCl solution was computed using Geochem-PC. The objective was to analytically confirme the performance of the model.

A solution of 0.01 M of HCl was prepared, and its Cl^- content was determined by the mercury (II) thiocyanate method. The pH was determined using a common pH meter, already calibrated. The results for this simple experiment and the predicted concentrations are given in table 6.2.

Table 6.2. Predicted versus observed values for a 0.01 M HCl solution.

	Measured	**Predicted**
pH	$2.05 \pm 0.0_1$	2.045
Cl^-, μgL^{-1}	364.6 ± 1.3	354.5

6.3.2. Modelled inorganic species in soil solution

The data shown in Table 6.1. were entered in a seed file and run in Geochem-PC, the following assumptions were applied:

- pH was fixed at 7.5, this is the most common- median- pH value in the liner samples.
- The soil solution was considered to be concentrated and affected by the chemical species present in it. That is, activity coefficients were corrected considering the ionic strength. The activity coefficients were calculated, using the Davis equation:

$$\log \gamma_i = -Az^2\left(\frac{\sqrt{I}}{1+\sqrt{I}} - 0.24I\right) \quad 6$$

where: A ~0.51 at 298 K

where the ionic strength (I) of the solution was given by:

$$I = \frac{1}{2}\Sigma C_i z_i^2 \quad 7$$

where z_i is the charge on the ion

- No redox reactions were considered in the modelling, because the pH used for the modelling was 7.5. That is why Fe^{2+} species were not reported
- Three more chemical species (taken from literature as the common concentration found in soils (Lindsay, 1979)) were included: CO_3^{2-}, NO_3^-, Mn^{2+}; to balance the system to a near equilibrium. This indicates that more determinations should be carried out to speciate the soil solution.
- The system was considered to be open
- Simple solid phases were allowed, but not imposed

Results are given in Table 6.3.

Zn was the only heavy metal under study that was speciated. This was because it was the only heavy metal present in a detectable concentration in the soil solution. Around 25 % (~ 0.6 mg/L) of the total concentration in soil solution will be as a free metal ion, whereas 23 % (~ 0.55 mg/L) will be complexed by different ligands. Free metal ions are probably the most bioavailable heavy metal species for plants and microorganisms, whereas the heavy metal complexes are usually important for mobility (Temminghoff, 1998). Zn availability or mobility does not represent a hazard in this soil system, a high concentration of zinc in the soil solution will precipitate as carbonate.

Table 6.3. Primary distribution of metals and ligands in the soil solution extracted from the Lower Oxford Clay samples.

Metal	Ligand
Ca^{2+}	**CO_3^{2-}**
54.53 % as a free metal	0.18 % as a free ligand
1.25 % complexed with CO_3^{2-}	1.37 % complexed with Ca^{2+}
16.44 % in solid form with CO_3^{2-}	18.03 % in solid form with Ca^{2+}
22.83 % complexed with SO_4^{2-}	0.57 % complexed with Mg^{2+}
0.11 % complexed with PO_4^{3-}	1.30 % complexed with Na^{+}
4.83 % in solid form with PO_4^{3-}	0.03 % complexed with Zn^{2+}
	0.50 % in solid form with Zn^{2+}
Mg^{2+}	78.03 % complexed with H^{+}
73.77 % as a free metal	
1.42 % complexed with CO_3^{2-}	**SO_4^{2-}**
24.53 % complexed with SO_4^{2}	83.52 % as a free ligand
0.06 complexed with Cl^{-}	9.74 % complexed with Ca^{2+}
0.21 % complexed with PO_4^{3-}	3.80 % complexed with Mg^{2+}
	0.07% complexed with K^{+}
K^{+}	2.82 % complexed with Na^{+}
96.76 % as a free metal	0.04 % complexed with Zn^{2+}
3.22 % complexed with SO_4^{2}	
0.02 complexed with Cl^{-}	**Cl^{-}**
	98.99 as a free ligand
Na^{+}	0.01 % complexed with Ca^{2+}
97.47 % as a free metal	0.05 % complexed with Mg^{2+}
0.37 % complexed with CO_3^{2-}	0.94 % complexed with Na^{+}
2.04 % complexed with SO_4^{2}	
0.12 % complexed with Cl^{-}	
Fe^{3+}	**PO_4^{3-}**
0.01 % complexed with OH^{-}	2.92 % complexed with Ca^{2+}
99.99 % in solid form with OH^{-}	84.66 % in solid form with Ca^{2+}
	2.02 % complexed with Mg^{2+}
Mn^{2+}	0.07 % complexed with Zn^{2+}
64.10 % as free metal	10.32 complexed with H^{+}
8.84 % complexed with CO_3^{2-}	
26.83 % complexed with SO_4^{2-}	**NO_3^{-}**
0.22 % complexed with Cl^{-}	100 % as a free ligand
0.01 % complexed with OH^{-}	
Zn^{2+}	
24.93 % as a free metal	
2.75 % complexed with CO_3^{2-}	
51.88 % in a solid form with CO_3^{2-}	
10.43 % complexed with SO_4^{2-}	
0.05 % complexed with Cl^{-}	
0.32 % complexed with PO_4^{3-}	
0.03 % complexed with NO_3^{-}	
9.60 % complexed with OH^{-}	

6.4. Conclusions

The species predicted by the software Geochem-PC, agreed well with those predicted by means of stability diagrams. The stability diagrams identified the phase that controls the solubility on the solid phases, and express in graphical terms the possible species in solution for a familiar parameter such as pH. The geochemical model is an attractive tool to solve the many and sometime intricate equations necessary to describe the soil system equilibrium; however two main requirements should be fulfilled , i) the enclosed thermodynamic database should be extensive and accurate ii) the model should consider the common reactions that takes place in the soil system.

A verification of the geochemical equilibrium model database and algorithms is always recommended and the analytical scheme for confirmation ideally should be carried out for each type of reaction.

The modelling of inorganic metal species in the soil solution of Oxford Clay samples can be summarised as follows:

The essential metals- Ca, K, Mg, Na, Mn- would be as free ions

Fe would precipitate with OH- ligand

The common ligands in soil would be reactive towards metals, as expected.

Zinc would be available in 25 % of its total concentration in soil solution and inorganically complexed in 23 %

More analytical determinations should be carried out to describe chemical species in soil solution, such as Disolved Organic Matter.

Chapter 7. Statistical analysis of the measured parameters in the liner

7.1. Introduction

A methodology that includes both statistical and geostatistical treatment was applied to the results of the sequential extraction and geochemical parameters described in chapter 5. There were only enough data in nine populations to be treated in such a way: pH, organic matter, Cr, Cu and Zn as total fractions, Cr, Cu and Zn bound to organic matter and Zn bound to Fe-Mn oxides. Cd, Ni and Pb populations were not included because they were not considered reliable.

Bayesian probability was applied on the exchangeable Zn, Cr and Cu, and Zn and Cu bound to carbonates populations, because there were not enough data to apply the methodology mentioned above.

Non-parametric correlations coefficients were calculated for the Mg^{2+}, Ca^{2+}, K^{+} and Na^{+} and the CEC. This was because there were not enough data to apply a geostatistical analysis.

7.2. Descriptive Statistics

During the descriptive statistical analysis histograms and summary statistics were prepared for the nine soil parameters. The relationship between pH, organic matter and the operational defined species of Zn, Cu and Cr was measured through the rank -or non parametric- correlation coefficient (Spearman algorithm) using the statistical software SPSS for windows version 9.02. The results are shown in Table 7.1.

Each population was tested for normality using the Kolmogorov-Smirnoff test. When the population was found not normal, a Box-Cox transformation was applied, and the new transformed population was tested for normality once more.

Table 7.1. Rank correlation coefficients.

	pH	Organic matter
pH	1.000	0.414*
Organic matter	0.414*	1.000
Cr_{org}	0.430**	0.258
Cr_{tt}	0.466**	0.409*
Cu_{org}	0.647**	0.387*
Cu_{tt}	0.451**	0.438**
Zn_{FeMnox}	0.529**	0.204
Zn_{org}	0.648**	0.231
Zn_{tt}	0.564**	0.420*

* Correlation is significant at the 0.05 level (2-tailed)

** Correlation is significant at the 0.01 level (2-tailed)

Where the variance increased by more than 30%, the original population was reflected and tested for normality. To reflect a population, a value of one (1) was added to the highest value of the population, from this constant each datum was subtracted. When the population was transformed, both the original and the transformed population were geostatistically treated and tested again during the error analysis.

7.3. Geostatistics

Variogram

An Iterative Exploratory Variography (IEV) using VARIOWIN version 2.2 was applied to the original and transformed population.

- Four different directional variograms were calculated at 0°, 45°, 90°, 135° with an angular tolerance of 22.5°. After exhaustive trial and error, the optimum number of lag and lag distances were set at (10,10) m
- The four variograms were fitted to a model, using the Indicative of Goodness of Fit (IGF) (Pannatier, 1995)

The model parameters (type of model, nugget value, range, sill and anisotropy) for each of the structures, if more than one, were used for the point estimation utilising the ordinary kriging algorithm.

Estimation

The estimation was made using the module KB2D of GSLIB version 2.0. The 2D program was run for each variable using their respective fitted model parameters for ordinary kriging. The cell size to calculate the point estimates was (13 x 10) to the north-east and south-west respectively; the number of cell to the north-east were 10 and 5 to the south-west, covering a total area of 6500 square meters. In the case of the samples taken randomly, an approximate location was assigned and the estimation was carried out one by one , by defining in the parameter file [nx=1 x-coord xsiz=1, ny=1 y-coord ysiz=1]. The maximum search radius was set at 20. The minimum and maximum data for kriging were 3 and 6.

Cross-validation

The cross-validation of the estimated versus the observed values was carried out using the module SCATPLT of GSLIB version 2.0. A file containing the observed and estimated values for the population in question, was prepared and a scatterplot was made to compare the two sets of data. If the two distributions were similar the data would plot as a straight line at the 45° bisector. Values for the correlation and rank correlation were calculated as well.

Analysis of cross-validated residual or errors

An analysis of estimation errors was carried out as follows:

- Histograms for each error population were prepared using the HISTPLT module of GSLIB, to check the distribution of the errors
- Variograms were prepared using VARIONWIN to check independence of errors

Both transformed and original populations were geostatistically treated and a comparison of their model errors was conducted. The best way to describe a particular variable population was selected, based on the model that produces the error population with the best performance.

Mapping

Gray scale maps of kriging estimates were prepared in GSLIB version 2.0; using the module PIXELPLT.

7.4. Results

7.4.1. soil pH

Soil pH varies from a very acid zone, where pH values as low as 2.7 were found, to a neutral-alkaline zone. Around 83 % of data were in the second region. A bimodal distribution was found to represent best these two regions. This distribution was considered an extreme platykurtic distribution (Sokal and Rohlf, 1995) and was transformed in order to normalise it.

The transformation was:

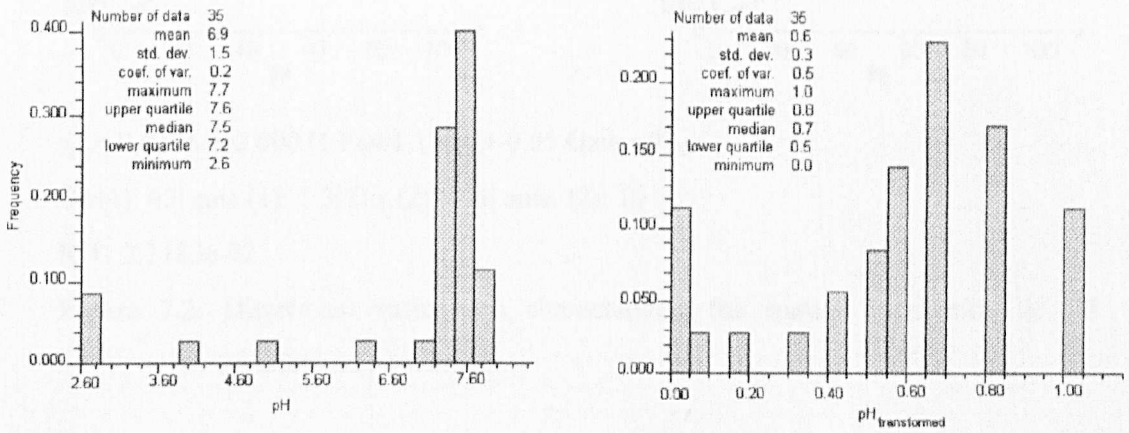
$$pH_{bc} = \frac{1}{(pH_{ref})^2}$$

$$pH_{ref} = 8.7 - pH_i$$

where:

bc = Box-Cox transformed population, ref = reflected population, 8.7 = the highest value in the population + 1, pH_i = the original population, i = sample id, for i= 1 to 35

In the error comparison, the best performance was given by the transformed population model. The histograms and descriptive statistics for the original and transformed pH population are shown in Figures 7.1a and b.

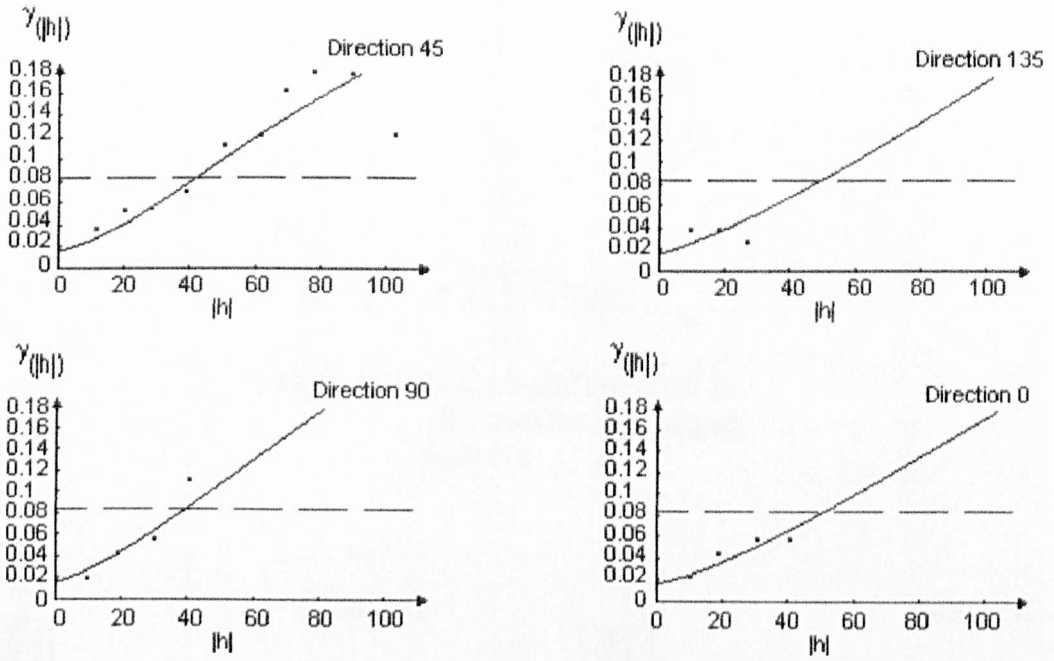


a. original **b.** transformed

Figure 7.1. Histogram and descriptive statistics for the pH populations.

The directional variogram characterising the spatial distribution of the pH transformed populations are given in Figure 7.2. This spatial variability can be described as a nested guassian and power model, as shown in the Figure 7.2. The histogram of the ordinary kriging estimates and the scatterplot of observed versus estimated values are given in Figures 7.3 and 7.4 respectively.

The histogram of ordinary kriging estimate errors and the variogram of errors are given in Figures 7.5 and 7.6 respectively.



$\gamma_{(h)}$= 0.0176 + 0.00071 Pow1.175$_{(h)}$+ 0.05 Gauss 92$_{(h)}$

Dir(1): 63| anis.(1): 1.3| Dir.(2): 191| anis. (2): 10

IGF: 3.1183e-02

Figure 7.2. Directional variograms characterising the spatial distribution of pH transformed population.

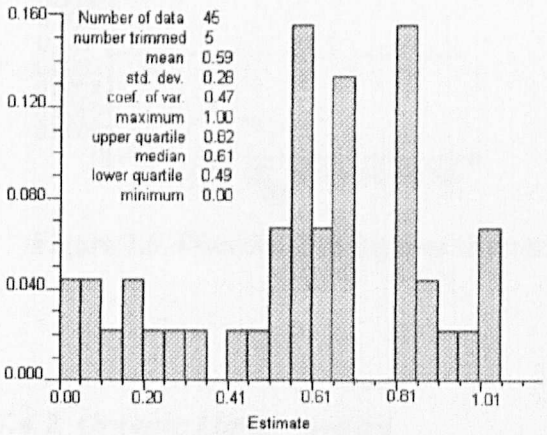


Figure 7.3. Histogram and descriptive statistics of the ordinary kriging estimates for the pH transformed population.

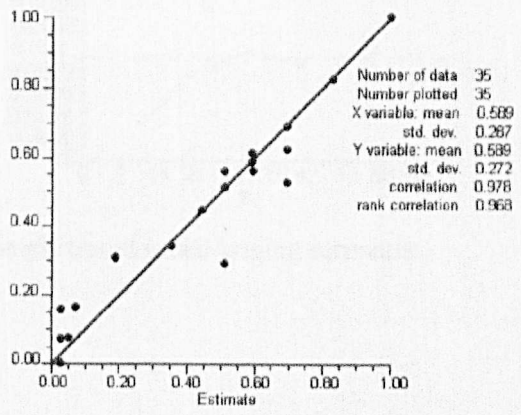


Figure 7.4. Scatterplot of observed versus estimated values for the soil pH transformed population.

The gray scale map of the ordinary kriging estimates for the pH transformed population is shown in Figure 7.7.

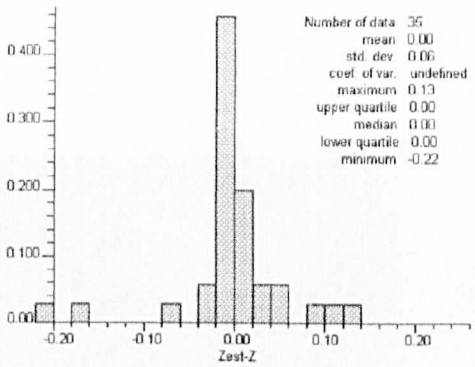


Figure 7.5. Histogram of errors for the pH transformed kriging estimates.

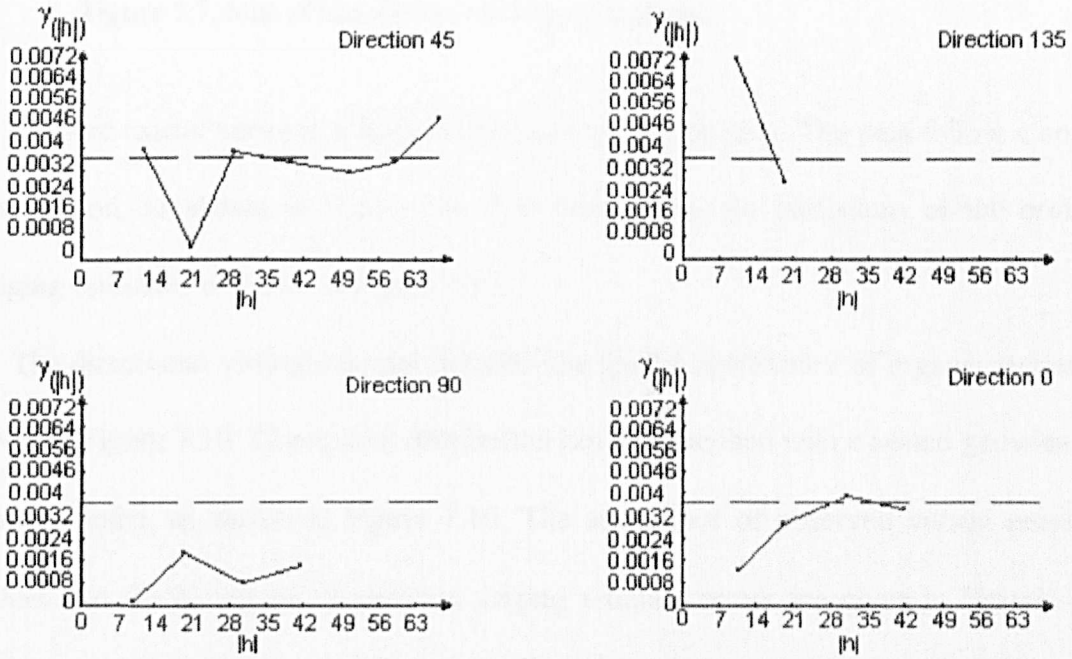


Figure 7.6. Directional variograms of errors for the pH transformed kriging estimates.

7.4.2. Organic Matter content

Organic matter content shows a positive correlation with pH. This could be due to the oxidation of pyrite and the resulting low pH values in the acid zone. One of the oxidation reactions could take place if the ferric iron (Fe^{3+}) acts as an oxidising agent in the aqueous system. The ferric iron could be in solution either because the low pH or by complexation with organics such as humic acid.

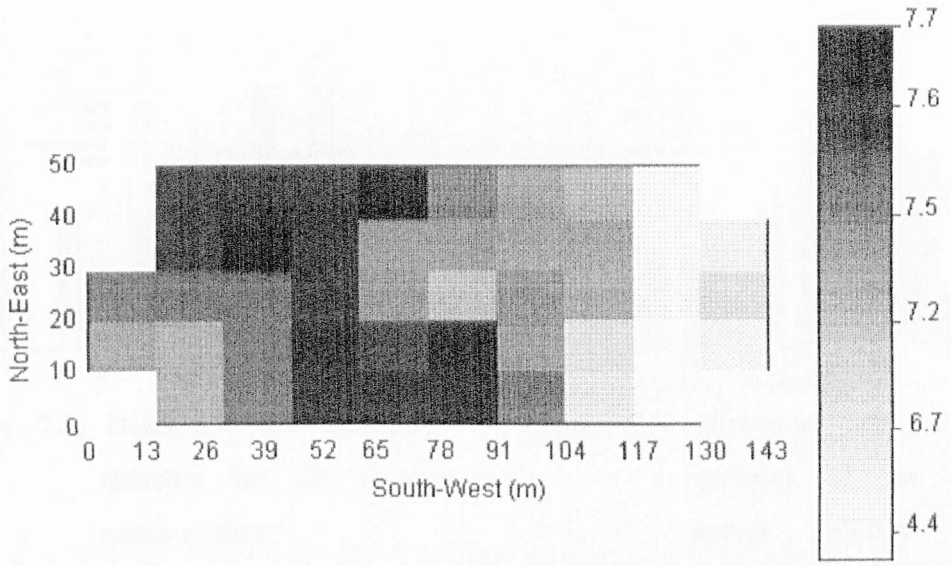


Figure 7.7. Map of transformed pH kriging estimates.

Organic matter varies in a fairly continuous way in the area. The data follow a normal distribution, as shown in Figure 7.8. For comparison, the histogram of the ordinary kriging estimates is shown in Figure 7.9.

The directional variograms that describe the spatial distribution of organic matter are given in Figure 7.10. This spatial distribution can be described with a nested gaussian and power model, as shown in Figure 7.10. The scatterplot of observed versus estimated values and the histogram of ordinary kriging estimate errors are given in Figures 7.11 and 7.12 respectively.

The directional variograms of errors are given in Figures 7.13. The gray scale map of the kriging estimated values is given in Figure 7.14.

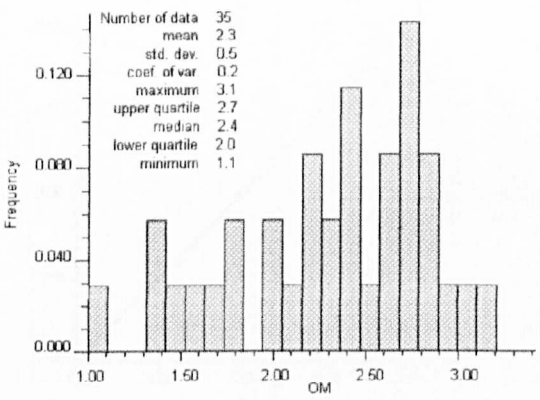


Figure 7.8. Histogram and descriptive statistics for the organic matter content.

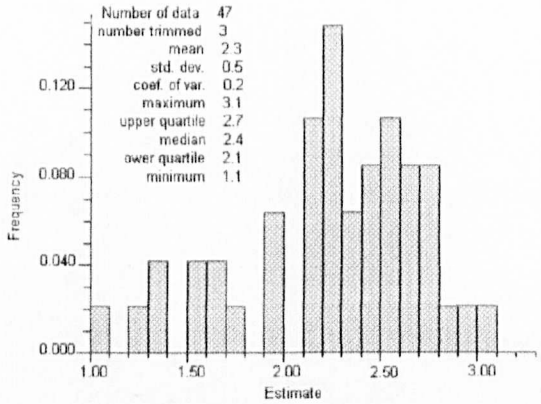
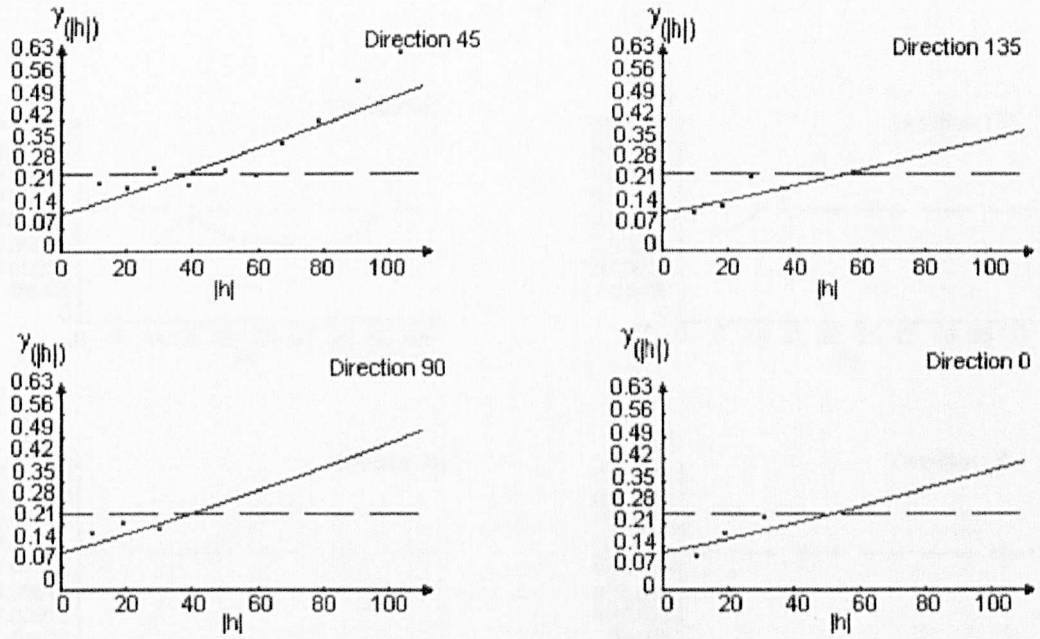


Figure 7.9. Histogram and descriptive statistics of the organic matter ordinary kriging estimates.



$\gamma_{(h)} = 0.1252 + 0.00137\ \text{Pow1.104}_{(h)} + 0.003\ \text{Gauss 110}_{(h)}$

Dir(1): 106| anis.(1): 0.61| Dir.(2): 94| anis. (2): 5.3

IGF: 4.7742e-02

Figure 7.10. Directional variograms characterising the spatial distribution of the organic matter content population.

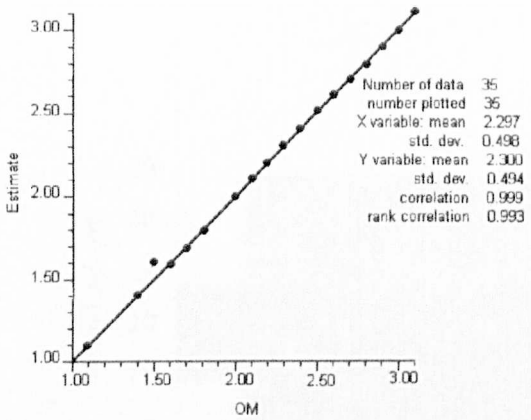


Figure 7.11. Scatterplot of observed versus estimated values for the organic matter content population.

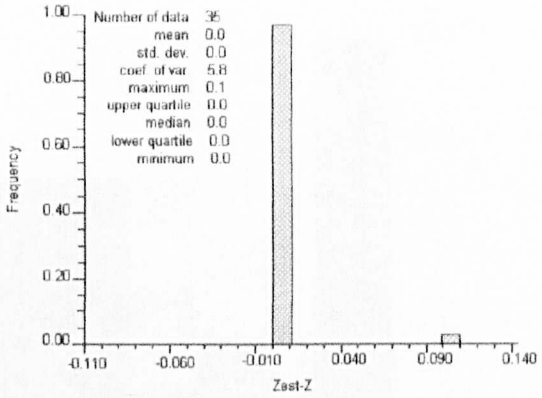


Figure 7.12. Histogram of errors for the organic matter content kriging estimates.

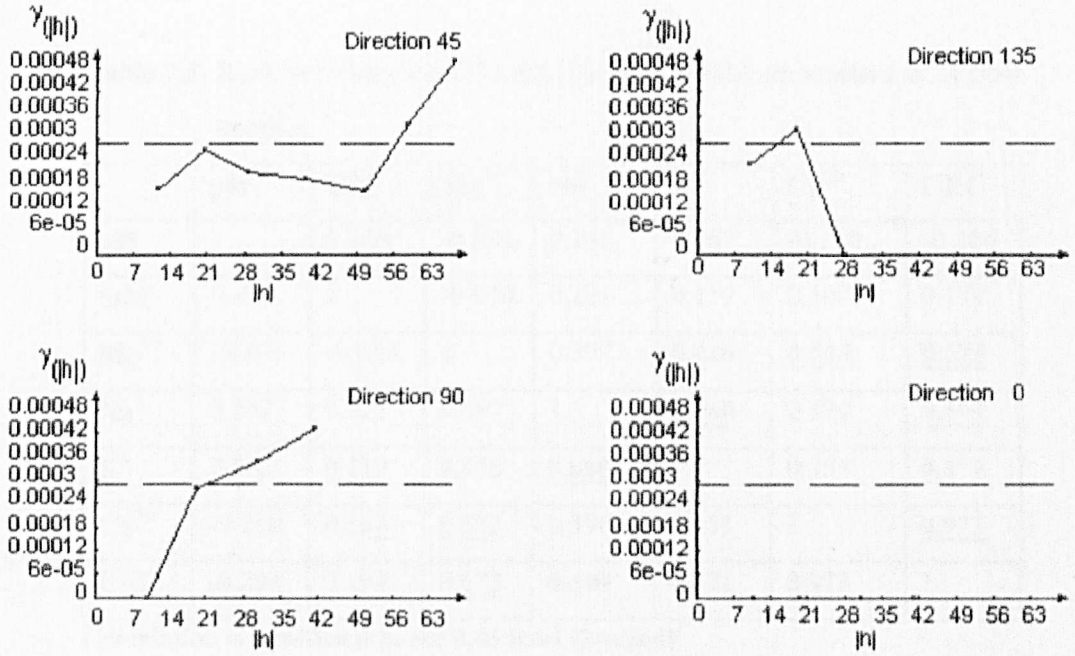


Figure 7.13. Directional variograms of errors for the organic matter content kriging estimates.

7.4.3. CEC and exchangeable cations

The rank correlation coefficients calculated for Mg^{2+}, Ca^{2+}, Na^{+}, K^{+}, CEC, pH and organic matter content are given in Table 7.2.

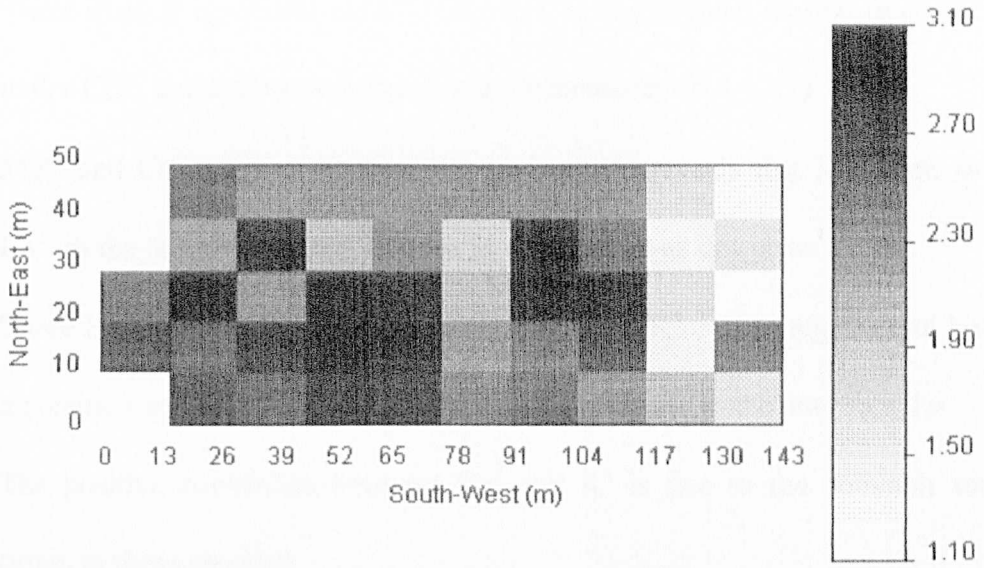


Figure 7.14. Gray scale map of organic matter kriging estimates.

Table 7.2. Rank correlation coefficients for geochemical parameters in 24 liner samples.

	pH	OM	Mg^{2+}	Na^{+}	K^{+}	Ca^{2+}	CEC
pH	1	0.158	-0.206	0.252	0.262	-0.260	-0.204
OM	0.158	1	-0.010	0.221	0.119	0.167	0.199
Mg^{2+}	-0.206	-0.010	1	0.397	**0.416**	**0.553**	**0.673**
Na^{+}	0.252	0.221	0.397	1	**0.680**	0.370	**0.499**
K^{+}	0.262	0.119	**0.416**	**0.680**	1	0.351	**0.471**
Ca^{2+}	-0.260	0.167	**0.553**	0.370	0.351	1	**0.973**
CEC	-0.204	0.199	**0.673**	**0.499**	**0.471**	**0.973**	1

Correlation is significant at the 0.05 level (2-tailed)

Correlation is significant at the 0.01 level (2-tailed)

Observations:

- There is no correlation between CEC and pH, this means that most of the of the CEC is due to the permanent fixed charge at the clay surface, that is, the contribution of the pH dependent charge (sesqioxides, kaolinite and allophane) is null above pH 6

- There is no a significant contribution to CEC by organic matter, in the pH range under CEC and cation exchangeable were measured (6.3 - 7.7)
- Mg^{2+} and Ca^{2+} show a positive correlation, this reveals that Mg^{2+} can substitute Ca^{2+} in the calcite lattice or a common origin, such as dolomite
- There is a positive correlation between Mg^{2+} and K^{+} , this suggests that both have a common source of origin, such as illite and smectite in the liner samples
- The positive correlation between Na^{+} and K^{+} is due to the common source of origin in these samples

7.4.4. Cu, Cr and Zn

7.4.4.1. Exchangeable fraction

Zn, Cu and Cr were found as exchangeable forms, particularly in the samples collected in the acid zone. The concentration of the three metals increased as pH decreased.

Bayesian probability concepts-the Bayes theorem- were applied to the exchangeable Zn, Cu and Cr populations, because of the few data in each population. Using this type of probability, it is possible to combine new evidence concerning a hypothesis with prior knowledge. This allows an estimate of the likelihood that the hypothesis is true to be calculated from one or more items of evidence. The Bayes theorem is given by (Hoshmand, 1998):

$$p(h|e) = \frac{p(e|h) \times p(h)}{\sum_i p(e|h_i) \times p(h_i)}$$

where:

h = the hypothesis, there will be a number, i, of possible outcomes, but these must be mutually exclusive, for example, samples could either have a metal as exchangeable cation, or do not have it

e = evidence, for example, observations of pH (acid or neutral-alkaline)

Σ = sum each of the I possible outcomes

p(e|h) = the probability of the evidence occurring given that the hypothesis is true, for example, samples with an acid pH, are more likely to have metals as exchangeable cations, but not all samples with an acid pH will have metals as exchangeable cations

p(h) = the prior probability, the probability of the hypothesis is being true regardless of the new evidence, for example, the likelihood of the site having exchangeable cations

p(h|e) = the posterior probability, the probability of the hypothesis being true given the evidence, for example; the probability of the metals as exchangeable cation being present given the observed pH

The results of the Bayes theorem applied to exchangeable Cr, Cu and Zn populations are given from Figures 7.15 to 7.17.

Observations:

- The posterior probability of Zn being an exchangeable cation given the occurrence of acid pH is high, around 1. Whereas, the posterior probability of Zn being as exchangeable cation given a neutral-alkaline pH is null
- The posterior probability of Cu being as an exchangeable cation given the occurrence of pH acid is 0.5, whereas, the posterior probability of Cu as an exchangeable form given the occurrence of a neutral-alkaline pH is null
- The posterior probability of Cr being as an exchangeable cation given the occurrence of pH acid is 0.33, whereas the posterior of the presence of exchangeable Cr, given the occurrence of a neutral-alkaline pH is low (0.069), but possible

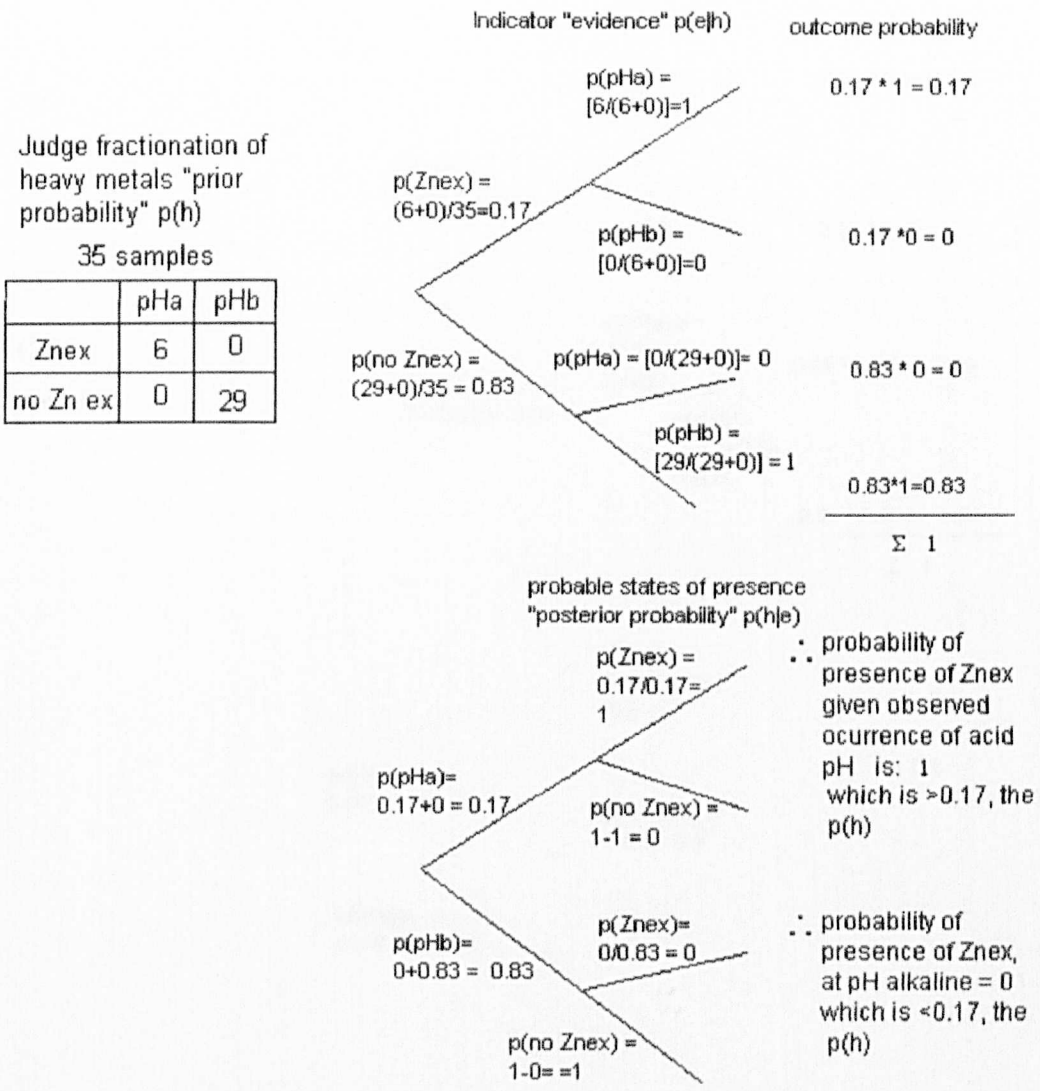


Figure 7.15. The Bayes theorem applied on the exchangeable Zn results.

– Even that exchangeable Cu and Cr are influenced by pH changes, the most affected one metal was Zn. This could be due to the fact that the selectivity of adsorption by the charged surface depends on the ion charge and the radius of the hydrated ion, thus, Zn having the largest hydrated radius, it is not as selectively absorbed as the others are

Judge fractionation of heavy metals "prior probability" p(h)

35 samples

	pHa	pHb
Cuex	3	0
noCuex	3	29

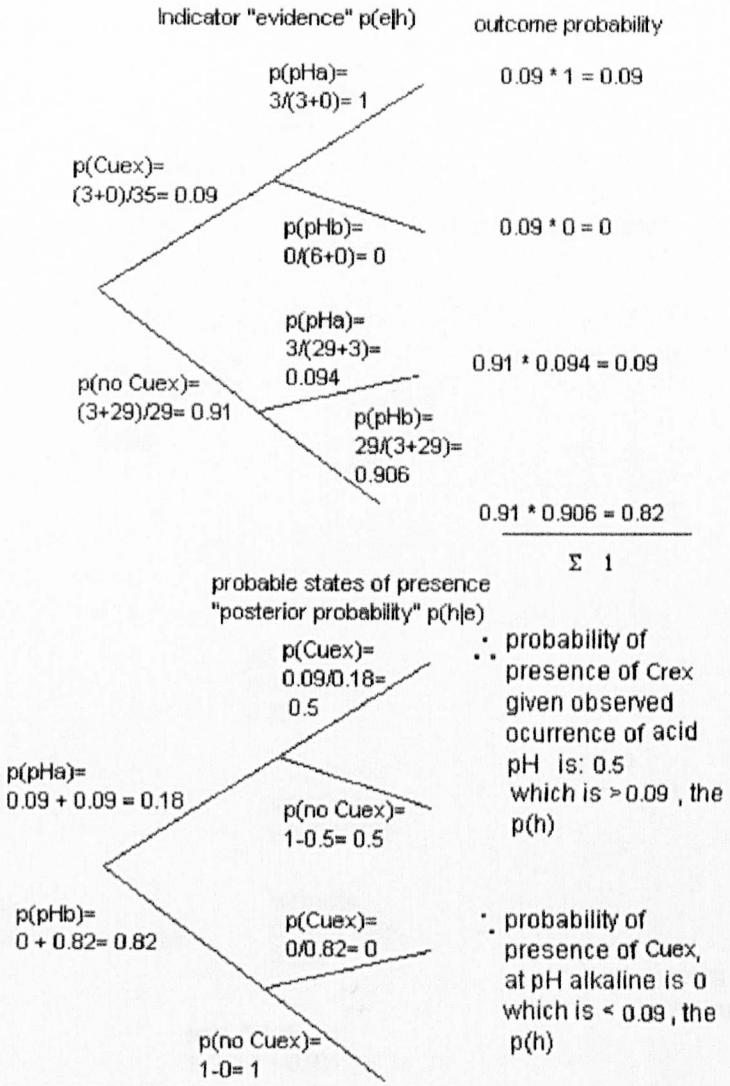


Figure 7.16. The Bayes theorem applied on the exchangeable Cu results.

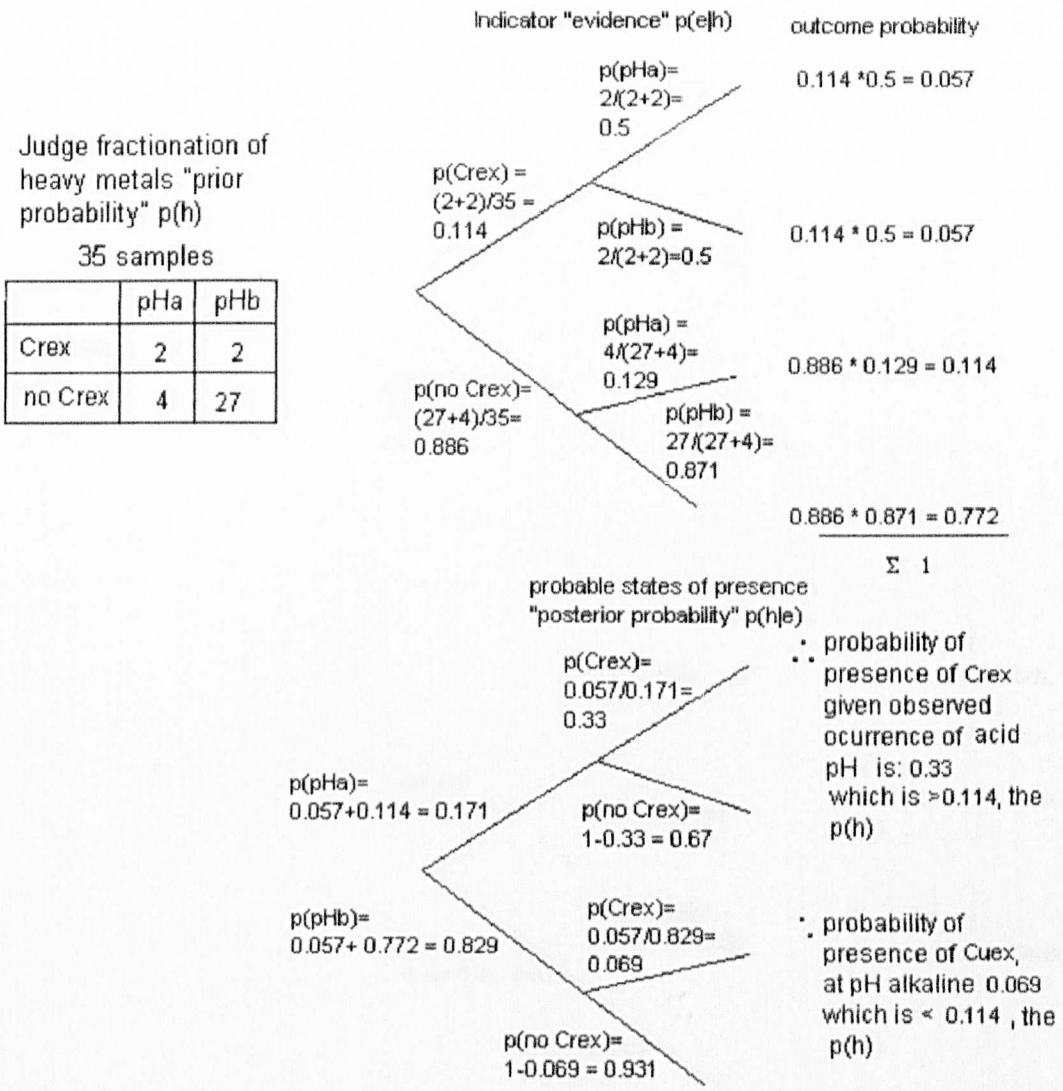
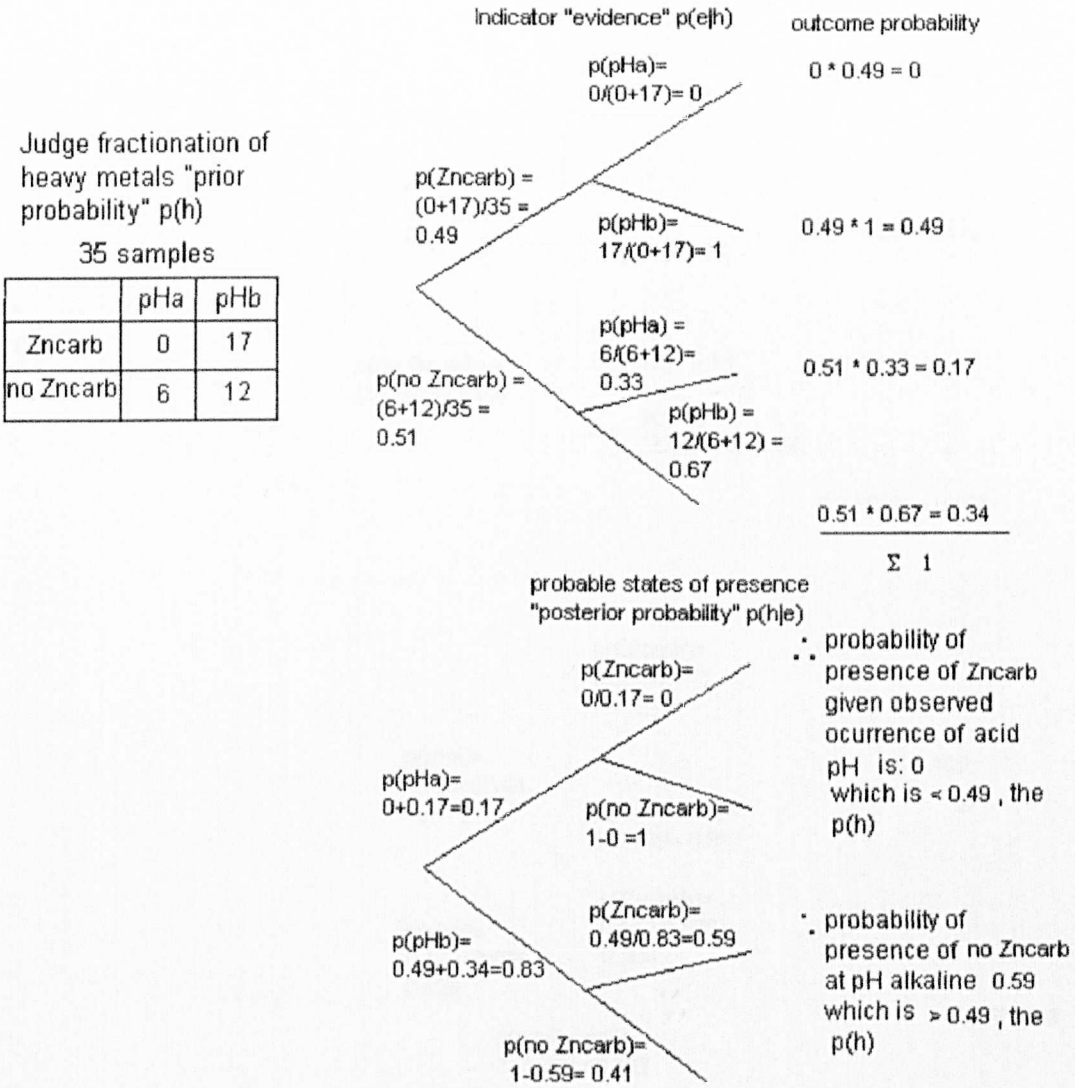


Figure 7.17. The Bayes theorem applied on the exchangeable Cr results.

7.4.4.2. Fraction bound to carbonates

Zn and Cu were found in some samples bound to carbonates. The Bayes theorem was applied to the results of metals bound to carbonates. The results are shown in Figures 7.18 and 7.19.



	pHa	pHb
Zncarb	0	17
no Zncarb	6	12

Figure 7.18. The Bayes theorem applied to the Zn bound to carbonates results.

Observations:

- Zn and Cu could be bound to calcite by a sorption mechanism in areas where the pH varies from neutral to alkaline. In the acid zone they could be bound to gypsum in the acid zone, the other main mineral source of carbonates in that zone.

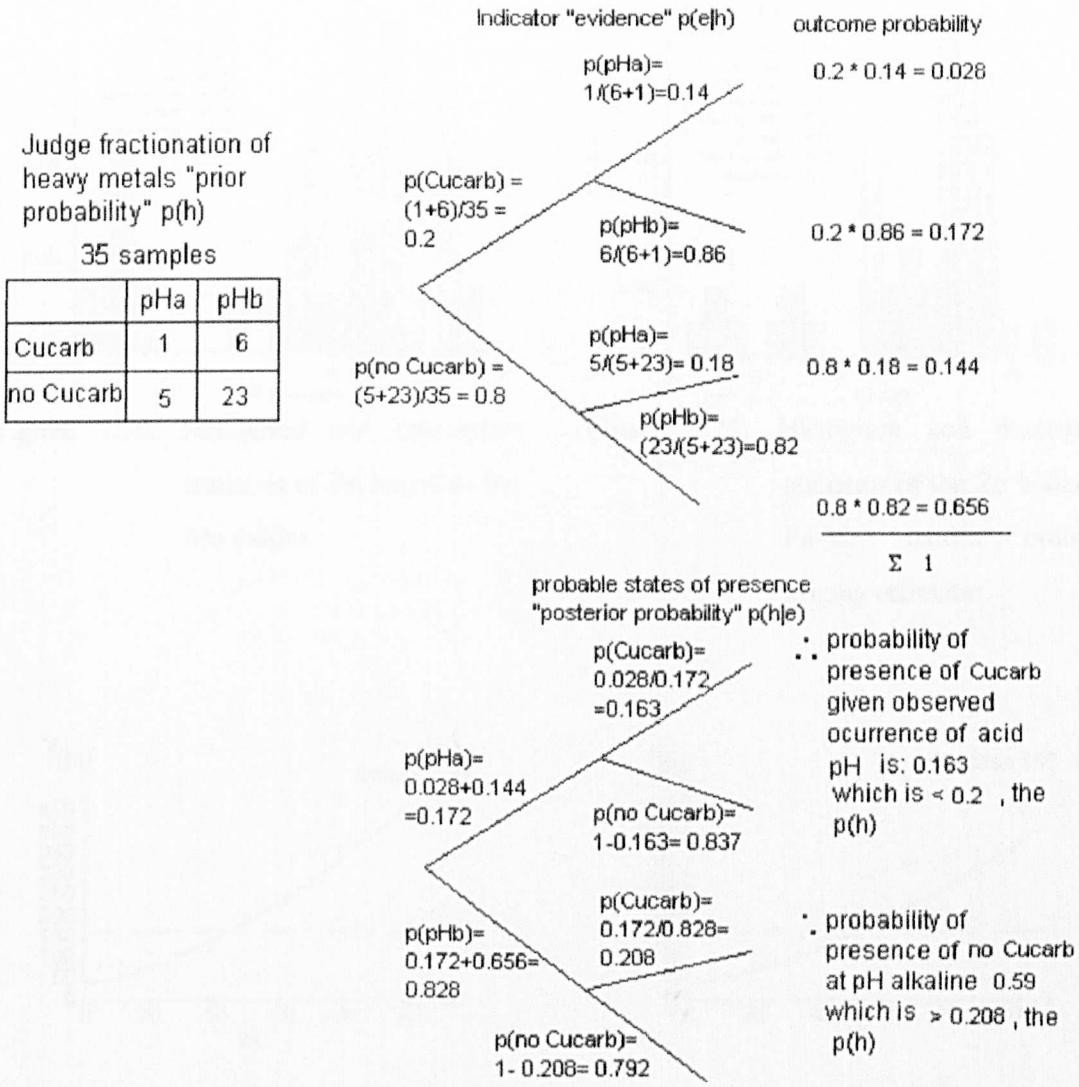


Figure 7.19. The Bayes theorem applied on the Cu bound to carbonates results.

7.4.4.3. Fraction bound to Fe-Mn oxides

Zn was the only metal bound to Fe-Mn oxides and the population has a normal distribution. The histogram and descriptive statistics are given in Figure 7.20; the modelled population of Zn bound to Fe-Mn oxides is shown in Figure 7.21. The directional variograms characterising the spatial distribution of the Zn bound to Fe-Mn oxides are given in Figure 7.22. This spatial variability can be described by a power model, as shown in Figure 7.22.

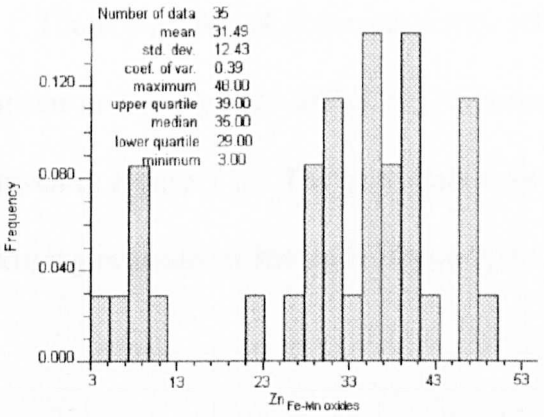


Figure 7.20. Histogram and descriptive statistics of Zn bound to Fe-Mn oxides.

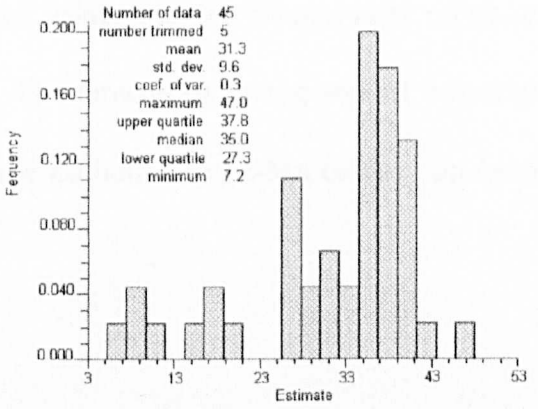
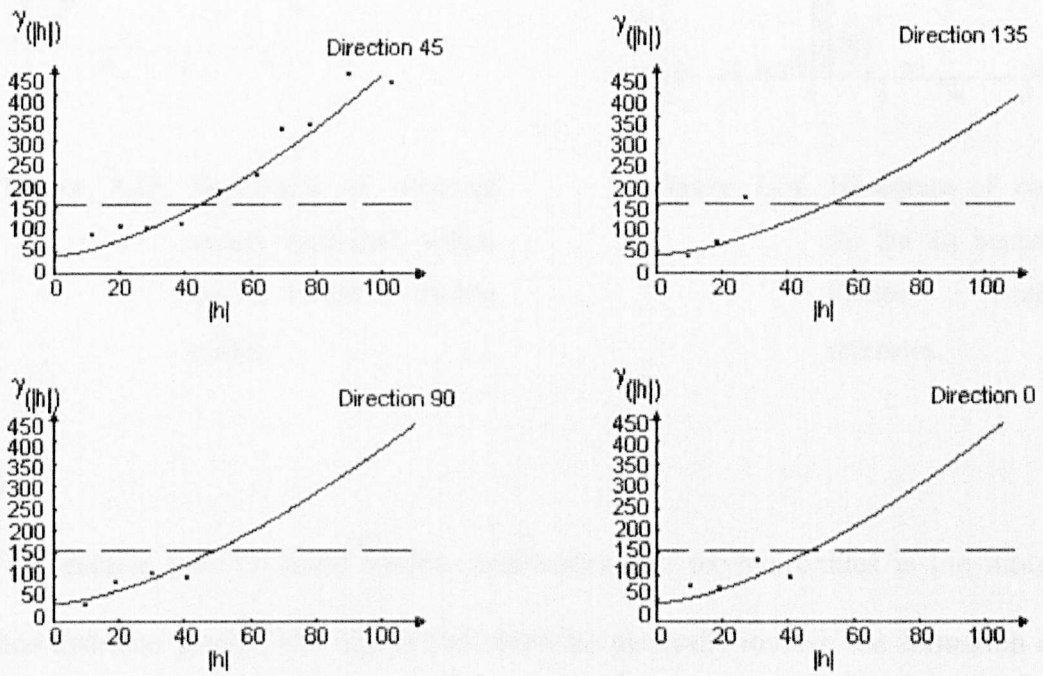


Figure 7.21. Histogram and descriptive statistics of the Zn bound to Fe-Mn oxides ordinary kriging estimates.



$\gamma_{(h)}$= 43.329 + 0.3624 Pow1.526$_{(h)}$

Dir: 173| anis.: 1.2

IGF: 4.3285e-02

Figure 7.22. Directional variograms characterising the spatial distribution of Zn bound to Fe-Mn oxides.

The scatterplot of observed versus estimated values and the histogram of errors are given in Figures 7.23 and 7.24, respectively. The directional variograms of errors are given in Figure 7.25. The gray scale map for the Zn bound to Fe-Mn oxides population kriging estimates is shown in Figure 7.26.

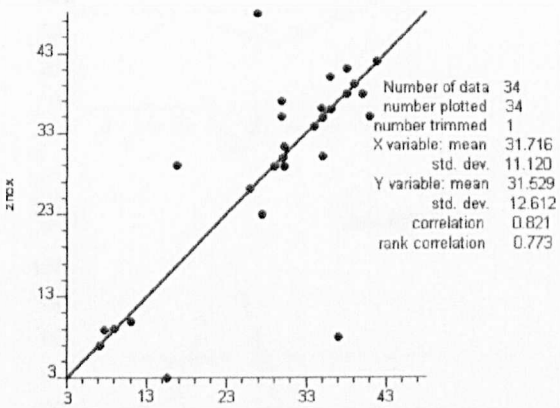


Figure 7.23. Scatterplot of observed versus estimated values for Zn bound to Fe-Mn oxides.

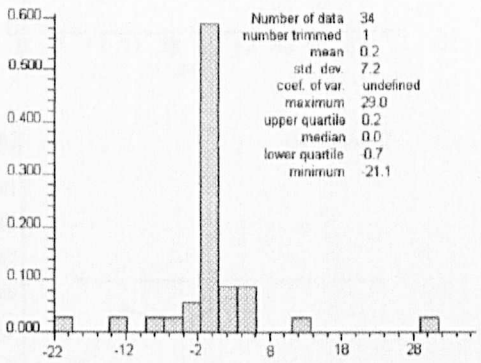


Figure 7.24. Histogram of errors for the Zn bound to Fe-Mn oxides estimates.

Note:

The reactive part of metal oxides, hydroxides and oxyhydroxides is the inorganic surface hydroxyl group. The adsorption reactions generally involve the formation of an inner sphere complex (formed largely via covalent metal-ligand bonds) between the hydroxo metal ion and the deprotonated negatively charged surfaces of Al, Mn and Fe. The specific adsorption of a ion metal by this reaction, occurs most readily for metals that hydrolyse in water. The relative affinities of the metals tend to follow the Irving-Williams order: $Hg^{2+} > Pb^{2+} > Cu^{2+} > Zn^{2+} > Ni^{2+} \sim Co^{2+} > Cd^{2+}$ (Naidu *et al*, 1996).

The above mentioned explains why Zn was preferentially bound to Fe-Mn oxides over Cu and Cr.

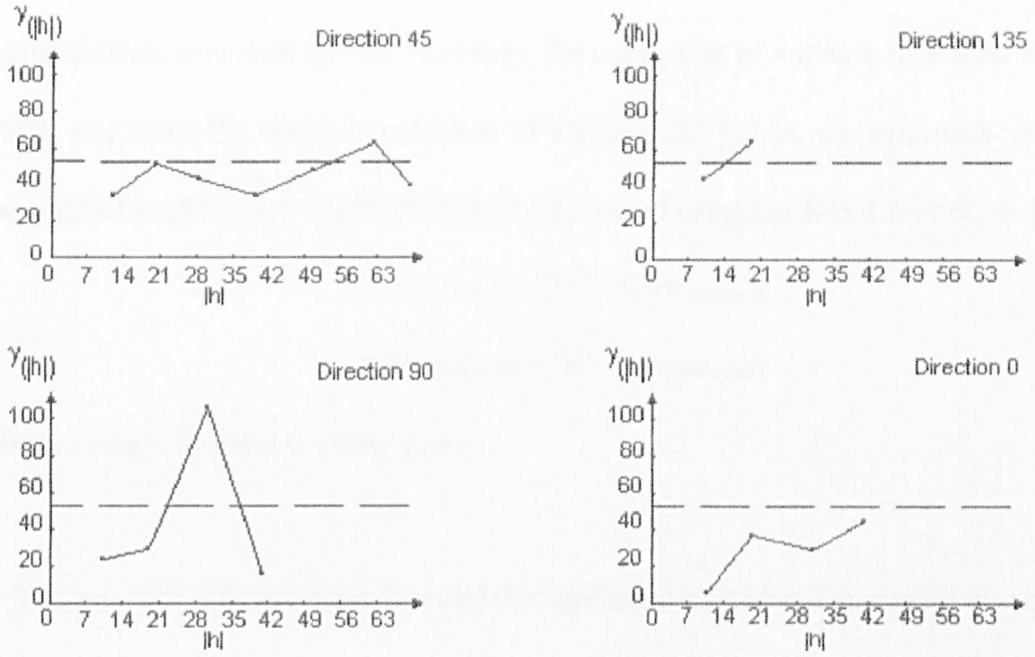


Figure 7.25. Directional variograms of the errors for the kriging estimates of Zn bound to Fe-Mn oxides.

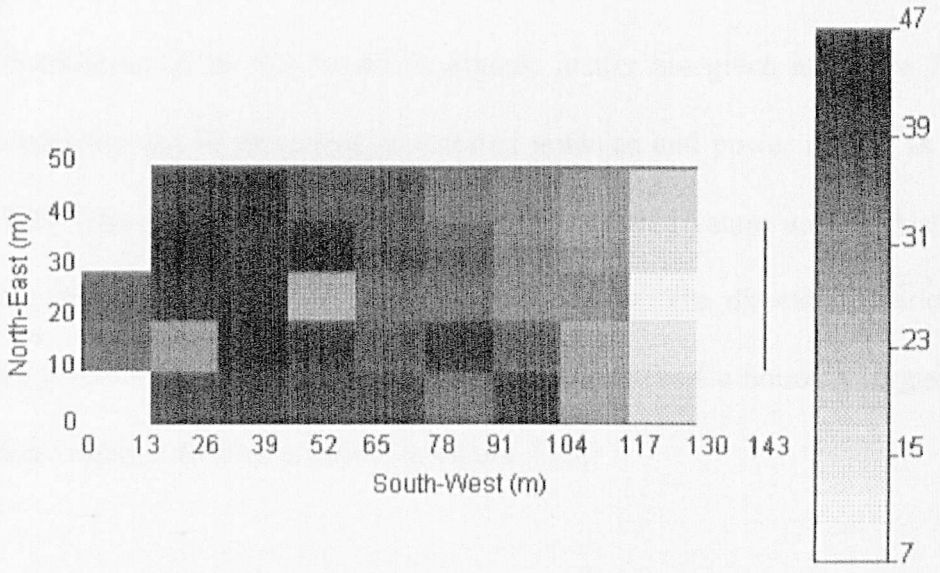


Figure 7.26. Gray scale map of the Zn bound to Fe-Mn oxides kriging estimates.

7.4.4.4. Fraction bound to Organic Matter

Cu

The original population did not have a normal distribution (Skewness: -1.6630, Kurtosis: 4.8194) when the Kolmogorov-Smirnoff test was applied and to normalise it a Box-Cox transformation was used (λ =2). However, the coefficient of variance increased to 50 %, which was twice the original coefficient of variance (27 %). A new approach was tried, the original population was reflected and transformed using the Box-Cox test, as follows:

$$Cuorg_{reflected} = 21.7 - Cuorg_{original}$$

$$Cuorg_{transformed} = \ln (Cuorg_{reflected})$$

where: Cuorg = Cu bound to organic matter

The new population was normal and the coefficient of variance increased by only 6 %.

During the errors comparison, the original population model gave better results and was chosen to be reported. The histogram and descriptive statistics are given in Figure 7.27. The histogram and descriptive statistics of the modelled Cu bound to organic matter population are given in Figure 7.28. The directional variograms characterising the spatial distribution of the Cu bound to organic matter are given in Figure 7.29. This spatial variability can be described as a nested guassian and power model, as shown in Figure 7.29. The scatterplot of observed versus estimated values and the histogram of errors are given in Figures 7.30 and 7.31 respectively. The directional variograms of errors are given in Figures 7.32. The gray scale map of the Cu bound to organic matter population kriging estimates is shown in Figure 7.33.

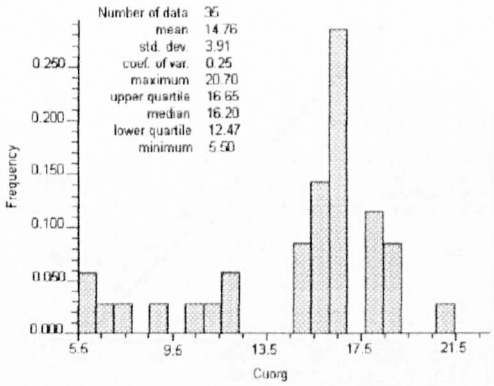


Figure 7.27. Histogram and descriptive statistics for Cu bound to organic matter.

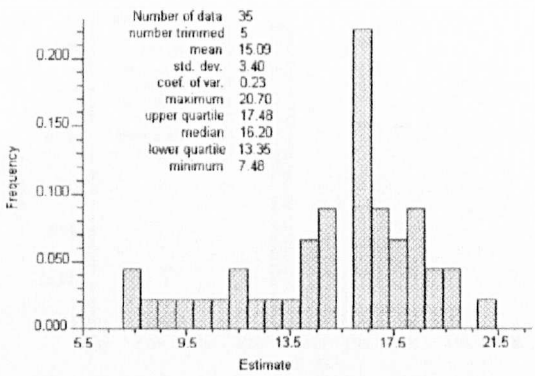
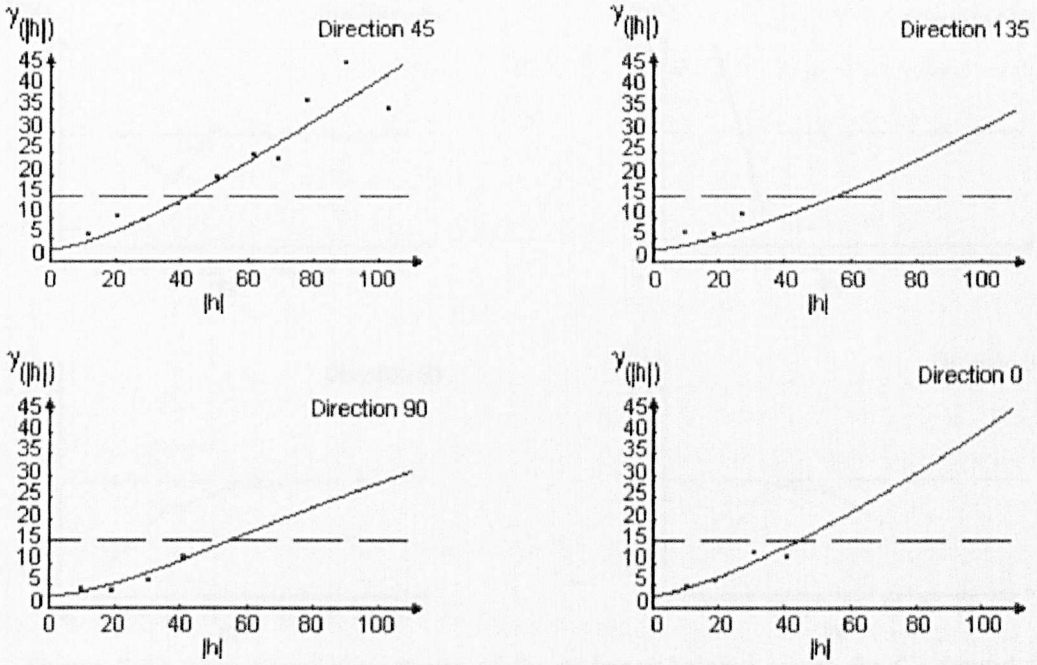


Figure 7.28. Histogram and descriptive statistics of the ordinary kriging estimates for Cu bound to organic matter.



$\gamma_{(h)}$= 3 + 0.081 Pow1.33$_{(h)}$+ 10.3 Gauss 110$_{(h)}$

IGF: 3.48e-02

Dir(1): 145| anis.(1): 1.9| Dir.(2): 210| anis. (2): 31

Figure 7.29. Directional variograms characterising the spatial distribution of Cu bound to organic matter.

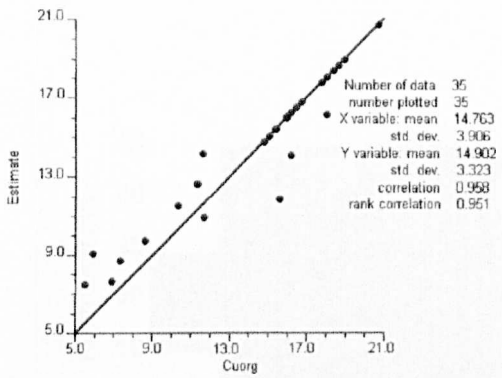


Figure 7.30. Scatterplot of observed versus estimated values for Cu bound to organic matter.

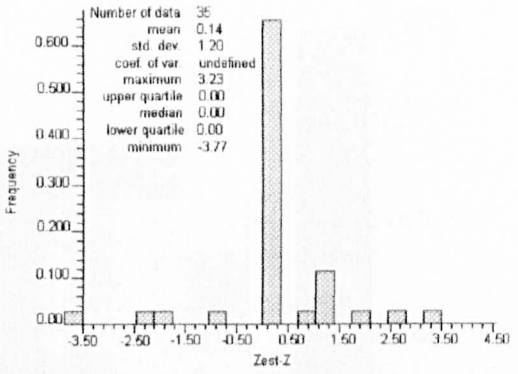


Figure 7.31. Histogram of errors for the Cu bound to organic matter estimates.

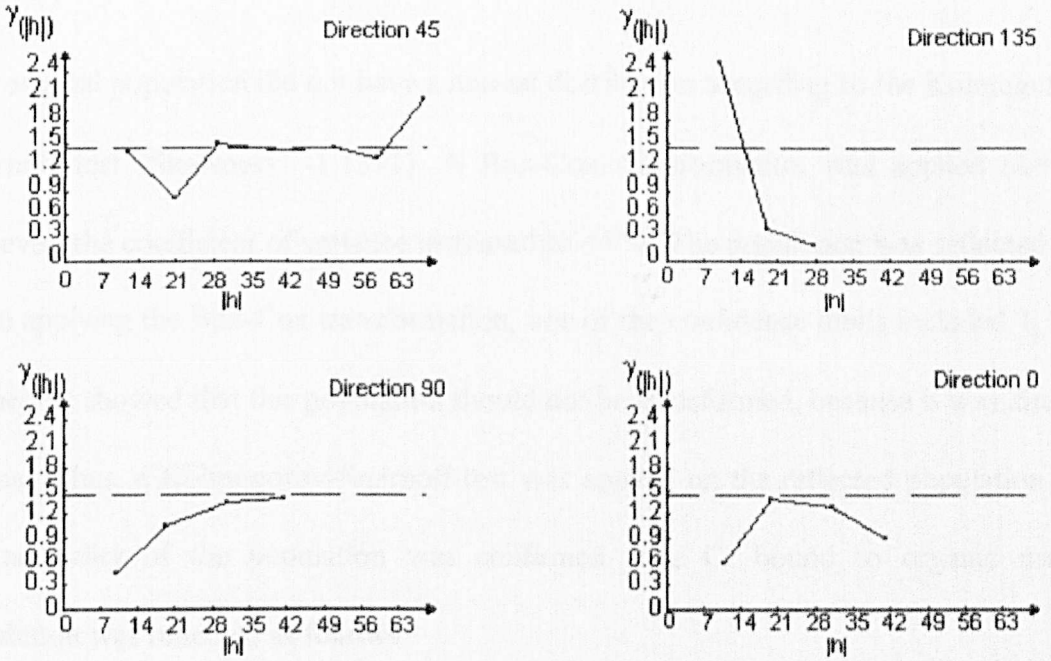


Figure 7.32. Directional variograms of the ordinary kriging errors for Cu bound to organic matter.

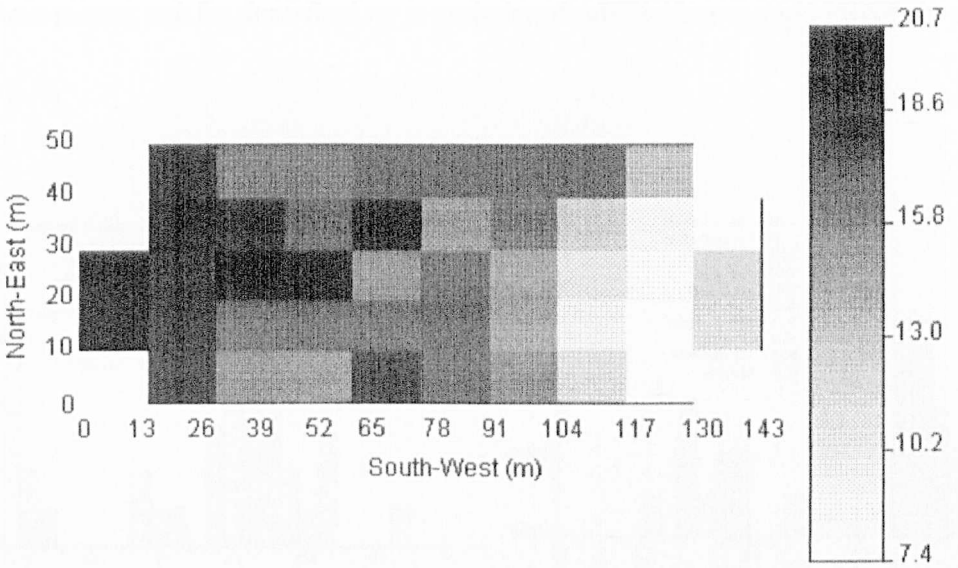


Figure 7.33. Gray scale map of Cu bound to organic matter kriging estimates.

Cr

The original population did not have a normal distribution according to the Kolmogorov-Smirnoff test (Skewness: -1.1331). A Box-Cox transformation was applied (λ= 2), however, the coefficient of variance increased to 44 %. The population was reflected and when applying the Box-Cox transformation, one of the confidence limits included 1, that is, the test showed that this population should not be transformed, because it was already normal. Thus, a Kolmogorov-Smirnoff test was applied on the reflected population and the normality of the population was confirmed. The Cr bound to organic matter population was reflected as follows:

$$Crorg_{reflected} = 7.4 - Crorg_{original}$$

During the errors comparison the original population model gave better results and was the one chosen to be reported. The histogram and descriptive statistics for the original population and the modelled original population are given in Figures 7.34 and 7.35 respectively. The directional variograms characterising the spatial distribution of the Cr bound to organic matter are given in Figure 7.36. The spatial variability of Cr bound

to organic matter can be described by a guassian model with a nugget effect, as shown in Figure 7.36.

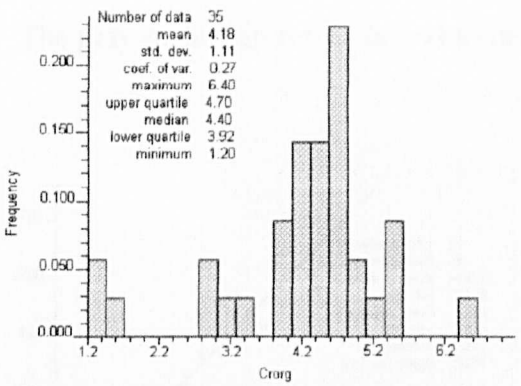


Figure 7.34. Histogram and descriptive statistics of Cr bound to organic matter.

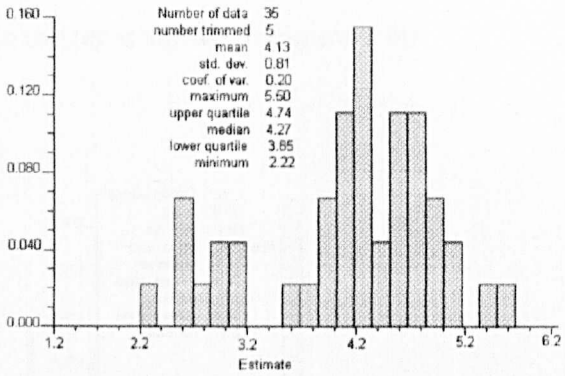
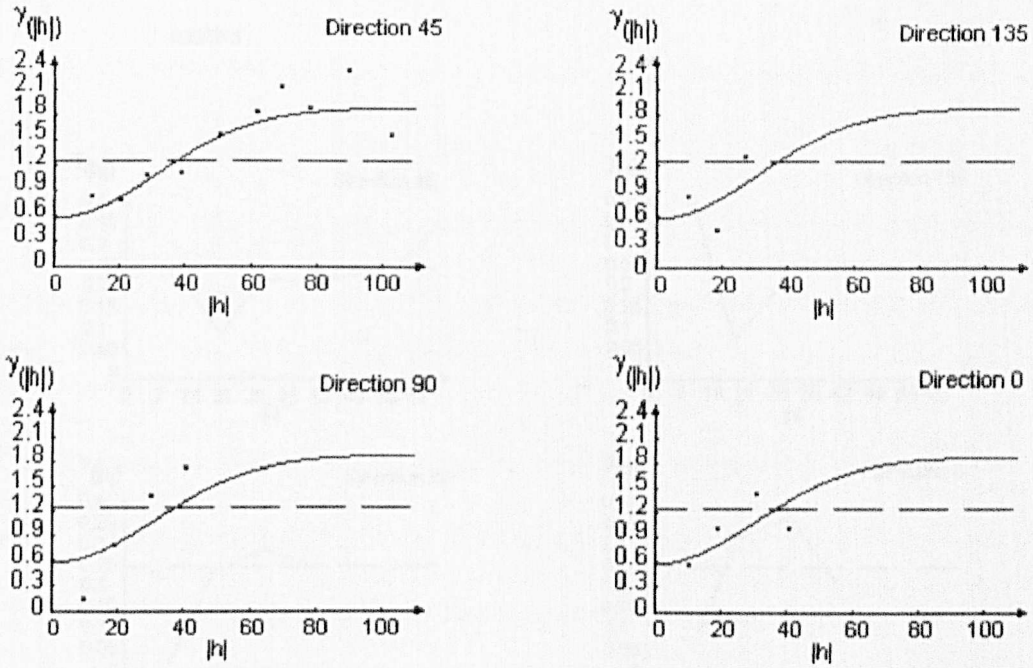


Figure 7.35. Histogram and descriptive statistics of the ordinary kriging estimates for Cr bound to organic matter.



$\gamma_{(h)}$= 0.6 + 1.3 Gauss 76$_{(h)}$

Dir: 32| anis.: 0.97

IGF: 7.667e-02

Figure 7.36. Directional variograms characterising the spatial distribution of the Cr bound to organic matter.

The scatterplot of observed versus estimated values and the histogram of errors are given in Figures 7.37 and 7.38, respectively. The variogram of errors are given in Figure 7.39.

The gray scale map for Cr bound to organic matter is shown in Figure 7.40.

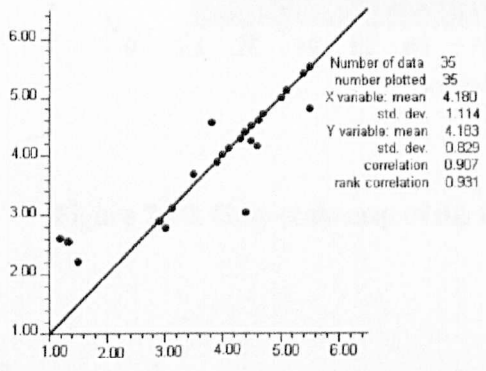


Figure 7.37. Scatterplot of observed versus estimated values for Cr bound to organic matter.

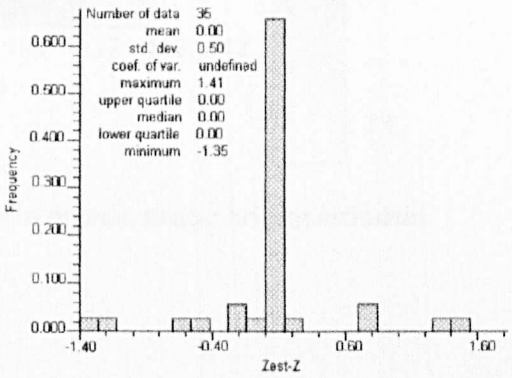


Figure 7.38. Histogram of errors for Cr bound to organic matter ordinary kriging estimates.

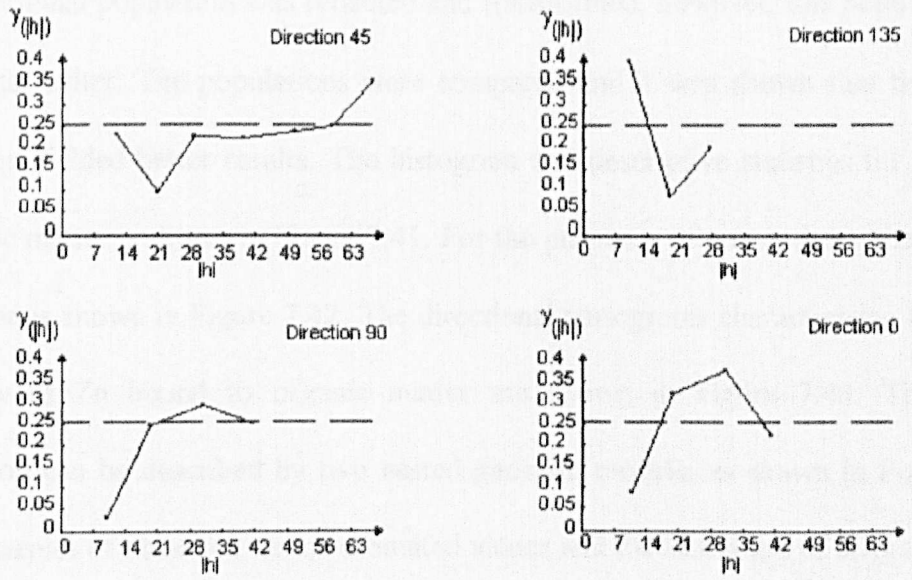


Figure 7.39. Directional variograms of errors for the Cr bound to organic matter estimates.

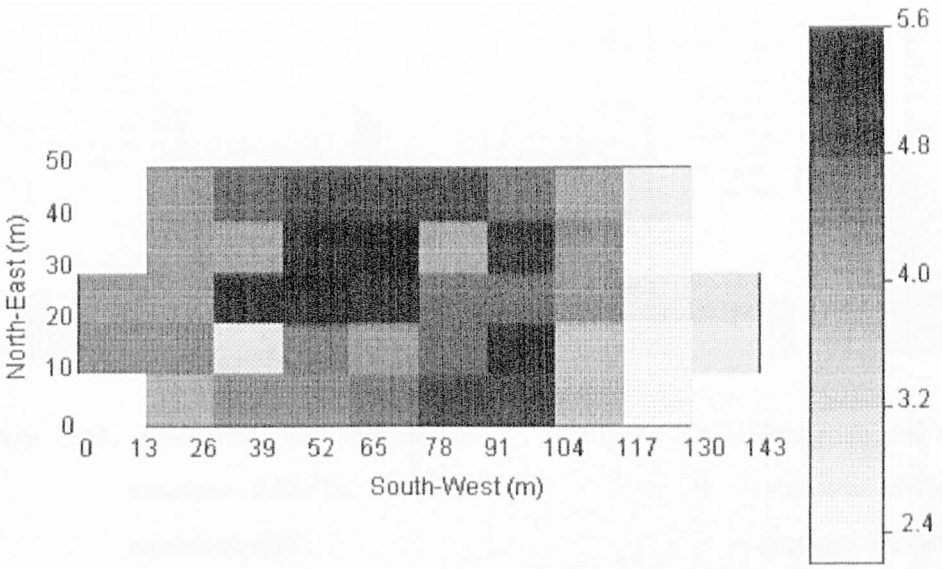


Figure 7.40. Gray scale map of the Cr bound to organic matter kriging estimates.

Zn

The original population was not normal according to the Kolmogorov-Smirnoff test (Skewness: -1.6630, Kurtosis: 4.8194). A Box-Cox transformation ($\lambda = 2$) was applied to normalise the original population, however, the coefficient of variance increased to 45 %. The original population was reflected and transformed, however, this population was not normal either. The populations were compared and it was shown that the original population yielded better results. The histogram and descriptive statistics for Zn bound to organic matter is shown in Figure 7.41. For the purposes of comparison, the modelled population is shown in Figure 7.42. The directional variograms characterising the spatial variability of Zn bound to organic matter are shown in Figure 7.43. This spatial distribution can be described by two nested gaussian models, as shown in Figure 7.43. The scatterplot of observed versus estimated values and the histogram of errors are given in Figures 7.44 and 7.45, respectively. The directional variogram of errors are given in Figure 7.46. The gray scale map for Zn bound to organic matter is shown Figure 7.47.

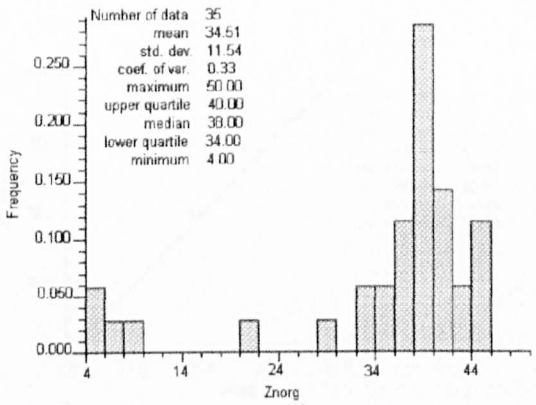


Figure 7.41. Histogram and descriptive statistics of the Zn bound to organic matter.

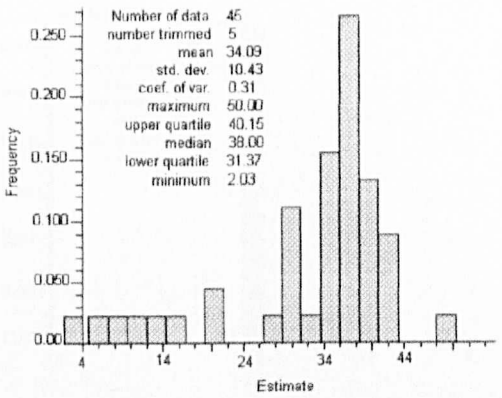
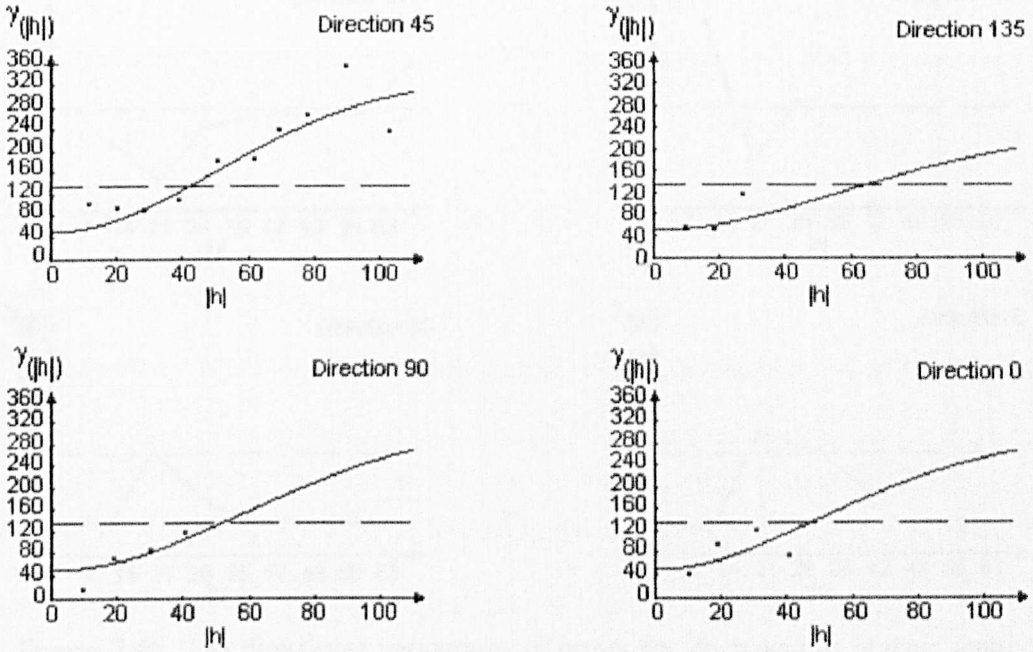


Figure 7.42. Histogram and descriptive statistics of Zn bound to organic matter ordinary kriging estimates.



$\gamma_{(h)}$= 53.7 + 140 Gauss $110_{(h)}$ + 140 Gauss $105_{(h)}$

Dir(1): 193| anis.(1): 8.9| Dir(2): 133| anis.(2): 1.7

IFG: 6.4604e-02

Figure 7.43. Directional variograms characterising the spatial variability of the Zn bound to organic matter.

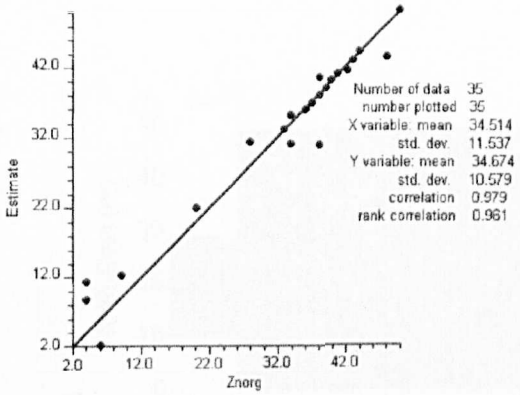


Figure 7.44. Scatterplot of observed versus estimated values for Zn bound to organic matter.

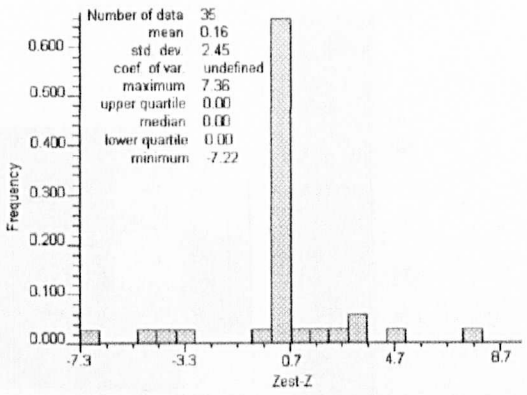


Figure 7.45. Histogram of errors for Zn bound to organic matter estimates.

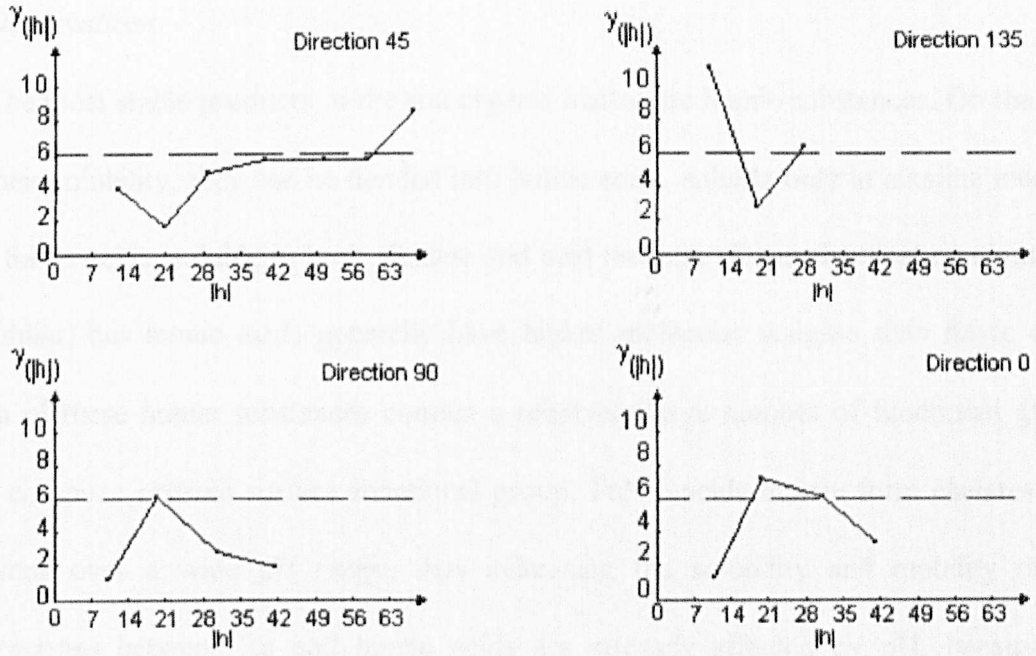


Figure 7.46. The directional variograms of errors for Zn bound to organic matter estimates.

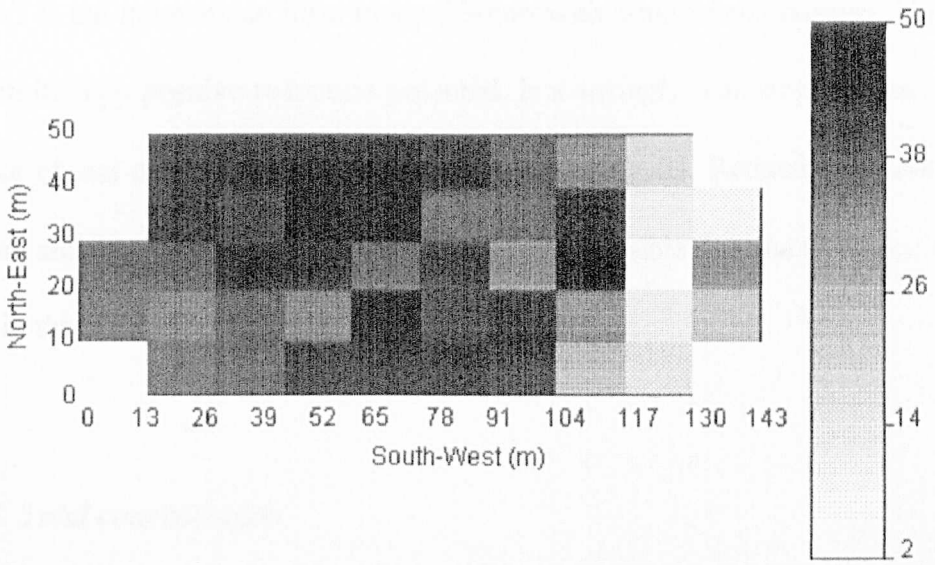


Figure 7.47. Gray scale map of Zn bound to organic matter kriging estimates.

Observations:

The most stable products of the soil organic matter are humic substances. On the basis of their solubility, they can be divided into humic acids, soluble only in alkaline medium, and fulvic acids, soluble in both alkaline and acid medium. Their chemical configuration is similar, but humic acids generally have higher molecular weights than fulvic acids. Both of these humic substances contain a relatively large number of functional groups that compose organic surface functional group. Fulvic acids mainly form chelates with Zn ions over a wide pH range, thus increasing the solubility and mobility of Zn. Interactions between Zn and humic acids are strongly affected by pH, because the solubility of Zn and humic acids is inversely dependent on pH. In acid conditions most of Zn is soluble, while humic acids are insoluble (Alloway, 1995). This could explain why in samples in the acid region the concentration of Zn is very small in comparison to those in the neutral-alkaline zone. Finally, it should be emphasised that simple organic compounds, such as aminoacids, hydroxy-acids and phosphoric acids are also effective complexing or chelating agents for Zn, thus increasing its mobility and solubility in soils.

Cr VI is the more stable form in equilibrium with atmospheric oxygen. However, Cr IV, with its high positive reduction potential, is a strongly oxidising species, and in the presence of soil organic matter Cr IV is reduced to Cr III. Reduction is more rapid in acid than alkaline soils. (Alloway, 1995). It is quite possible that the Cr bound to organic matter in this study is CrIII.

7.4.4.5. Total concentration

Cr

The original population was not normal (Skweness: -1.3137, Kurtosis: 5.3486), when a Box-Cox transformation was applied ($\lambda = 2.8$) the coefficient of variance increased to 43 %. The original population, then, was reflected in the following way:

$$Cr_{total_{reflected}} = 127 - Cr_{total}$$

and transformed using a Box-Cox test ($\lambda = 0.5$), as follows:

$$Cr_{total_{transformed}} = \sqrt{Cr_{total_{reflected}}}$$

This last population was normal. However, during the model error comparison the original population model gave the best results; which are reported in the following paragraphs.

The histogram and descriptive statistics for total concentration of Cr are shown in Figure 7.48, the modelled population of total concentration of Cr in shown in Figure 7.49. The directional variograms characterising the spatial variability of the total concentration of Cr are shown in Figure 7.50. This spatial distribution can be described by a spherical model, as shown in Figure 7.50. The scatterplot of observed versus estimated values and the histogram of errors are given in Figures 7.51. and 7.52.

respectively. The variogram of errors are given in Figure 7.53. The gray scale map of the total concentration of Cr is shown in Figure 7.54.

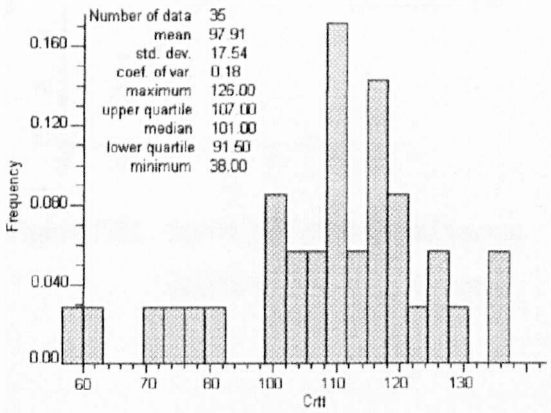


Figure 7.48. Histogram and descriptive statistics of the total concentration of Cr.

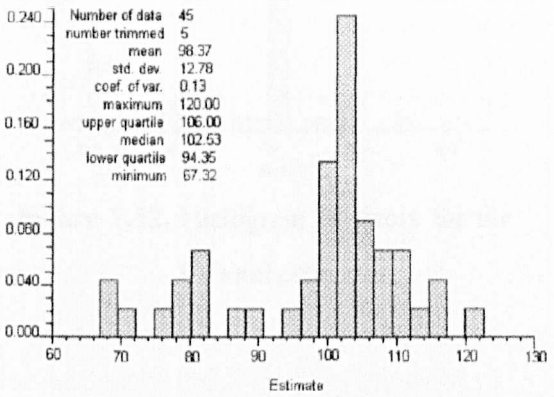
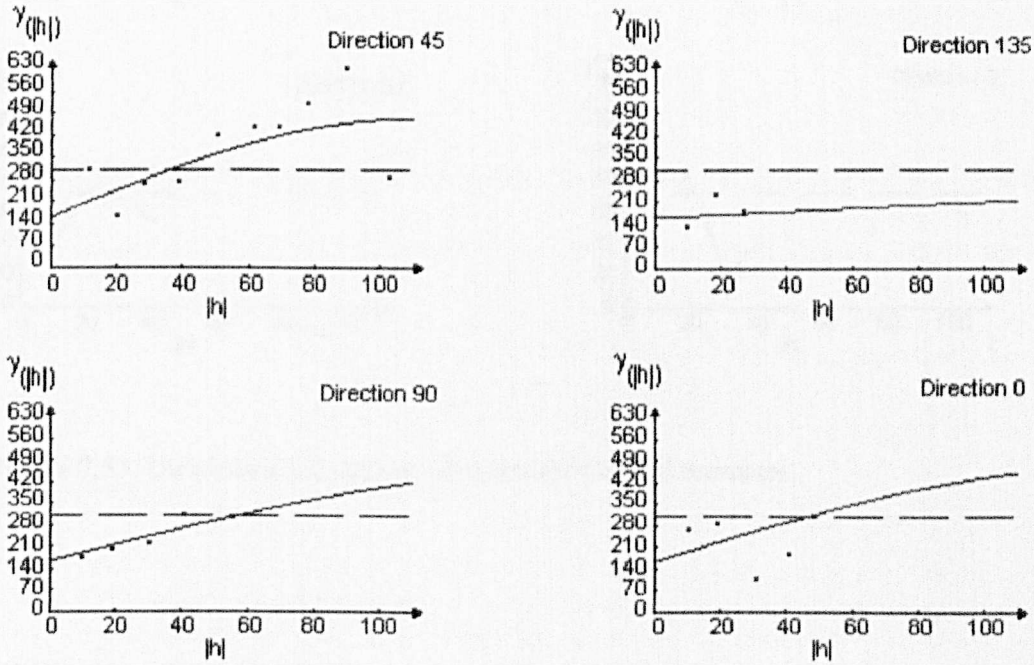


Figure 7.49. Histogram and descriptive statistics of the ordinary kriging estimates for Cr total.



$\gamma_{(h)}$= 167 + 310 Sph. $107.3_{(h)}$

Dir: 173.9| anis.: 55

IGF: 8.72e-02

Figure 7.50. Directional variograms characterising the spatial variability of the total concentration of Cr.

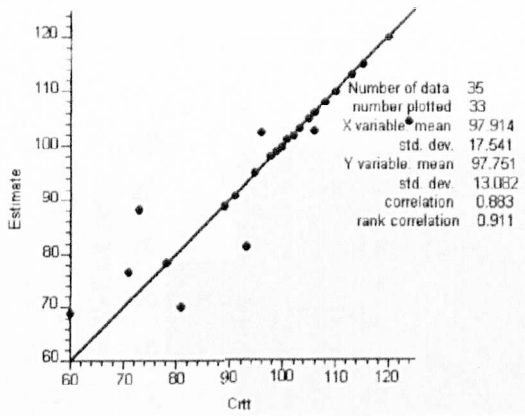


Figure 7.51. Scatterplot of observed versus estimated values for Cr total.

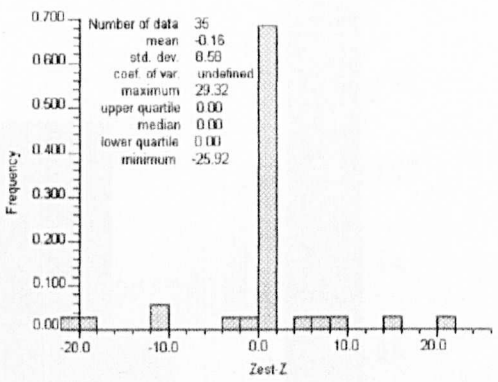


Figure 7.52. Histogram of errors for the Cr total estimates.

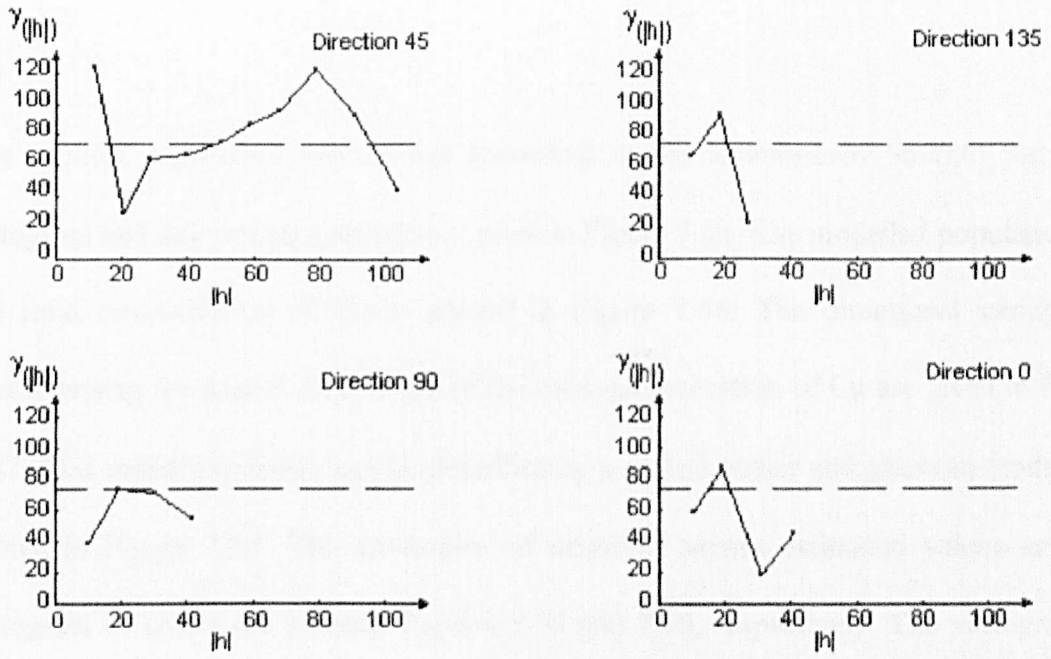


Figure 7.53. Directional variograms of errors for Cr total estimates.

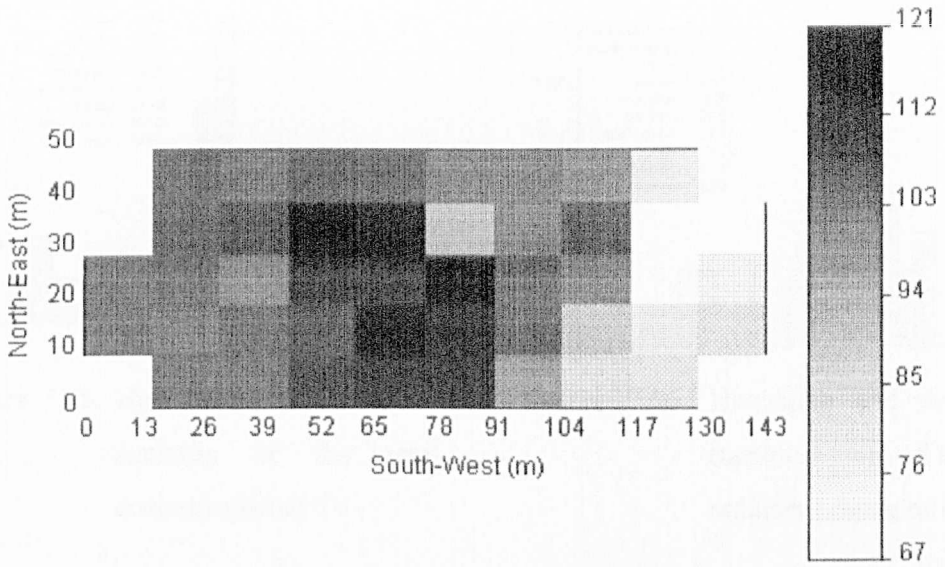


Figure 7.54. Gray scale map of total concentration of Cr kriging estimates.

Cu

The original population was normal according to the Kolmogorov-Smirnof test. The histogram and descriptive statistics are given in Figure 7.55. The modelled population for the total concentration of Cu is shown in Figure 7.56. The directional variograms characterising the spatial distribution of the total concentration of Cu are given in Figure 7.57. This spatial variability can be described by a nested power and gaussian models, as shown in Figure 7.57. The scatterplot of observed versus estimated values and the histogram of errors are given in Figures 7.58 and 7.59, respectively. The variogram of errors are given in Figure 7.60. The gray scale map of the total concentration of Cu is shown in Figure 7.61.

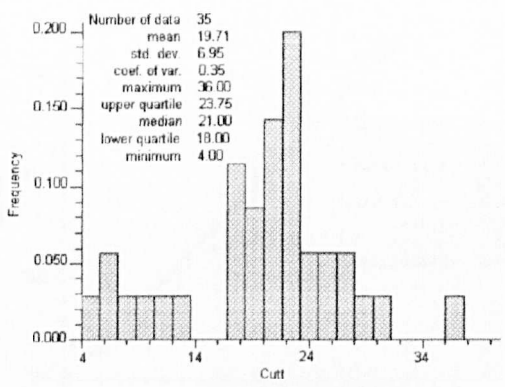


Figure 7.55. Histogram and descriptive statistics of the total concentration of Cu.

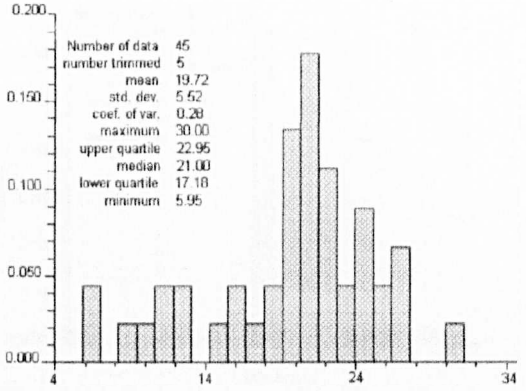
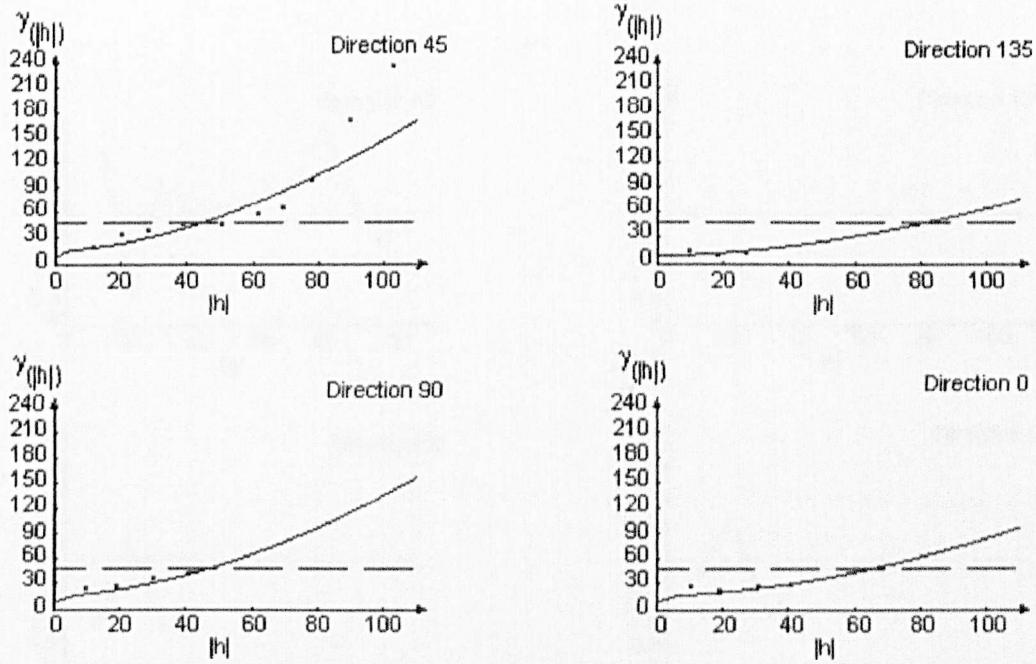


Figure 7.56. Histogram and descriptive statistics of Cu total ordinary kriging estimates.



$\gamma_{(h)}$= 11 + 0.0531 Power 1.71$_{(h)}$ + 7 Gauss 4.9$_{(h)}$

Dir(1): 17| anis.(1): 1.9| Dir(2): 0| anis(2).: 70

IGF: 6.6326e-02

Figure 7.57. Directional variograms characterising the spatial distribution of the total concentration of Cu.

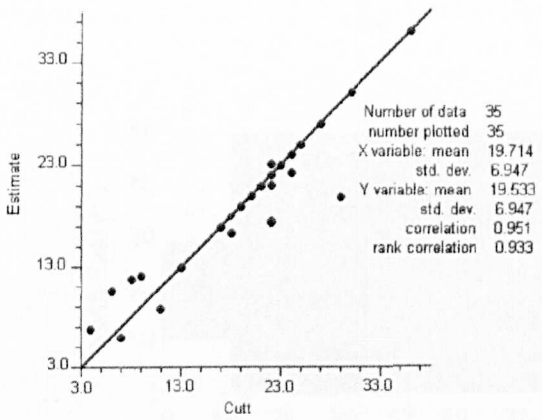


Figure 7.58. Scatterplot of the observed versus the estimated values for Cu total.

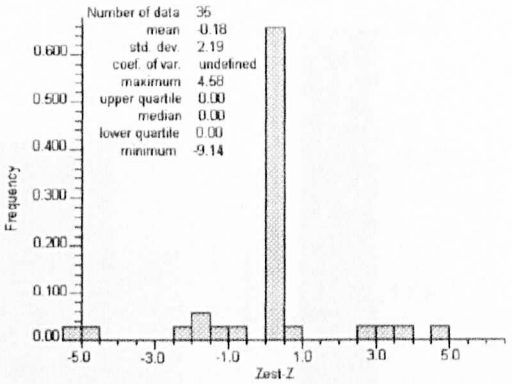


Figure 7.59. Histogram of errors for Cu total estimates.

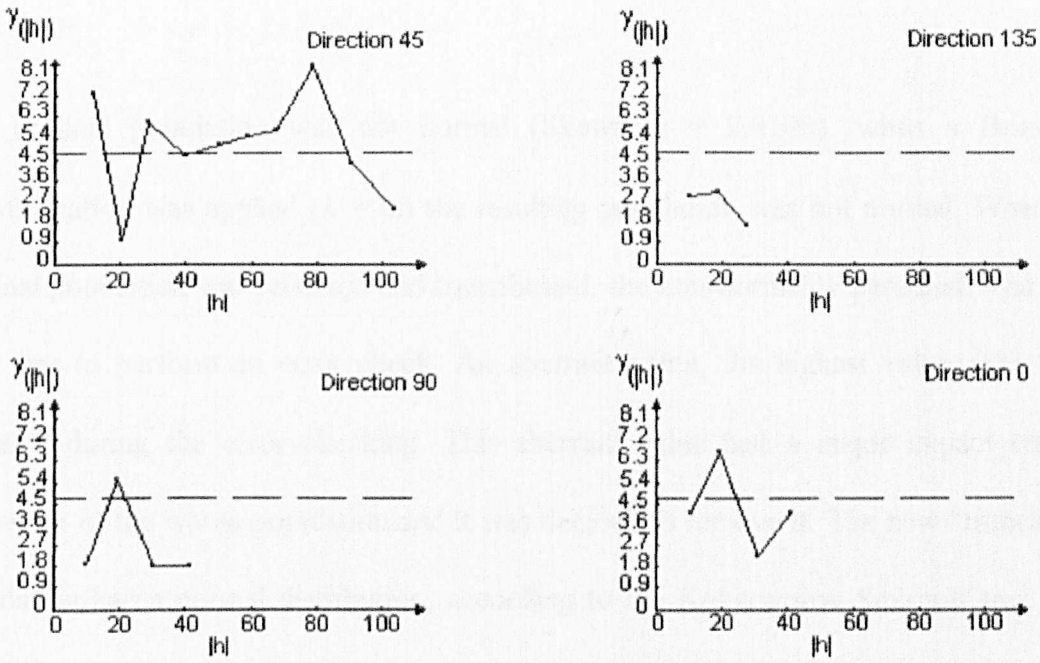


Figure 7.60. Directional variograms of errors for the Cu total estimates.

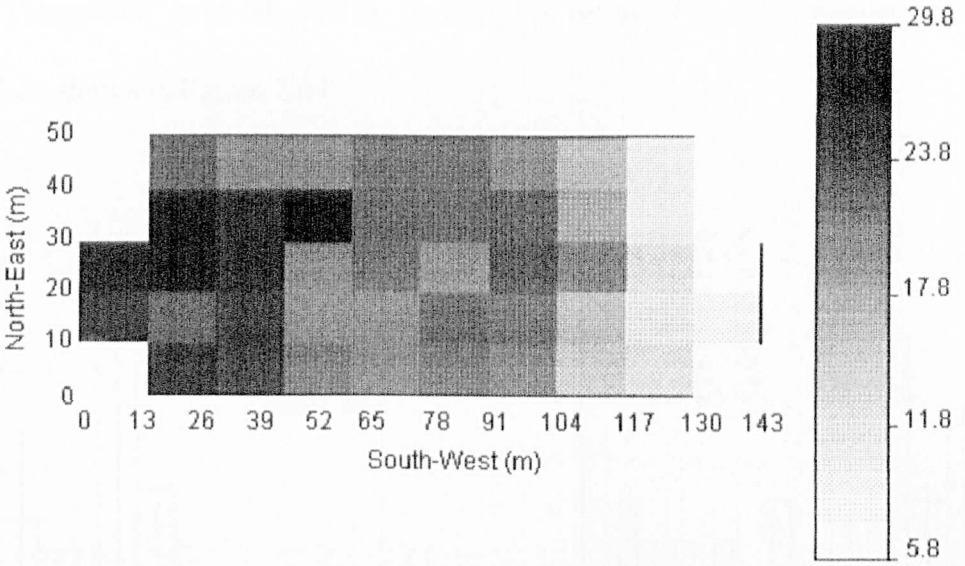


Figure 7.61. Gray scale map of total concentration of Cu kriging estimates.

Zn

The original population was not normal (Skewness = 2.8108), when a Box-Cox transformation was applied (λ = ln) the resulting population was not normal. When the original population was reflected and transformed, the non-normality persisted. The next step was to perform an error check. An aberrant value, the highest value: 353, was revealed during the error checking. This aberrant value had a major impact on the behaviour of the whole population and it was decided to remove it. The new "truncated" population had a normal distribution, according to the Kolmogorov-Smirnoff test. The three populations, the original , the original transformed and the truncated were geostatistically treated, during the error estimation comparison; the first one gave the best performance.

The histogram and descriptive statistics for the original population are given in Figure 7.62. The modelled population is shown in Figure 7.63. The directional variograms characterising the spatial distribution of the total concentration of Zn are given in Figure

7.64. This spatial variability can be described in terms of a nested nugget and guassian model, as shown in Figure 7.64.

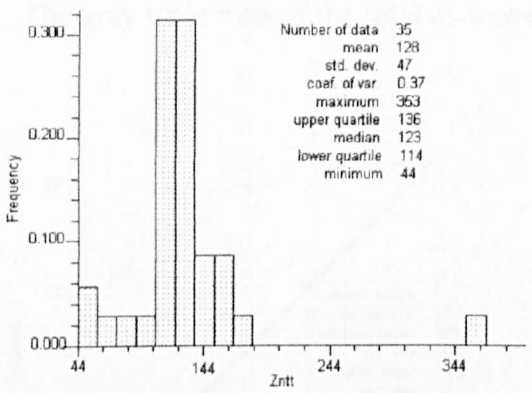


Figure 7.62. Histogram and descriptive statistics of the total concentration of Zn.

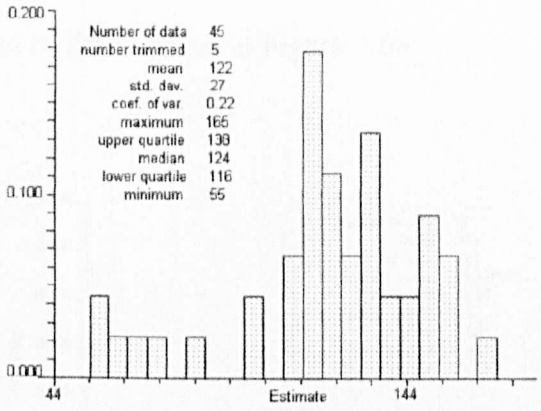
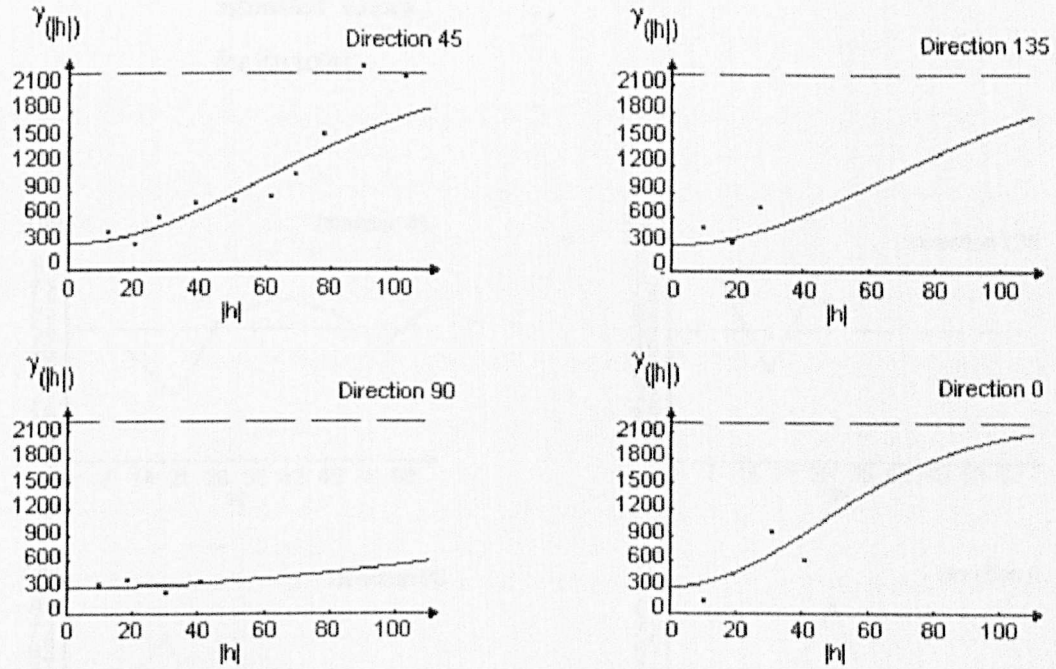


Figure 7.63. Histogram and descriptive statistics of the ordinary kriging estimates for Zn total.



$\gamma_{(h)} = 319 + 1884\ \text{Gauss}\ 110_{(h)}$

Dir.: 137 | anis: 4.2

IGF: 1.023e-02

Figure 7.64. Directional variograms characterising the spatial distribution of the total concentration of Zn.

The scatterplot of observed versus estimated values and the histogram are given in Figures 7.65 and 7.66 respectively. The directional variogram of errors are given in Figure 7.67.

The gray scale map of the total concentration of Zn is shown in Figure 7.68.

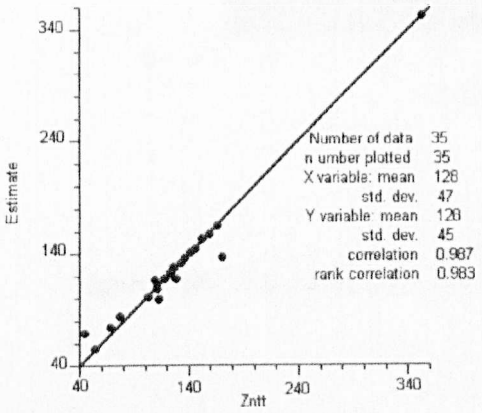


Figure 7.65. Scatterplot of observed versus estimated values for Zn total.

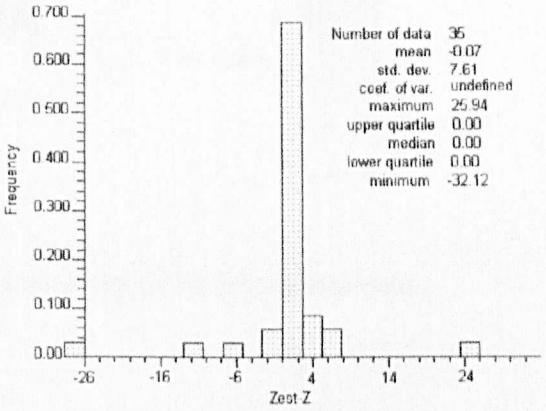


Figure 7.66. Histogram of errors for Zn total estimates.

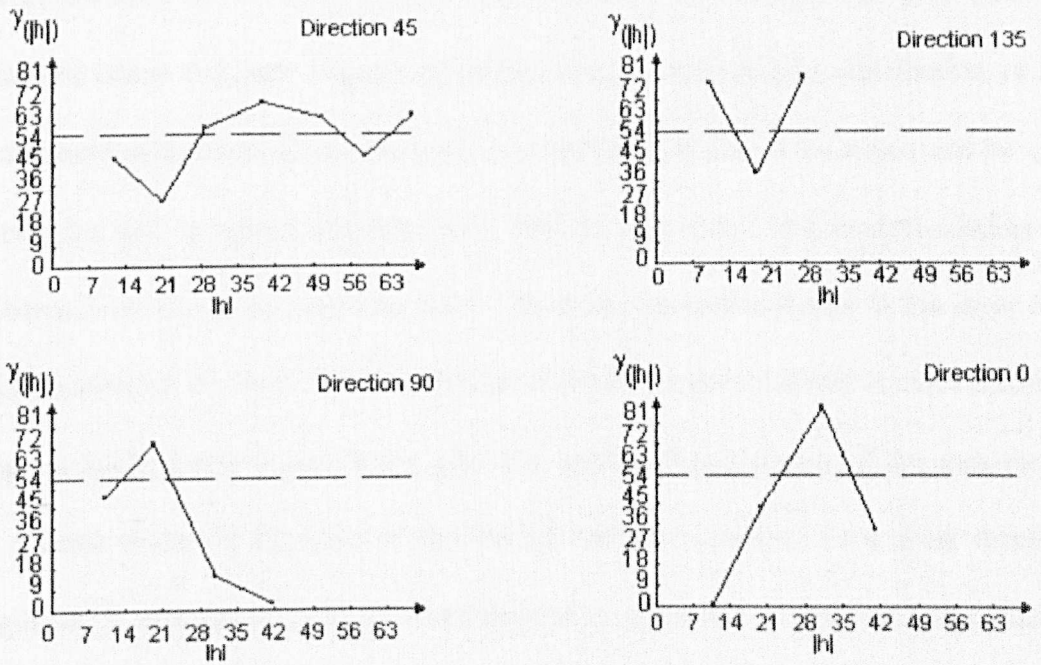


Figure 7.67. Directional variogram of errors for Zn total estimates.

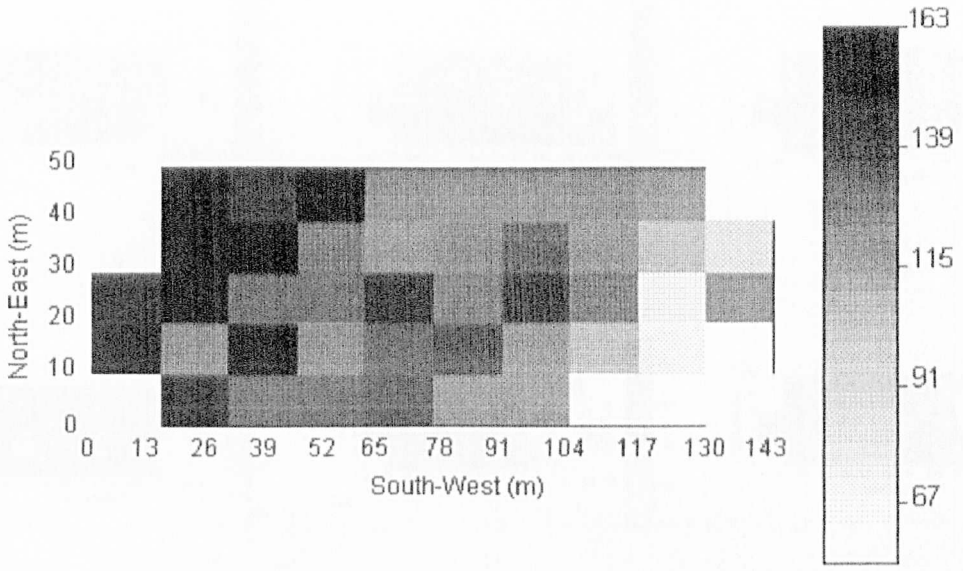


Figure 7.68. Gray scale map of the total concentration of Zn kriging estimates.

7.5. Conclusions

The variograms for pH and organic matter content illustrated a high degree of spatial dependence for sampling points within 10-120 m of one another. Nugget variances were around 10 % of structural variances, indicating that the sampling was carried out in an appropriate scale to reflect the spatial autocorrelation in the area. The gray scale maps calculated using ordinary kriging algorithms had a non-uniform distribution of these geochemical parameters along the bottom of the landfill cell. Two zones can be clearly defined for pH, a neutral-alkaline zone and an acid one. The neutral-alkaline zone corresponds to the compacted clay liner. The acid zone corresponds to the layer rich in pyrite underneath the liner. The distribution of organic matter content is more continuous along the south-western part of the cell. The spatial characteristics of the measured pH and organic matter at the base of the landfill cell are complex. To a great extent this complexity is associated with the mineralogical composition of the site and particularly with the oxidation of the pyrite in the surface. The spatial complexity affects the spatial distribution of Cr, Cu and Zn bound to solid phases in the area (Figure 7.69).

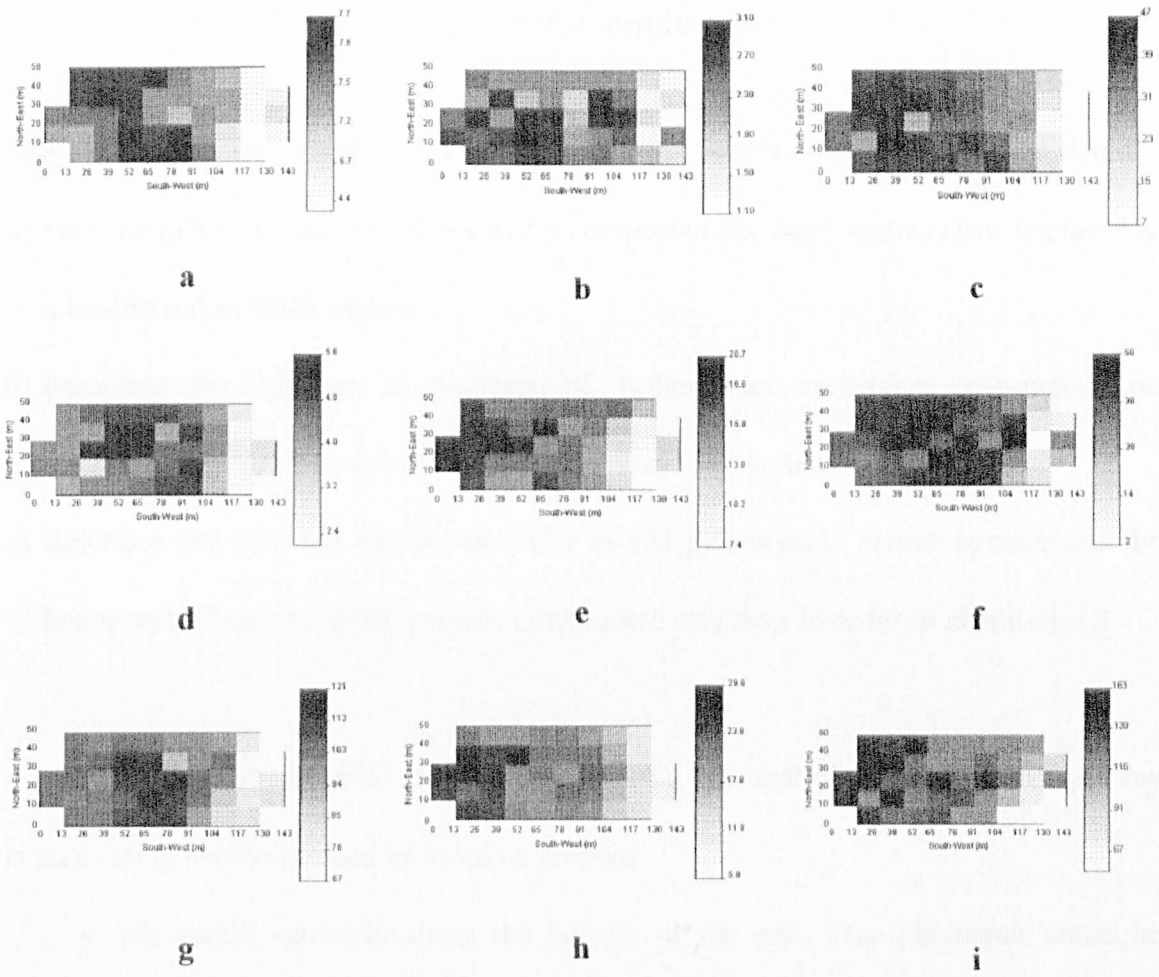


Figure 7.69. Summary figure showing grey scale maps of: **a)** pH, **b)** organic matter, **c)** Zn bound to Fe-Mn oxides, **d)** Cr bound to organic matter, **e)** Cu bound to organic matter, **f)** Zn bound to organic matter, **g)** Total concentration of Cr, **h)** Total concentration of Cu, and **i)** Total concentration of Zn.

Variograms for Cr, Cu and Zn exhibited a high degree of spatial continuity too. However, with the exception of Cr, Cu and Zn bound to organic matter and the total concentration of Zn, the spatial autocorrelation variances could be attributed at scale less than 10 m. The CEC in the liner will be controlled particularly by the permanent charge in the clay. This will gives it an homogeneous capacity to the liner almost independent of the pH changes.

Chapter 8. Conclusions

This work describes an approach which has not been used before. It is original in that it:

a) was conducted in actual conditions of a compacted clay liner system already placed in a landfill cell in Bedfordshire

b) considers the influence of geochemical, rather than mechanical, parameters on attenuation of heavy metals by a compacted clay liner system

c) describes and uses the spatial variability of soil pH, organic matter content and the heavy metal fractions along a newly constructed clay liner in order to charaterise it

Results from the ***chemical characterisation*** of a new cell of engineered Oxford Clay in an existing landfill site can be listed as follows:

- pH varied markedly along the bottom of the cell. Two pH zones could be identified, 1) a neutral alkaline zone with pH values within a range of 7-7.7; most of samples belong to this zone 2) an acid zone with pH values within a range of 2.6- 6.5
- Organic matter content varied within the range of 1-2.3 %
- Cation exchange capacity (CEC) varied between 19 and 71 $cmol_c\,kg^{-1}$. Ca^{2+} (63-84 %) dominated the CEC in the assessment samples. Mg^{2+} (11-29 %) was the second most important exchangeable cation. The Ca^{2+}:Mg^{2+} ratios varied from 1:2 to 1:7. Na^{+} and K^{+} were 1-12 % and 0-4 % of the CEC
- Results from the fractionation of Cr, Cu and Zn in solid phases showed that the metal concentration in the acid zone was lower than in the alkaline zone, this suggested that metals had been solubilised and mobilised in the zone with acid pH. Other important results from the fractionation of metals in solid phases

were that Zn was distributed in all fractions, whereas Cr and Cu were mainly bound to organic matter

- The modelling of inorganic metal species in the soil solution of Oxford Clay samples can be summarised as follows: the essential metals- Ca, K, Mg, Na, Mn- would be as free ions, Fe would precipitate with OH- ligand, Zn would be available in 25 % of its total concentration in soil solution and inorganically complexed in 23 %. However, more analytical determinations should be carried out to describe chemical species in soil solution, in particular Dissolved Organic Matter determination

It is important to remark that the sequential extraction scheme used to fraction the metals in solid phases offers a simple approach to the assessment of metal speciation in soil, and it can produce meaningful results only if:

- the effectiveness of each extraction step is confirmed. This can be achieved by using additional analysis along with the sequential extraction. It is also recommended to use thermodynamic calculations
- The stability of the extracts obtained using the sequential extraction scheme versus time is assessed
- A soil solution study is carried out as a complementary analysis
- The mineralogical composition is considered at all times when estimating side reactions and interferences arising from the extractions

Results from the ***mineralogical characterisation*** of a new cell of engineered Oxford Clay in an existing landfill site explained the pH variation found during the chemical characterisation, as follows:

- The acid pH zone is due to a layer rich in pyrite that is still undergoing a weathering process, with pyrite as the most redox sensitive component. Oxidation of pyrite produces sulphuric acid, leaching of carbonate minerals, and increasing gypsum and amorphous Fe oxides. Gypsum may cause expansion and disruption of the clay or concrete fabric. However, the increase of the amorphous Fe oxides will enhance the sorption and cation exchange properties of the clay
- On the other hand, the neutral-alkaline zone belongs to the compacted clay liner, which is more stable, where pyrite has not been oxidised and gypsum has not been generated. The clay mineral concentration in the compacted clay liner is high; this will increase the cation exchange properties of the clay. From the clay minerals, smectite (for its swelling properties) will give the effective "seal" character to the clay.

A recommendation to Shanks and McEwan is that they should consider the hazard represented by the layer rich in pyrite underneath the liner system. The pyrite could undergo oxidation that will impact on the mobilisation of heavy metals.

From the ***spatial characterisation*** of a new cell of engineered Oxford Clay in an existing landfill site it can be noted that:

- The soil pH and organic matter content variabilities were explained by changes at short distances. The spatial characteristics are complex and to a large extent this complexity is associated with the mineralogical composition of the site, particularly with the oxidation of pyrite in the surface

- The spatial description of the metal fractions bound to specific clay liner pools showed strong correlation with soil pH, which were explained and described in relation to the changes of the mineralogical composition in the area. The spatial variations of metal bound to specific clay pools at short distances can be used to assess the effect of geochemical parameters on the localisation of heavy metals in the liner

The results of this study are meaningful to:

a) Landfill related people since the spatial description of the liner will produce useful information to asses the continuity of the liner and its properties

b) Researchers, for the technical and methodological aspects described along this work

This work forms the basis for alternative studies such as,

- Speciation of soil solution, the technical details and some values are already given in this work, these could be taken into consideration for further analysis. The organic contribution must be considered for a complete characterisation of the species in the soil solution
- The spatial variability developed in this work revealed invaluable information to assess the natural attenuation of the liner. It would be interesting to study to what extent the parameters that limited the natural attenuation are the subject of temporal variation. It is expected to be significant, for example for the oxidation of the pyrite in surface. This oxidation rate is expected to be different in the dry season
- The spatial variability of permeability of the liner along the bottom of the cell

Finally, this work has demonstrated that:

- Geochemical attenuation variability is a predictable, dependable and quantifiable (via determination of the metal reactivity) mechanism which can be used to advantage in the design of a landfill site and in the operations of a monitoring system
- Hazards maps can be used to illustrate the variability of geochemical attenuation and spot future problems that can impact on the performance of a compacted clay liner system

References

Adams F. 1971. Ionic Concentrations and Activities in Soil Solution. Soil Science Society of America Journal 35, 420-426.

Allison J. D., Brown D. S. and Novo-Gradac K. J., 1991. MINTEQA2/PRODEFA 2, A Geochemical Assessment Model for Environmental Systems: Version 3.0. User's manual. EPA/600/3-91/021. Environmental Research Laboratory, Office of Research and Development. U.S. Environmental Protection Agency, Athens, Georgia, USA.

Alloway B. J. (ed.), 1990. Heavy Metals in Soils, Blackie, London.

Amacher M. C., 1984. Determination of Ionic Activities in Soil Solutions and Suspensions: Principal Limitations. Soil Science Society of America Journal 48, 519-524.

APHA, AWWA, WEF, 1992. Standard methods for the examination of water and wastewater, ed. 18th.

Amrhein C. and Suarez D. L., 1990. Procedure for determining sodium-calcium selectivity in calcareous and gypsiferous soils. Soil Science Society of America Journal 54, 999-1007.

Ball S. and Bell S., 1994. Environmental Law, the law and policy relating to the protection of the environment, 2nd edition. Blackstone Press Limited, London, UK.

Batchelder M., 1995. The performance of mudrocks for leachate containment: physical and chemical constraints. PhD thesis, University of London.

Batchelder M. and Cressey G., 1998. Rapid, accurate quantification of clay bearing samples by X-ray diffraction whole pattern stripping. Clay and Clay Minerals 46 (2), 183-194.

Batchelder M., Mather J. D. and Joseph J. B., 1998. The Stability of the Oxford Clay as a Mineral liner for Landfill. J. CIWEM 12, 92-97.

Bermoind A., Yousfi I. and Ghestern J. P., 1998. Kinetic Approach to the chemical speciation of trace metals in soils. Analyst 123, 785-789.

Bermond A. P., 1992. Thermodynamics Applied to the study of the Limits of Sequential Extraction Procedures Used for the Speciation of Trace Elements in Sediment and Soils. Environmental Technology 13, 1175-1179.

Brown K. W. and Thomas J. C., 1984. Conductivity of three commercially available clays to petroleum products and organic solvents. Hazard Waste. 4, 545-553.

Burgess T. M. and Webster R., 1980. Optimal Interpolation and Isarithmic Mapping of Soil Properties. III. Changing Drift and Universal Kriging. Journal of Soil Science XX, 505-524.

Burgess T. M. and Webster R., 1980a. Optimal Interpolation and Isarithmic Mapping of Soil Properties. I. The Semi-Variogram and Punctual Kriging. Journal of Soil Science 31, 315-331.

Burgess T. M. and Webster R., 1980b. Optimal Interpolation and Isarithmic mapping of Soil Properties. II. Block Kriging. Journal of Soil Science 31, 333-341.

Candelaria L. M. Chang A. C and Amrhein C., 1995. Measuring Cadmium Ion Activities in Sludge-Amended Soils. Soil Science 159 (3), 162-175.

Carter R. M. (ed.); 1993. Soil Sampling and Methods of Analysis. Canadian Society of Soil Science. Lewis Publisher, London.

Cliff A. D. and Ord J. K.; 1975. Model Building and the analysis of spatial pattern in human geography (with Discussion). Journal of the Royal Statistical Society B 37, 297-348.

Commission of the European Communities, Directive relating to the quality of water intended for human consumption, 80/778/ EEC, OJ L 229, 11.

Cressie N. A. C., 1993. Statistics for Spatial Data. John Wiley & Sons, New York.

Daniel David E. (ed.), 1993. Geotechnical Practice for Waste Disposal. Chapman and Hall, London.

Daniel D. E. and Liljestrand H. M., 1984. Effects of landfill leachates on natural liner systems. A report to the Chemical Manufacturers Association.

Daniel D. E., Liljestrand H. M, Broderick G. P. Bowders J. J., 1988. Interaction of Earthern Liner Materials with Industrial Waste Leachate. Hazard Waste, Hazard Mater 5, 93-108.

Das K. A.C., Cervera M. L. and de la Guardia M., 1995. Metal Speciation in Solid Matrices. Talanta 42, 1007-1030.

Department of the Environment, 1993. Waste Management Paper No 26A: A Technical Memorandum Providing Guidance on Assessing the Completion of Licensed Sites. HMSO, London

Deutsch C V. and Journel A. G., 1998. GSLIB: Geostatistical Software Library and User's Guide. Oxford University Press, Oxford.

Deutsch W. J., 1997. Groudwater Geochemistry. Fundamentals and Applications to Contamination. Lewis Publishers, Boca Raton, Florida.

Englund E. and Sparks A., 1991. GEO-EAS 1.2.1. Geostatistical Environmental Assessment Software User's Guide EPA 600/4-88/033. Environmental Monitoring Systems Laboratory, Office of Research and Development U.S. Environmental Protection Agency, Las Vegas, Nevada.

Ehrig H. J. (1988). Water and element balances of landfills, in Lecture Notes in Earth Sciences. (ed. P. Baccini) Springer-Verlag, Berlin.

Fernandez-Boy M. E., Cabrera F. and Moreno F.; 1998. Analysis of inorganic anions in drainage water and soil solution by single-column ion chromatography. Journal of Chromatography A 823, 285-290.

Gardiner J., 1974. The Chemistry of Cadmium in Natural Water-I. A study of cadmium complex formation using the Cadmium Specific -Ion Electrode. Water Research 8, 23-30.

Gesler W., 1986. The uses of spatial analysis in medical geography: a review. Soc. Sci. Med. 23, 963-973.

Goodchild M. F., Parks B. O. and Steyaret L. T. (eds.), 1993. Environmental Modelling with GIS. Oxford University Press. New York.

Goovaerts P., 1997. Geostatistics for natural resources characterisation. Oxford University Press, New York.

Grantham G. and Robinson H. D. (1988). Instrumentation and monitoring of bentonite landfill liner. Waste Manage 78, 134-148.

Griffin R. A. and Jurinak J. J., 1973. Estimation of Activity Coefficients from the Electrical Conductivity of Natural Aquatic Systems and Soil Extracts. Soil Science 116 (1), 26-30.

Hann F. A. M de, Keizer M.G., Lexmond T. M., Reimsdjik W. H. van, Zee S. E. A. T. M. van der, 1986. Some recent developments and approaches in soil protection research. Netherlands Journal of Agricultural Science 34 (3), 361 - 370.

Harmsen K. (1977). Behaviour of heavy metals in soils. Centre for Agricultural Publishing and Documentation, Wageningen.

Hester R. E. and Harrison R. M., 1995. 3. Waste Treatment and Disposal. The Royal Society of Chemistry. Letchworth, Herts.

Horton A., Shephard-Thorn E. R and Thurrell R. G., 1974. The geology of the new town of Milton Keynes. IGS-NERC report 74/16. HMSO. London.

Hoshmand R. A., 1998. Statistical Methods for Environmental and Agricultural Sciences. CRC Press, Boca Raton, Florida.

Issaks E. H. and Srivastava R. M., 1989. An introduction to Applied Geostatistics. Oxford University Press, New York.

Jackson J. O., 1973. The alteration characteristics of the Lower Oxford Clay. Clay Minerals 10, 113-126.

Jackson J. O. and Fookes P. G.; 1974. The relationship of the Estimated Former Burial Depth of the Lower Oxford Clay to some soil properties. Q. J. Engng Geol. 7, 137-179.

Johnson R. L., Cherry J. A. and Pankow J. F., 1989. Diffusive containment transport in natural clay: A field example and implications for clay-liner waste disposal sites. Environmental Science and Technology 23 (3), 340-349.

Journel A. G and Huijbregts C. J., 1978. Mining Geostatistics. Academic Press, London.

Krebbs C. J., 1999. Ecological Methodology. Addison Wesley Logman Inc., Menlo Park, California.

Lake D. L., Kirk P. W. W, and Lester J. N., 1984. Fractionation, Characterisation, and Speciation of Heavy Metals in Sewage Sludge and Sludge-Amended Soil: A Review, Journal of Environmental Quality 13 (2), 175-181.

Lake J. V., Bock G. R. and Goode J. A. (ed.), 1997. Precision Agriculture: Spatial and Temporal Variability of Environmental Quality. John Wiley & Sons, West Sussex England.

Langford C. H. and Cook R. L., 1995. Kinetic versus Equilibrium Studies for the Speciation of Metal Complexes with Ligands from soil and water. Analyst 120, 591-596.

Liddell K. C., 1994 in Metals and Materials Waste, Reduction, Recovery and Remediation edited by K. C Liddell, R. G. Bautista and R. J. Orth. The Minerals, Metals & Minerals Society.

Liebhold A. M., Rossi R. E. and Kemp W. P., 1993. Geostatistics and Geographic Information System in Applied Insect Ecology. Annual Review of Entomology 38, 303-327.

Lindsay W. L., 1979. Chemical Equilibria in soils. John Wiley & Sons. Chichester.

Loeppert R. H., Schwab A. P and Goldberg S., 1995. Chemical Equilibrium and Reaction Models. Soil Society of America Inc. American Society of Agronomy, Inc. Madison.

Luoma S. N. and Bryan G. W., 1981. A statistical Assessment of the form of trace metals in oxidised estuarine sediments employing chemical extractants. The Science of the Total Environment 17, 165-195.

McBride M. B., Bolt G. H., Hayes M. H. B., De Strooper E. B. A. (eds.), 1991. Interactions at the soil colloid-soil solution interface. Kluwer, Dordrecht.

McBride m. B. 1994. Environmental Chemistry of Soils. Oxford University Press. New York.

McLean Joan E. and Bledsoe Bert E., 1992. EPA/540/S-92/018: Ground Water Issue. Behaviour of Metals in Soils. Office of Solid Waste and emergency Response, Office of Research and Development Environmental Protection Agency. Las Vegas.

Michalke B., 1994. Quality Control in Speciation investigations, Fresenius J. Anal. Chem. 350, 2-6.

Milodowski A. E., Bloodworth A. J. and Wilmot R. D., 1986. Report FLPU 85-13: Long Term Effects on Potential Repository Sites: The Alteration of the Lower Oxford Clay during Weathering, British Geological Survey-Natural Environment Research Council, Nottigham.

Minnich M. M and McBride M. B., 1987. Copper Activity in Soil Solution: I. Measurement by Ion-selective Electrode and Donnan Dialysis. Soil Science Society of America Journal 51, 568-572.

Myers J. C., 1997. Geostatistical Error Management. Van Nostrand Reinhold, New York.

Naidu R., Kookana D. S., Oliver D. P., Rogers S. and McLaughlin M.J. (eds.) (1996). Contaminants and the soil environment in the Australasia-Pacific Region. Kluwer Academic Publishers. London.

Olea R, (ed.), 1991. Geostatistical Glossary and Multilingual Dictionary. Oxford University Press, Oxford.

O'Leary P. and Walsh P., 1992. Solid Waste Landfills. Solid and Hazardous Waste Education Centre. University of Wisconsin, Madison.

Pannatier Y., 1995. Variowin 2.2 User's manual.

Parker D. R., 1997. Geochem-PC version 2.0. User Manual.

Parker A. and Rae J. E. (eds.) (1998). Environmental Interactions of Clays. Clays and the Environment. Springer-Verlag Berlin.

PetersT., 1993. Chemical and Physical changes in the Subsoil of Three Waste Landfills. Waste Manage Research 11, 371-376.

Pickering W. F., 1979. Copper retention by soil/sediment components. In: Nriagu J. O (ed.). Copper in the environment. I. Ecological cycling. John Wiley, New York.

Piwoni Marvin D. and Keeley Jack W., 1990. Basic Concepts of Contaminant Sorption at Hazardous Waste sites EPA/540/4-90/053. United States Environmental Protection Agency, Las Vegas.

Quevauviller Ph., Maier E. A., 1994. Single and Sequential Extraction of Trace Metals in Soils and Sediments. Conclusions of the workshop held in Stiges (E) on 29-31 March 1992 in Research trends in the field of environmental analysis, European Commission, Brussels.

Quigley R. M., Fernandez F., Yanful E., Helgason T., Margaritis A. and Whitby J. L., 1986. Hydraulic Conductivity of Contaminated Natural Clay Directly Below the Confederation Road Domestic Waste Landfill, Sarnia, Ontario. GEOT-13-86. Geotechnical Research Centre Report. Ontario.

Rapin F., Tessier A. and Campbell P. G. C. and Richard Carignan R. (1986). Potential Artifacts in the Determination of Metal Partitioning in Sediments by a Sequential Extraction Procedure. Environ. Sci. Technol. 20 (8), 836-840.

Robertson G. P., 1987. Geostatistics in ecology: interpolating with known variance. Ecology 68 (3), 744-748.

Rowell D. L., 1994. Soil Science: Methods and Applications. Longman Scientific and Technical, Essex.

Rossi R. E., Mulla D. J., Journel A. G. and Franz E. H., 1992. Geostatistical tools for modelling and interpreting ecological spatial dependence, Ecological Monographs 62, 277-314.

Rubio R. and Ure A. M., 1993. Approaches to Sampling and Sample Pretreatment for Metal and Sample Pretreatments for Metal Speciation in Soils and Sediments. Intern. J. Environ. Anal. Chem. 51, 205-217.

Skitt J., 1992. 1000 terms in Solid Waste Management. ISWA, Denmark.

Skoog D. A., West D. M. and Holler F. J., 1996. Fundamentals of Analytical Chemistry, seven edition. Saunders College Publishing, U. S. A.

SME (Southern Waste Services) LTD, 1976. Geological and Hydrogeological Survey of L-field area Stewartby for waste Disposal purposes. Technical and Research Department SME (Southern Waste Services) LTD, 1996. L-field landfill site fact file.

Sokal R. R. and Rohlf J. F., 1995. Biometry. W. H. Freeman and Company, New York.

Sparks D. L., Page A. L., Helmke P. A., Loeppert R. H. Soltanpour R. H., Tabatabai M. A., Johnston C. T and Summer M. E. (eds.), 1996. Methods of Soil Analysis. Part 3. Chemical Methods. Soil Science Society of America, Inc. American Society of Agronomy, Inc. Madison.

Szpunar-Lobinska J., Witte C., Lobinski R. and Adams F. C., 1995. Separation techniques in speciation analysis for organometallic species. Fresinius J. Anal. Chem. 351, 351-377.

Tan K. H., 1996. Soil Sampling, Preparation and Analysis. Marcel Dekker, Inc. New York.

Tessier A, Campbell P. G. C., and Bisson M., 1979. Sequential Extraction Procedure for the Speciation of Particulate Trace Metals. Analytical Chemistry 51 (7), 844-851.

United States Salinity Laboratory Staff, 1969. Diagnosis and Improvement of Saline and Alkali Soils. Agricultural Handbook No. 60. United States Department of Agriculture. 84,88.

Ure A. M. and Davidson C. M., 1995. Chemical Speciation in the Environment. Blackie Academic & Professional. Glasgow.

Ure A.M, Quevauviller Ph., Muntau H. and Griepink B., 1993. Speciation of Heavy Metals in Soils and Sediments. An Account of the Improvement and Harmonisation of Extraction Techniques Undertaken under the Auspices of the BCR of the Commission of the European Communities. International Journal of Environment Analytical Chemistry 51, 135-151.

Viera S. R., Hatfield, Nielsen D. R. and Biggard J. W., 1983. Geostatistical theory and application to variability of some agronomical properties. Hilgardia 51, 1-75.

Walker T., 1991. Managing Leachate, One day symposium, Baden Powell House, Kensington, London.

Wolft R. S. (1979). Methanogenesis, in Microbial Biochemistry, Int. Rev. of Biochemistry, 21 (ed. J. R. Quayle) University Park Press, Baltimore, MD.

Wolin M. J. and Miller T. L. (1985) in Biology of Industrial Microorganisms (eds. A. L. Demsin and N. A. Solomon) Benjamin/Cumings Publ. Co. Inc. Menlo Park, CA.

Wolt J., 1994. Soil Solution Chemistry: Applications to Environmental Science and Agriculture. John Wiley, New York.

Xiao-Quan S. and Bin C., 1993. Evaluation of Sequential Extraction for Speciation of Trace Metals in Model Soil Containing Natural Minerals and Humic Acid. Analytical Chemistry 65, 802 -807.

Zehnder A. J. B. (1978). . Ecology of methane formation, in Water pollution Microbiology, 2, (ed. R. Mitchell). John Wiley & Sons, N. Y.

Zeikus J. G. (1980). Microbial populations in digesters, in Abaerobic Digestion, (ed. D. A. Stafford) Appl. Sci. Publishers, London.

Appendix 1. The certified values of the reference material and the recovery percentage of exploratory samples

a) GSS-1

Brown Soil

National Research Center for CRMs (China)

Description:

The material used for this CRM was collected at Yichun, Heilongjiang, China. The soil is dark brown padzolitic soil typical of the mountanous and hilly terrain of northeast China. The underlaying bedrock is granite in a district of Pb-Zn mineralization.

Certified concentrations (μg/g dry weight unless noted):

Component	Value	Uncertainty (±)	Component	Value	Uncertainty (±)
Li	35.3	0.6	Mo	1.4	0.06
Be	2.5	0.13	Ag	0.35	0.03
B	50	2	Cd	4.3	0.2
F	506	19	In	0.081	0.011
Na_2O(%)	1.66	0.02	Sn	6.1	0.4
MgO(%)	1.81	0.04	Sb	0.87	0.12
Al_2O_3(%)	14.18	0.08	I	1.9	0.2
SiO_2(%)	62.60	0.09	Cs	9.0	0.4
P	735	13	Ba	590	15
S	310	60	La	34	1
K_2O (%)	2.59	0.02	Ce	70	2
CaO (%)	1.72	0.03	Pr	7.5	0.3
Sc	11.2	0.3	Nd	28	1.4

Component	Value	Uncertainty (±)	Component	Value	Uncertainty (±)
Ti	4830	70	Sm	5.2	0.2
V	86	2	Eu	1.0	0.04
Cr	62	2	Gd	4.6	0.16
Mn	1760	24	Tb	0.75	0.04
Fe_2O_3(%)	5.19	0.04	Dy	4.6	0.17
Co	14.2	0.4	Er	2.6	0.1
Ni	20.4	0.6	Yb	2.66	0.12
Cu	21	0.6	Lu	0.41	0.03
Zn	680	11	Hf	6.8	0.5
Ga	19.3	0.8	Ta	1.4	0.1
Ge	1.34	0.12	W	3.1	0.14
As	33.5	1.7	Hg(ng/g)	32	3
Se	0.14	0.02	Tl	1.0	0.08
Br	2.9	0.3	Pb	98	3
Rb	140	3	Bi	1.17	0.06
Sr	155	3	Tm	0.42	0.04
Y	25	1	Th	11.6	0.4
Zr	245	6	U	3.3	0.3
Nb	16.6	0.7			

Noncertified concentrations (μg/g dry weight unless noted):

Component	Value
Cl	78
Te	0.051
Au (ng/g)	0.55

Order information:

Contact NRCCRM.

Reference:

Institute of Geophysical and Geochemical Exploration (1986). Certificate of geochemical standard reference materials. Institute of Geophysical and Geochemical Exploration, Langfang, Hebei, China.

b) Recovery Percentage for the exploratory samples

Element	Concentration, μg/g
Cr	61 ± 4
Ni	20 ± 1
Cu	20 ± 1
Zn	690 ± 23
Cd	4 ± 0.3
Pb	96 ± 6

Appendix 2. The assessment sampling report

Date: November 20th, 1997

Period of time: 12:00 - 14:30

Location: Northern part of the L-field site, liner made of virgin strata of Lower Oxford Clay

Sampling protocol: Regular grid

Specifications: 27 sampling points and eighth random replicates.

Samplers:

- Greg Anderson
- Alma Eslava-Gomez
- Gabriela Muñoz-Meléndez

Sampling tools:

- Poly-twist andersons, twist ties with cutter
- Heavy duty plant labels (plastic)
- Durable glass fibre filled polyamide trowel
- Thermos Cooler Box
- Plastic bags (to storage samples)

Weather: it was raining in the three days previous to the sampling, and it rained sometimes during the sampling. The temperature was around 12 °C, it was windy. At around 14:00 the sun shined for a while.

Soil horizon: Virgin strata of Lower Oxford Clay

Occurrence of alien elements:

The auger sampler was broken when taking the first sample, because the sample was highly disturbed, it was sampled again this time with the trowel.

Observations:

There are a "red" zone, presumably pyrite zone from sample 22. The water accumulated in that region had a reddish colour.

Samples were kept in the cooler box at around 5 ° C and transported to the laboratory on the same day. They were in the laboratory at around 19:00.

Appendix 3. The hexaquo ion $[M(H_2O)_6]^{n+}$

It is because water is a ligand that it is impossible to place a transition-metal ion in aqueous solution without complex formation occurring; if no other co-ordinating groups are present, this complex will usually be the hexaquo ion $[M(H_2O)_6]^{n+}$, as shown in Figure A2.1.

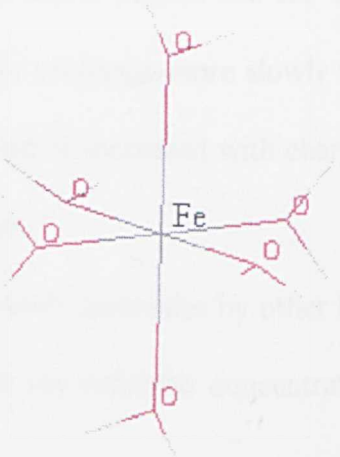


Figure A2.1 Fe^{3+} hexahydronium ion

The hexaquo-ion will reacts mainly by substitution and acid base reaction.

In case of acid-base reaction, the Lowry-Bronsted acidity should be recall to explain the following reaction:

$$[M(H_2O)_6]^{n+} + H_2O \Leftrightarrow [M(H_2O)_5(OH)]^{(n-i)+} + H_3O^+$$

for simplicity the water molecules are omitted in the hexaquo ion and the hydronium ion is considered as H^+

The greater the charge on the aqueo ion the greater its acidity, that is dipositive transition metals ions are only weakly acidic, the tripositive ions are strong acids, in this last case any attempt to raise the pH above the formation constant the reaction proceed

to the right, that is to the formation of aqueous complex, and eventually in the final equilibrium the neutral specie $M(H_2O)^3(OH)_3{}^0$ precipitates.

In addition to the mononuclear hydroxo-species, the formation of binuclear cation occurs by the olation reaction:

$$[2M(H_2O)_6]^{n+} + 2H_2O \Leftrightarrow [M(H_2O)_8(OH)_2]^{n+1} + 2H_3O^+$$

In case of substitution reactions, these should considered the octahedral stereochemistry of hexaquo ion. The fundamental substitution reaction will be given by the water exchange between hydrated cations and the solvent water. The more highly charged M^{3+} ions undergo water exchange more slowly than the M^{2+} and M^+ ions. The M-OH_2 bond strength is expected to increased with charge in M and decrease with size of M for ions of the same charge.

The rate of replacement of water molecules by other ligand in general depend on the concentration of metal ion but not only the concentration of the added ligand, they follow a first-order rate law.